Norwegian University of Science and Technology

*Faculty of Engineering Science and Technology, Department of Energy and Process Engineering*

# Project Work

## Assessment of an advanced heating and cooling system with thermal storing

*Author:*
J.W.P. Vervoort

*Supervisor:*
Natasa Nord (NTNU)
*Co-supervisor:*
Hanne Kauko (Sintef)
Christian Schlemminger (Sintef)

December 21, 2016

**Norwegian University of Science and Technology**

**Faculty of Engineering Science and Technology**
**Department of Energy and Process Engineering**

EPT-P-2016-94

NTNU

**PROJECT WORK**

for

Jill Vervoort

Autumn 2016

**Assessment of an advanced heating and cooling system with thermal storing**

Evaluering av avanserte oppvarmings- og kjølesystem med termisk lagring

**Background and objective**

To achieve Norway's goals for climate and energy policy it is necessary to reduce greenhouse gas emissions, increase the use of renewable energies and reduce energy use effectively. Housing and building complexes account for approximately 40% of the Norwegian energy use and there is a great potential for energy efficiency and energy integration. SINTEF project INTERACT extends towards solutions for optimal design, integration and management of complex thermal energy systems. The work in this project assignment is directly linked to subjects and researchers in this project.
The aim of the thesis is energy analysis of a college building in Norway with an advanced energy supply system. The system utilizes phase change materials as a cold storage and energy wells for seasonal thermal storage. To understand and document the system operation, energy flows and temperature levels in different parts of the system should be analyzed at various heating and cooling loads to evaluate. The student will log and analyze real data from this energy system. A further development of the study is to model building and energy system with an appropriate modeling tool (IDA-ICE, MATLAB) to optimize the system performance.
The goal of the thesis is to estimate, document, and suggestion operation optimization for the advanced heating and cooling system with thermal storing.

**The following tasks are to be considered:**

1. Literature study on advanced heating and cooling system with thermal storing. Literature study has to include life-time commissioning and optimization of the building energy performance.
2. Collect documentation about the heating and cooling plant at the college building in Norway. Organize and understand the plant operation.
3. Collect measurement data on energy use, temperature, and other relevant energy performance data that can be logged via energy monitoring system. Analyse measurement data and define profiles and parameters that may be useful for the study.
4. Develop a simple model of the advanced heating and cooling system with thermal storing in MATLAB.
5. Calibrate the model based on the measurement data.
6. Perform sensitivity study of the results.
7. Optimize operation of the plant with the objectives: low energy use and relibility.
8. Present the results.

-- " --

The project work comprises 15 ECTS credits.

The work shall be edited as a scientific report, including a table of contents, a summary in Norwegian, conclusion, an index of literature etc. When writing the report, the candidate must emphasise a clearly arranged and well-written text. To facilitate the reading of the report, it is important that references for corresponding text, tables and figures are clearly stated both places. By the evaluation of the work the following will be greatly emphasised: The results should be thoroughly treated, presented in clearly arranged tables and/or graphics and discussed in detail.

The candidate is responsible for keeping contact with the subject teacher and teaching supervisors.

Risk assessment of the candidate's work shall be carried out according to the department's procedures. The risk assessment must be documented and included as part of the final report. Events related to the candidate's work adversely affecting the health, safety or security, must be documented and included as part of the final report. If the documentation on risk assessment represents a large number of pages, the full version is to be submitted electronically to the supervisor and an excerpt is included in the report.

According to "Utfyllende regler til studieforskriften for teknologistudiet/sivilingeniørstudiet ved NTNU" § 20, the Department of Energy and Process Engineering reserves all rights to use the results and data for lectures, research and future publications.

The report shall be submitted to the department via Its Learning.

Submission deadline: *December 21st, 2016.*

☐ Work to be done in lab (Water power lab, Fluids engineering lab, Thermal engineering lab)
☐ Field work

Department for Energy and Process Engineering, *August 22nd, 2016.*

Natasa Nord

Natasa Nord
Supervisor

Co-Supervisor(s): Hanne Kauko, hanne.kauko@sintef.no

**Abstract**

Within this project assignment the advanced heating and cooling system (AHACS) with thermal storing at Bergen University College (HiB) analysed. This AHACS is equipped with the following elements:

- A heat pumps/chiller system (HP system) consisting of three parallel connected HP's. The HP cycle runs on ammonia (R717). The maximal cooling capacity in cooling mode (CM) equals 1.400 $kW$. In heating mode (HM) the the maximal heating capacity is 1.600 $kW$. The total installed power of the compressors is $300kW$. In CM the outgoing condenser and evaporator temperature correspond $23°C$ and $5°C$. In HM the outgoing condenser and evaporator temperature correspond $50°C$ and $5°C$.
- A thermal energy storage (TES) consisting of 81 boreholes divided into 9 groups. Each well is about 220 $m$ deep and located 7 $m$ apart from each other. The total heat sink capacity is about 1.660 $kW$ and the cooling capacity is about 1.400 $kW$. In total the borehole system has a volume of 250 $m^3$. The temperature of the ground is $8 - 9°C$.
- Four phase change material (PCM) cold storage tanks with a volume of in total 228 $m^3$. This yields a capacity of 11.240 $kWh$ and a cooling supply of 1.600 $kW$ for 7 hours.. The PCM storage contains in total 47.000 encapsulated salt-hydrate PCM elements (freezing point 10°C). The PCM storage covers the peak cooling load on daily basis. During night the PCM storage is charged, while it it discharged during the day.
- A connection to the district heating (DH that covers the peak heating load.Heat is delivered for space heating at a temperature of 70°C and returns at approximately 35°C according to the design setpoint temperatures.
- 14 adiabatic cooling aggregates. This regards an evaporative ventilation air cooling system, which reduces the temperature of exhaust air by means of humidification. This adiabatic cooling effectively reduces the cooling power demand by around 40%.

Data is extracted from 15 energy measurements within the energy system, over a period from $1^{st}$ of November 2015 until $31^{st}$ of October 2016. All energy measurements are given in kWh per day over the given period and therefore the analysis gives a rough indication of the system performance during the given period. Within the period around 11 December until 1 February there is occurring an error in the measurement data, stating an average heating and cooling value to fill up the lack of data. The following was concluded from the data:

- The annual heating demand is 2.460 $MWh$ and the annual cooling demand is 1.010 $MWh$ given over the analysed period. The annual specific cooling demand is 21.3 $kWh/m^2.year$ and the annual specific heating demand is 52 $kWh/m^2.year$. This is in line with the designed values respectively $1.06GWh$ and $2.6GWh$ for annual demands and 22.4 $kWh/m^2.year$ and 54.9 $kWh/m^2.year$ for specific annual demands.
- The PCM cold storage is annually 94 $MWh$ charged, while it is $100MWh$ discharged. This means there is an imbalance of approximately 5.6%.
- Since 1171 $MWh$ heat is yearly extracted from the borehole system, while only 304 $MWh$ is rejected, the borehole system is in great imbalanced. This might lead to a soil temperature drop, and subsequently an efficiency drop.
- The energy input and output of the HP system shows a strong lineair relation. Meaning that the HP system is operation correctly. The yearly averaged coefficient of performance (COP) for heating is 4.7.

- The yearly averaged COP for cooling is 4.0. Seemingly the temperature levels at both evaporator and condenser side seem to be exceeding the designed values. Along with that the HP system has potential for a better COP.

The conclusion regarding potential optimization possibilities for the AHACS at HiB is that the balance of the borehole system should be further analysed and improved. Along with that the evaporator and condenser supply temperature should be decreased in order to improve the COP of the HP system. Two options are given to combine these optimization suggestions:

- In combination with trying to restore the balance in the borehole system, it would be interesting to see whether the more heat can be extracted from the space heating return temperature in order to realize a lower condenser supply temperature.
- Decrease the heat extracted from the borehole system in order to keep the evaporator supply temperature down. This might help balancing the heat extraction and rejection from the boreholes.

# Contents

# 1 Introduction

The Norwegian government has set strict targets concerning climate and energy policy. Last 15-4-2016 the government presented a white paper on Norwegian energy policy: Power for Change [1]. Key point in this paper is to secure an efficient and a climate friendly energy supply by considering the security of supply, effect on the climate, and the economic growth together. Besides, it is necessary to reduce greenhouse gas emissions, increase the use of renewable energy and reduce energy use.

Around 40% of the Norwegian energy use is accounted by the built environment. Along with that, the energy efficiency and energy integration shows a great potential for improvement [2]. SINTEF is researching this potential in their reseach project INTERACT. This project aims on optimal design, integration and management solutions of complex thermal energy systems within buildings. One example within this project is the energy analysis of the campus at the Bergen University College (HiB) in Norway. HiB has an advanced energy supply system which exploits phase change material (PCM) as a cold storage and energy wells for seasonal thermal energy storage (TES). This project assignment will delve further into the analysis of this specific supply system at HiB.

## 1.1 Problem description

The supply system of the college buildings is rather complicated due to the combination of the following components: heat pumps/chiller system (HP system), thermal energy storage (TES), phase change material (PCM) cold storage, district heating (DH), and adiabatic cooling. In order to document the system performance, several direct energy measurements are performed at the HPs, TES, PCM cold storage, and DH. Due to the complexity of the system, it is unknown weather the system is truly performing as intended. Therefor, it is questionable up to what extend the performed measurements are reliable. Use of indirect or even fused measurements may lead to better results[3, 4].

## 1.2 Research objective

The aim of this project assignment is to perform an energy analysis of the energy system at HiB. The goal of the thesis is to estimate, document, and suggest operation optimization for the advanced heating and cooling system (AHACS).

## 1.3 Research questions

The introduced problem is translated into the following research question:

*What potential optimization possibilities do exist for the advanced heating and cooling system that is used at HiB?*

The main research question is answered by researching the following sub-questions:

1. How is the energy use profile of the heating and cooling system?
2. Does the heating and cooling system perform as intended?

## 1.4 Structure

Before the main research question can be answered, the system operation should be fully understood. In order to do so, energy flows and temperature levels, logged in different parts of the system, are analyzed at various heating and cooling loads. A further development of the study is to model the energy system in MATLAB R2015a and to analyze the system performance.

**The project is addressed by performing the following steps:**

1. The literature study on advanced heating and cooling systems with TES is summarized in Chapter 2. The literature study includes also optimization of the building energy performance.
2. Specific information on the advanced heating and cooling system is given in Chapter 3
3. The method on how to investigate data regarding the the advanced heating and cooling system is given in Chapter 4. This chapter also explains how the HPs are analysed into further detail.
4. Measurement data on energy use and the outdoor temperature were analysed. The result of which are presented in Chapter 5.1. This section shows some useful energy profiles and parameters for this study.
5. The results of the model regarding the HPs in the advanced heating and cooling system is provided in Section 5.2. Within this model the sensitivity of the performed assumptions are tested in Section 5.2.2. In addition the HP performance is during a specific time of the year is calibrated to the HP design specifications.
6. The conclusion and discussion on the performed research and assembled recommendations for further research, are given in Chapter 6 and 7 with the objectives to keep energy usage low and to ensure the reliability of the system.

## 1.5 Limitations

During this project assignment several difficulties were faced. The data were provided quite late in the project. This induced slow research progression in the first two months. However, after all required data were available the research got accelerated quite fast. The delayed data analysis was affected by this rough start. Therefore, the research was not able to dig deeper in more than one of the system elements. The element analysed are the HPs. The provided data give only daily averages over the entire year. This means that daily fluctuation will not be able to analyze during the research.

# 2 Advanced heating and cooling system

Chapter 2 summarizes the literature study upon AHACS with thermal energy storing. First the design process of AHACS is described in Section 2.1. Whereafter three existing AHACS with thermal storing are shortly analysed and compared in Section 2.2. Subsequently, the basics of several different advanced energy system components are analysed. In relation to this research, it is important that the functioning of the HPs and the PCM cold storage is understood, following Section 2.3.2 and 2.3.3. Additionally, the basic functioning of the borehole system as TES, DH, and adiabatic space cooling will be clarified in Section 2.3.4, 2.3.5 and 2.3.6. Lastly, the the energy system monitoring considerations are discussed in Section 2.3.7.

## 2.1 Guiding steps for the energy system design

Energy system are designed in such a way that the energy demand of a building is covered. Many industrial and non-residential buildings show a high energy demand. At the same time these buildings often produce a lot of excess heat due to their processes or equipment [5], e.g. computer facilities at universities, refrigeration systems at supermarkets, or technical equipment at hospitals. Utilizing instead of wasting this excess heat would reduce the energy use. Inevitably the design strategy for energy systems is heading into a more sustainable direction. This leads to optimized energy systems, resulting into higher energy efficiency and reduced installed power.

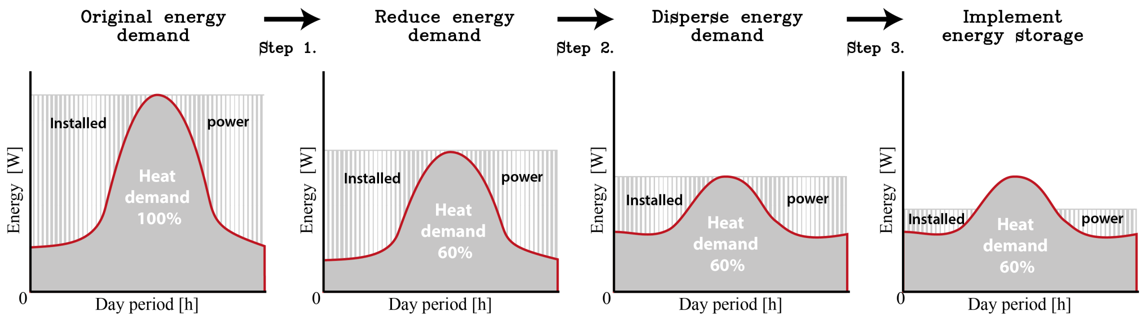


Figure 2.1: Energy system optimization steps

Figure 2.1 shows an schematic overview on three design steps related to the design of an advanced and sustainable the energy system with energy storage. The energy demand in buildings is continuously fluctuating. Mainly this fluctuation is related to the user profile and the outdoor climate. Building energy systems have often such high installed power to cover the peak demand, that it is redundant most of the time. Therefore, the first step is to reduce the energy demand in general and lower the peak demand. This is realised by a more efficient energy system, a reduction of the energy losses, reuse (waste) energy and optimizing the user profile in the best possible way. Though, the human behaviour is hard to control. People tend to forget about saving energy and frequently priority is given over occupants' comfort, well-being, and satisfaction within a building energy design [6]. Intelligent buildings create the opportunity to ensure the quality of the living environment with a sustainable approach. E.g. Altomonte et al. shows how knowledge on former research, human behavior, environmental impact, and climate scenario's are to translated into integrated creative and technical skills during the building energy design [6]. An intelligent building design helps optimizing the users' profile in the built environment. Secondly, it is rather important to disperse the energy demand over time in a way that the energy system might run on a less fluctuating power level with a lower peak demand. Lastly, the energy system can be designed in such a way that energy is stored during a low energy demand period. Later on, the stored energy can be released in order to meet up the peak demand. This results in a lower maximum installed power of the energy system.

## 2.2 Advanced heating and cooling system with thermal energy storing

More often AHACS with thermal storing are realised independent from the building sector. Per building sector a specific energy use can be expected, Figure 2.2 gives an overview of the average annual specific use for non-residential buildings. In principle this specific energy use is depending on the operation time, location, amount of technical equipment, and energy efficiency goal. Consequently hospitals and nursing homes show rather high specific energy use, while schools show rather low specific energy use [7]. Note that the specific energy use is not necessarily lower for newer buildings compared to the older ones. This is caused by the increase of technical equipment and longer operation time in many building types, even though the building (energy) regulations have become stricter. For example the requirements concerning the indoor air quality have become higher, leading to higher energy consumption [7]. Next, three different AHACS with thermal energy storing are shortly introduced and compare with each other. Each energy system is applied in a different building sector: office, commercial, and school buildings.

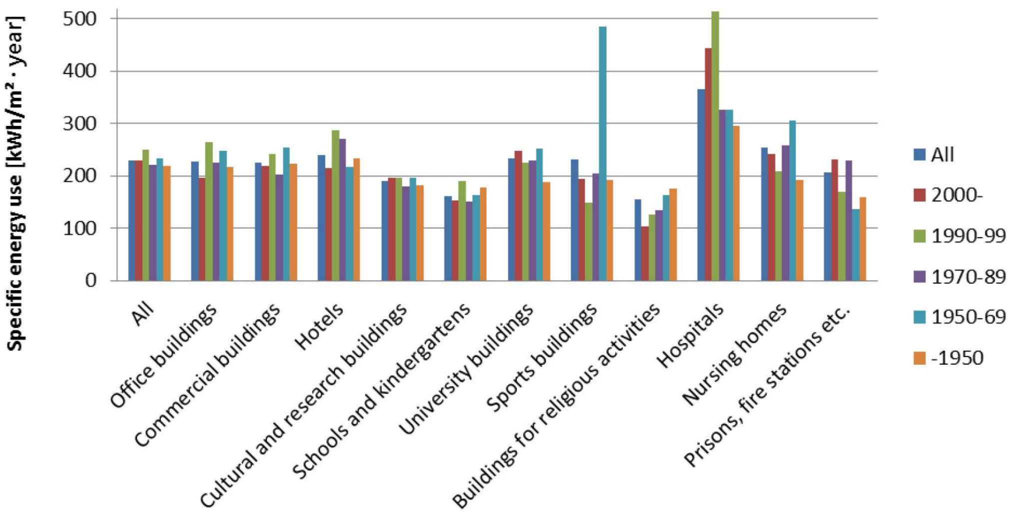


Figure 2.2: Average annual specific energy use according to the building category and building year in Norway in 2011 [7]

### 2.2.1 Powerhouse Kjørbo

April 2014 the renovated powerhouse Kjørbo opened its doors in Sandvika, Norway. The two connected, refurbished office buildings cover around 5.180$m^2$. The powerhouse is designed with the ambition of being a net zero emission building (ZEB), within the calculation the $CO_2$ emissions from construction, materials, operation, and demolition are taken into account. Figure 2.3 depicts the PID-chart of the energy system at the powerhouse. The heating and cooling demand of the building is covered by combined heat pump/chiller (HP) system, space heating heat pump (SH-HP) is entangled by a purple box, and bedrock borehole (BB) system, entangled by an orange box. The red entangled box consists the the space heating distribution loop, including district heating (DH). Whereas the blue entangled box describes the cold water distribution circuit towards ventilation, water, and computer cooling. The domestic hot water is generated with a separate domestic hot water heat pump DHW-HP, which is entangled by the green box.

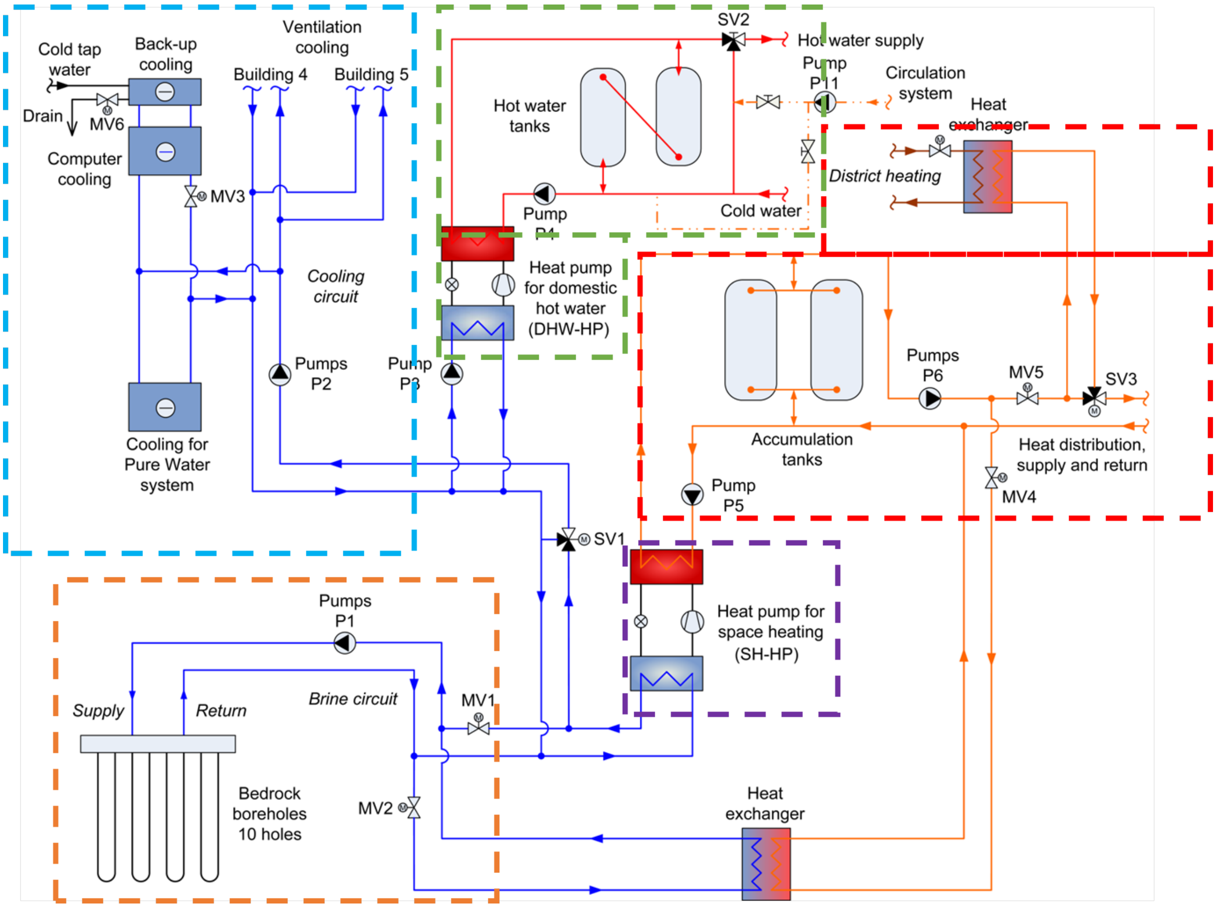


Figure 2.3: PID-chart of the energy system at powerhouse Kjørbo [8]

The SH-HP is designed to cover the entire heating demand of the building, however the DH is connected as back-up system. Besides the SH-HP provides cold for ventilative cooling. Within the space heating distribution loop two accumulation tanks of both 900 litres are parallel connected in between the SH-HP and the building heat supply. In case the SH-HP produces a surplus of heat, it is rejected into the BB [9].

In total ten BBs of approximately $225m$ depth are connected via a brine circuit with an ethanol-water mixture. The BBs are spaced respectively 10 and $15m$. apart from each other. This same brine circuit is part of the cooling system and therefore the BB is connected in series after SH-HP. This enables the option to utilize free cooling for process and ventilative cooling. Within the cold distribution loop ventilative cooling is supplied to both building, as well as cold for cooling computers and for the pure water system. In case the SH-HP is failing, the computers will be cooled with a back-up cooling, which is connected to the cold tap water [9].

The DHW-HP is connected in series to the returning pipeline of the cold distribution loop. Meaning that heat extracted from the building by the brine is used at the evaporator side of the DHW-HP to increase the evaporation temperature. Within the hot water distribution loop two in series coupled hot water tanks of each 600 liters are coupled in series to the hot water supply [9].

### 2.2.2 REMA 1000 Kroppanmarka

REMA 1000 is a supermarket chain, which opened one of the most energy efficient grocery stores in Northern Europe in August 2013. Namely REMA 1000 Kroppanmarka approximately uses 30% less energy compared to similar stores with conventional installations [5]. The annual specific energy use of Kropppanmarka is approximately $330kWh/m^2$, which is around 30% less than for similar supermarkets in Trondheim during summer and spring time, given by Stavset and Kauko. The energy system at Kroppanmarka supermarket is displayed in Figure 2.4. The system basically consists of five parts. The R744 refrigeration plant (REF) cycle is represented by the green lines, the heat storage (HS) distribution loop by the red lines, the floor heating (FH) distribution loop by the blue lines, and the energy well (EW) distribution loop by the black lines. The air handeling unit (AHU) is depicted in the upper right corner in the aqua blue colored box.

As can be seen in the REF cycle, the evaporation process is taking place at two different temperature levels via two stage compression and expansion. The heat from the REF is exchanged via the three gas coolers (plate heat exchangers) at different temperatures. The highest temperature is rejected to the HS loop via the first gas cooler. This high-temperature loop uses heat primarily to heat ventilation air in the AHU. Additionally heat is supplied to an air curtain (entrance) or the villa vent (common room) units. In times of low heat demand, the heat can be stored in the three hot water storage tanks. In total the tanks have a capacity of 2.700 litres. The tanks are able to exchange heat to the FH loop. In case the tanks are fully charged in combination with a relatively low heat demand, heat can be discharged through a dry cooler to the environment. In order to provide heating during major failure in the REF, the backup

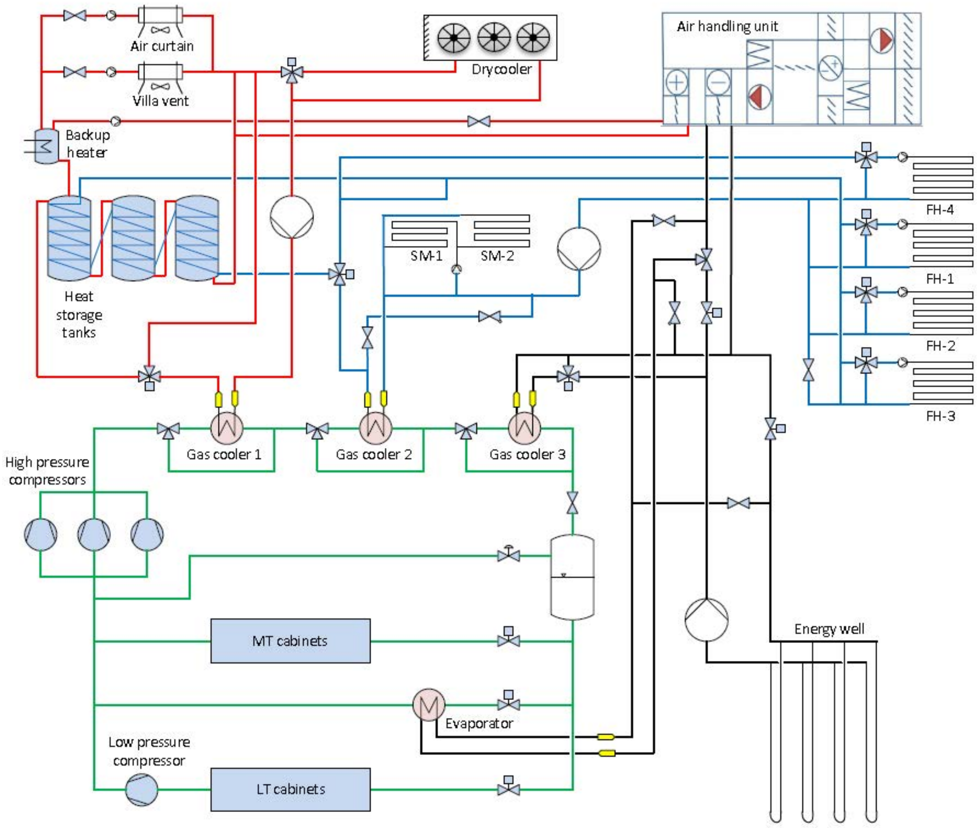


Figure 2.4: PID-chart of the integrated energy system at Kroppanmarka [5]

heater is activated [5].
The second gas cooler exchanges heat with the FH loop, at the medium temperature level. FH is delivered via four different groups, whereof three are supplied to sales area and one to the cooling chambers (keep ground frost free). In addition two snow melting circuits are connected to the FH loop, in order to keep entrance and service ramp snow and ice free [5].

The third gas cooler exchanges heat with the EW loop. The loop includes 4 vertical energy wills of approximately 170$m$ depth and about 8$m$ spaced from each other. The EW function as seasonal storage. Whereas during summer the EW provide free cooling and during winter provide extra heat. Additionally the EW loop is connected to provide cooling of ventilation air in the AHU during winter. Furthermore the EW loop is connected to the evaporator at the medium temperature level of the REF. This connection can be utilized as an additional cooling load given low internal cooling demands from the cabinets and high heating demand in de building [5].

The AHU utilizes thermal comfort and an acceptable indoor air quality. The operation mode of the AHU is based on five parameters: ambient temperature, shop temperature, $CO_2$ concentration, relative humidity, and heat available in the heat storage tanks. This way the supply of outdoor air is reduced without affecting the indoor air quality. When required, the outdoor supplied air can be preheated by the heat recovery wheel, resulting in a reduced heat demand [5].

### 2.2.3 Bergen University College

In 2014 the renovation of the campus of the Bergen University College (HiB) was completed. In August 2014 a new college building was opened, with a size of in total $50.983m^2$, including parking area of $3.650m^2$. The system is designed to supply $2.600MWh$ heating and $1.060MWh$ cooling on yearly basis. The peak load of the system is $2.830kW$ for heating load and $3.000kW$ for cooling load [10, 11]. The cooling capacity is relatively high, which attributed to the high amount of excess heat during summer related to the sun radiation and internal loads [5]. The main idea of the energy system design was to avoid energy disposal. As depicted in Figure 2.5, the energy system basically consists of five parts. The combined HP/chiller system is entangled with the purple box, the thermal energy storage (TES) with the orange box, the phase change material (PCM) cold storage with the blue box, DH with the red box, and the adiabatic cooling system with the green box.

In general the heat demand is covered by the HP system and the DH (only peak load). The HPs harvest heat from the TES (heat supply) and partial also from the space cooling. The heat generated at the condenser side of the HP system is supplied to the building space heating circuit, where DH only delivers the peak heat demand which the HP system is not able to produce. The heat pumps can run in both heating and cooling mode, depending on the cooling demand. When the cooling demand is increasing, the heat pumps will start to run in cooling mode[11].

While the HPs are running in cooling mode and the heating demand is low, there will be a surplus of energy generated at the condensor side of the HP system. In this case the heat is stored in the TES system. The TES system applied exists of 81 boreholes of approximately $220m$ depth, and $7m$ apart from each other. Occasionally, when there is no heat rejected into the boreholes, the temperatures in the boreholes can be low enough to cool down the return temperature at the evaporator side. In that case the borehole system will provide free cooling to the chilled water distribution loop instead of providing heat to the evaporators of the HPs[11].

The PCM-storage is applied within the chilled water distribution loop, providing space cooling. The PCM-storage contains in total 47000 encapsulated salt-hydrate PCM elements. These elements are stacked within four cylindrical tanks. The total capacity of the tanks is about $228m^3$. The connections are designed for different cooling demand modes. For example the PCM-storage can be connected inline to the building space cooling return in discharging mode. In case there is no cooling demand, the building space cooling is bypassed in charging mode[12]. In addition the adiabatic space cooling system are installed to pre-cool the ventilative air. This adiabatic cooling effectively reduces the cooling power demand by around 40% compared to the original cooling demand before it was implemented.[10]

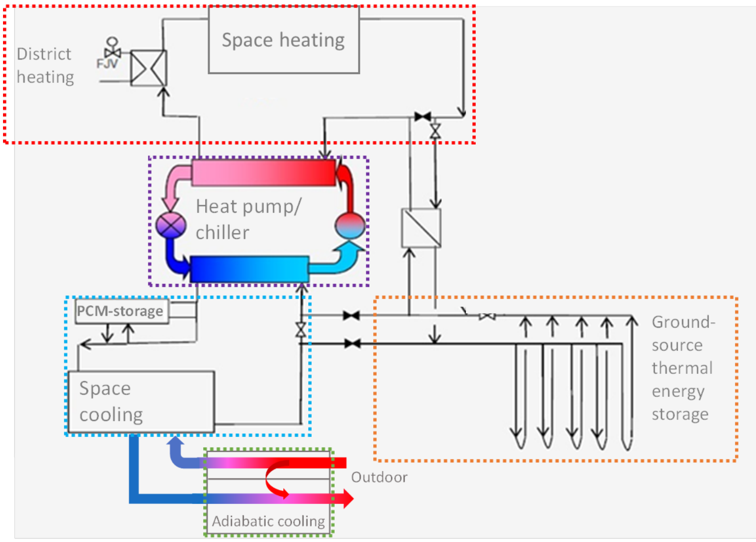


Figure 2.5: PID-chart of the energy system at HiB [10]

### 2.2.4 AHACS comparison

All three previously discussed AHACS are compared. In Table 1 the most important specifics on each energy system are summarized. The one element all three systems have in common is the HP. In all three cases both heating and cooling are extracted for respectively the condenser and evaporator side of the HP system. In each integrated energy supply system the HP is the key element. However, all three applications are integrated into the energy supply system each in their own unique way. Where REMA 1000 Kroppanmarka makes use of two different evaporation levels in one cycle, the powerhouse Kjørbo just adds an extra heat pump for how tap water supply only. Each case is designed for their specific needs. REMA 1000 Kroppanmarka has a extremely high cooling load due to numerous fridges and refrigerators applied in the supermarket. While HiB and powerhouse Kjørbo have high base cooling load due extensive computer use and data rooms. During summer the cooling load is peaking due to solar radiation and high internal loads caused by people and applications. While providing cooling to the building, the system will produce excess heat, which is ideally utilized during winter. In all three system this is translated into the application of ground TES for seasonal storing. Besides the seasonal storage all three system show periodic TES tanks to capture hourly and daily fluctuation in the thermal energy demand. This way the peaking energy demand can be covered without having to installing the maximum required capacity.

Table 1: AHACS comparison between 3 cases

| | Powerhouse Kjørbo | REMA 1000 Kroppanmarka | Bergen University College |
|---|---|---|---|
| Total heated area in $m^2$ | 5.180 | - | 47.333 |
| Building type | Office building | Commercial building | Educational building |
| Annual specific heating demand | 21.2 kWh/$m^2$.year | - | 54.9 kWh/$m^2$.year |
| Annual specific cooling demand | 20.3 kWh/$m^2$.year | - | 22.4 kWh/$m^2$.year |
| Annual specific energy demand | - | 330 kWh/$m^2$.year | - |
| District Heating | Back-up | No connection | Peak load |
| Seasonal TES | 10 bedrock boreholes depth +/-225 m. | 4 vertical energy wells depth +/- 170 m. | 81 boreholes depth +/- 220 m. |
| Periodic TES | spaced +/- 10 and 15 m. 2 accumulation tanks of 900 liters each 2 hot water tanks of 600 liters each | spaced +/- 8 m. 3 hot water tanks of 900 liters each | spaced +/- 8 m. 4 PCM storage tanks of in total 228$m^3$ |
| Cooling | Cooling brine cycle | Air handling unit | Adiabatic space cooling |
| Heat pump | 1 Combined heat pump chiller 1 Domestic hot water heat pump | 1 refrigeration plant with low and medium temperature level evaporation | 3 Combined heat pump chillers |
| Cold COP | - | 2.7-3.3 | - |
| Heat COP | DHW : 3.5 | - | 4.2 |

## 2.3 Core elements of AHACS installed at HiB

### 2.3.1 Counterflow heat exchanger

The energy system at HiB makes use of the counterflow heat exchanger at several different points in the system. The theory on all varying types of heat exchangers is kept the same. In general heat is exchanged via conduction or convection. In order to improve the heat exchange efficiency, the counterflow heat exchanger is used. This implies that the fluid at the primary side passes the fluid at the secondary side in a counter acting way. Meaning that the incoming hot air at the primary inlet first exchanges heat with the fluid at the outlet of the secondary side. The fluid at the secondary outlet is than already preheated by the primary outgoing fluid at the secondary inlet side. This enables the resulting outgoing fluid temperature at the secondary side to transcend the outgoing fluid temperature at the primary side, see Figure 2.6.

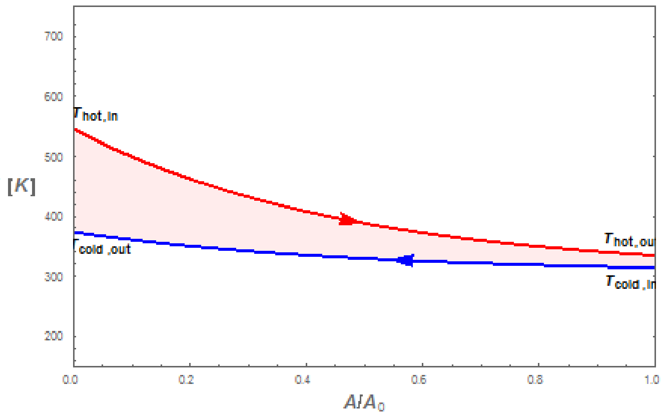


Figure 2.6: Operation of counter flow heat exchanger with equal heat capacity rates [13]

### 2.3.2 Heat pump/chiller system

In general a heat pump (HP) is able to supply both heat and cold, depending on purpose of use. A heat pump uses electricity and to extract heat from a low temperature source and deliver heat at a higher temperature level. A HP basically operates following the Carnot process, this means that the heat absorbed an rejected stays on a constant temperature, see state change 1-2 and 3-4 in Figure 2.7. This is roughly accomplished via isobaric evaporation and condensation, see state change 1-2 and 3-4 in the same figure. However, the ideal case is not fully met since it is hard to realize an adiabatic expansion and compression and therefore rather expensive. Due to internal friction and other irreversibilities, the 'real' operating cycle of the HP will operate more likely in a cycle 1-2'-3'-4, as shown in Figure 2.7 [14].

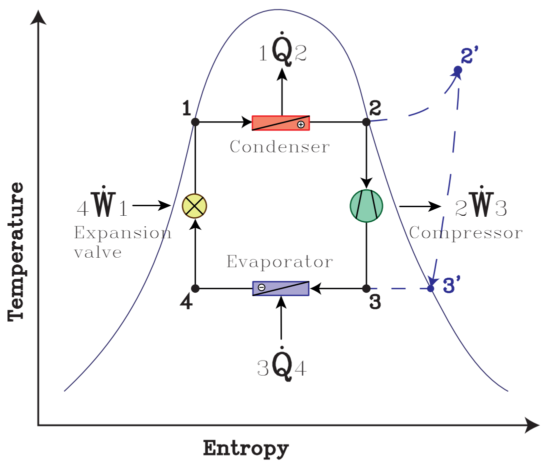


Figure 2.7: T-s diagram of the theoretical and 'real' Carnot cycle of a HP

The choice of the circulating refrigerant depends highly on the required design characteristics of the cycle. The thermophysical properties of the refrigerant have a considerable effect on thermodynamic losses related to heat transfer, flow resistance and compressor losses [15]. Therefore, a low molar mass and suitably high pressure at working conditions is favorable. In the past a several working media have been discarded as unsuitable for various reasons. A good example is the banishment of the halocarbon (HFC) refrigerants, due to the degrading effect on the ozone layer [15] caused by HFC leakage. Subsequently, natural refrigerants where put to use like, for instance, air, water, nitrogen, ammonia, hydrogen, and hydrocarbons. Depending on the operation temperatures a suitable refrigerant needs to be picked. Just like the refrigerant in the HPs at HiB, ammonia is an often picked refrigerant. Rather important advantages of ammonia are good thermodynamic and transport properties, low sensitivity to small amounts of water int the system, simple leak detection, 'unlimited' availability, and low pricing [15].

A heat pump is designed with a certain coefficient of performance (COP). The COP is given by the ratio of heating or cooling supplied to respectively the evaporator or condenser, to the electricity delivered to the compressor [14], given Equation 1. Higher COPs equate to lower operating costs [16]. A perfectly suitable example to increase the COP is to re-use the waste heat, generated at the condenser side, in case the HP is operating in cooling mode. Instead of wasting this heat, it might be stored underground in order to put it to use on a different moment of time [16]. This theorie is also put to use in the heating and cooling system at HiB.

$$COP_h = \frac{Q_h}{P_{el}} \quad \text{and} \quad COP_c = \frac{Q_c}{P_{el}} \tag{1}$$

With:

| | | |
|---|---|---|
| $COP =$ | Coefficient of performance | [-] |
| $Q =$ | Heat supply | $[kWh]$ |
| $P_{el} =$ | Electricity supply | $[kWh]$ |

The carnot efficiency is the theoretical maximum COP of a HP. This is defined as the ratio of heating or cooling supplied to the work required, given Equation 2. This equation is expressed in the designed temperature levels of both the evaporator (low temperature) and the condenser (high temperature) [14].

$$\epsilon_h = \frac{Q_h}{W} = \frac{T_H}{T_H - T_L} \quad \text{and} \quad \epsilon_c = \frac{Q_c}{W} = \frac{T_L}{T_H - T_L} \tag{2}$$

With:

| | | |
|---|---|---|
| $\epsilon =$ | Carnot efficiency | [-] |
| $Q =$ | Heat supply | $[kWh]$ |
| $W =$ | Electricity supply | $[kWh]$ |
| $T_L =$ | Low temperature | $[K]$ |
| $T_H =$ | High temperature | $[K]$ |

The thermal efficiency is represented by the ratio of the COP to the carnot efficiency. By combining equation 1 and 2, the thermal efficiency for HP's is defined as the ratio of the net useful work produced to the heat energy supplied [14].

$$\eta_h = \frac{COP}{\epsilon_h} \quad \text{and} \quad \eta_c = \frac{COP}{\epsilon_c} \tag{3}$$

With:

| | | |
|---|---|---|
| $\eta =$ | Thermal efficiency | [-] |
| $Q =$ | Heat supply | $[kWh]$ |
| $W =$ | Electricity supply | $[kWh]$ |

### 2.3.3 PCM cold storage

Cold storage helps to avoid heat disposal. PCM cold storage is a relatively new technology to do this. PCM's are defined by their freezing and melting points, which are above or below the water freezing temperature of 0°C. This makes the materials perfectly suitable for thermal management solutions via storing and releasing thermal energy during the melting and freezing process (phase change) [17]. Compared to water and ice cold storage, the PCM-storage provides nearly an ideal solution in terms of temperature and volume compared with ice and water [10]. Zhai et al. performed a rather interesting research upon PCM-storage for air conditioning systems [18]. Within the built environment PCM's are integrated within the the building envelope to increase the thermal storage density of buildings. PCM's might also be installed as a cold storage device at the chilled water side of the air-conditioning system. Usually the working fluid in this system regards water [18]. Figure 2.8 shows three possible running modes of the chilled water distribution loop. During off peak hours the cold storage will be charged. In this case the chillers generate cold and supply it to the PCM-storage (cycle 1). During a moderate cold demand, the stored cold is released and supplied to the building via the air-conditioning terminal (cycle 2). During peak hours the chiller will start to provide cold directly to the air conditioning terminal (cycle 3).

Ure et al. notes the application of PCM storage with a chilled water system [17]. Conform their work a PCM cold storage, with a melting temperature of +8 +10°C, a conventional water chiller can be utilised without the need for low temperature Glycol chillers. In Figure 2.9 the charging for air cooled chiller operation over a range of operating temperatures are given. This shows the benefits of applying PCM instead of water/ice low temperature chillers. The From Figure 2.9 can be concluded that low ambient temperatures coupled with higher evaporation temperatures offer a significant overall COP improvement, in the region of 17-36 % depending on the type of unit and location [17].

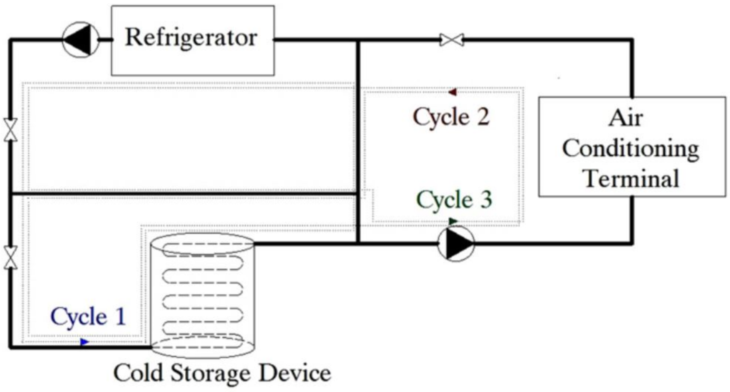


Figure 2.8: Diagram of PCM-storage air-conditioning system [18]

A proper designed PCM cold storage system will help spreading the cooling loads over a period of 24 hours. This means that the storage needs to be balanced carefully. Only then the initial investment and operational costs can be reduced. Depending on the scale of the system, a PCM cold storage might be applied as a diversification utility. The AHACS at HiB employs this utility. This means that the storage operates as a buffer to intercept peak loads, while the general system overall performs rather steady.

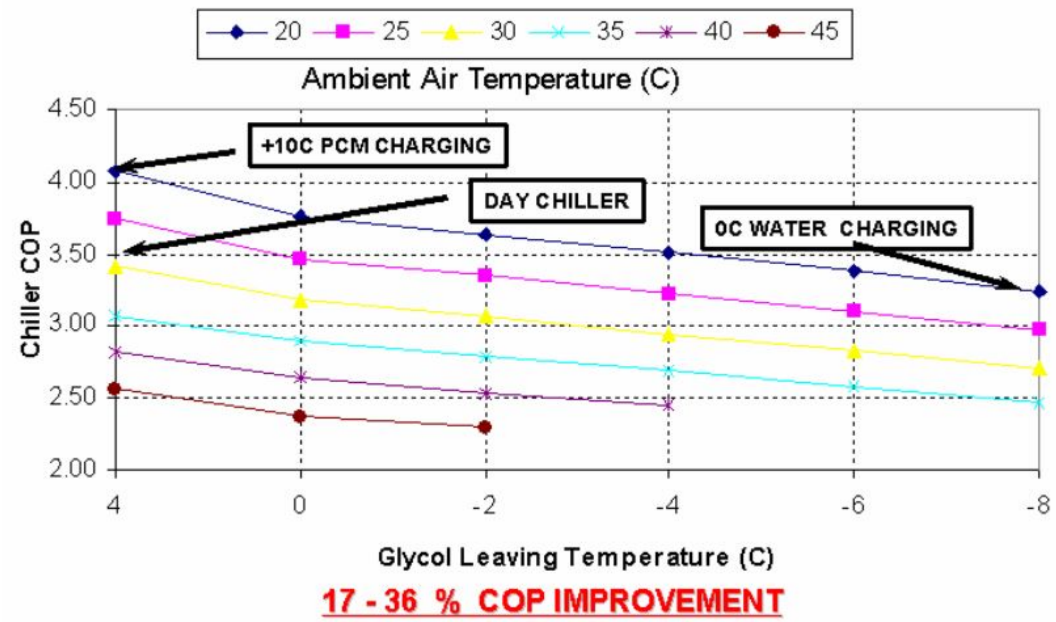


Figure 2.9: PCM Based Vs Conventional Ice TES charging comparison [17]

### 2.3.4 Borehole system

Underground energy storage is an important technology to cover the mismatch in demand and supply, related to fluctuating renewable energy sources [19]. Underground energy storage is a relative mature technology. This technology uses the stability of the ground temperature conditions. Usually this is designed as buried pipes horizontal along the length of a building or in a nearby field vertically into the ground. A borehole system, as it is applied at HiB, uses the verticale implementation. Basically the systems works as follows, in summer the generated surplus heat is stored in order to supply it during winter period. Vice verse cold is stored during the winter in order to be put to use during summer period. This seasonal storage helps balancing the thermal conditions in the system. In cold regions the implementation of underground cold storage is evolving. A ground source heat pump will enable us to reject or extract heat into the ground, ground water of surface water. A borehole system wields a ground coupled heat pump (GCHP) to circulate the fluid. This system is built on the assumption that at a sufficient depth, the ground temperature is always higher than the outdoor air temperature in winter and lower in summer [20].

A critical issue during system operation might be the risk of thermal imbalance in the GCHP. Especially in heating dominated building, this risk is rather high [20, 21]. The soil temperature gradually decreases, as the temperature recovery ability of soil after long-term heat extraction is limited. Over time the GCHP output will deteriorate until the GCHP is not functioning as desired. Based on earlier research [21, 22], a borehole system with free cooling is interesting for the HiB campus due to its relatively high cold demand. Free cooling helps to delay the process of soil temperature deterioration. Instead of extracting and rejecting heat from and to the soil alone, cold can be extracted as well. The efficiency of the free cooling will depend on the outdoor temperature and humidity as well as the indoor thermal and moisture conditions [22].

### 2.3.5 District heating

The principle of a DH is to distribute heat to many different buildings via the distribution grid, while heat is generated in a central energy plant. As a result, buildings served by a DH system do not need their own boilers or furnaces. DH provides valuable benefits regarding energy efficiency, fuel flexibility, enhanced environmental protection, easy/low maintenance, and reliability of the regarding energy system [23]. The AHACS at HiB is connected to the DH. However, the DH only covers the peak load of the heating demand at HiB. This way the HPs will only need to cover the base load of the heating demand and therefore less designed capacity is required.

### 2.3.6 Adiabatic space cooling

In buildings with relatively high cooling load, an adiabatic space cooling system could be a rather useful application, see Figure 2.10. The main principle of the system is that the exhaust air is pre-cooled by adding moisture to the air, this happens in the green entangled box in Figure 2.10. On top of the pre-cooling, the fresh outdoor air will be cooled a via rotary heat exchanger as shown in the green boxes in Figure 2.10. The indirect evaporative units cool fresh air by means of heat exchangers, isolated from the water. Riffat et al. describes it in a way that primary air is cooled by thin dry metal or plastic surfaces, of which the opposite sides are covered by water films that evaporate into a secondary air stream [24]. This way the fresh air will be pre-cooled by the returning hot space air via evaporative cooling before delivering it to the cold distribution loop. The cold distribution loop will now deliver the remaining cold which is required to fulfil the cooling demand [10]. By applying this passive technology of evaporative cooling, the cooling demand reduces substantially at the heat source. Therefore, the need for extensive ductwork, fans and their associated noise might be diminished [24]. The main drawback of the application it that fresh cold air supplied by the cold water distribution loop directly interacts with returning hot air from the building. This implies that the system is not applicable in buildings where fresh air regulations are strict. This is rather important for buildings like hospitals.

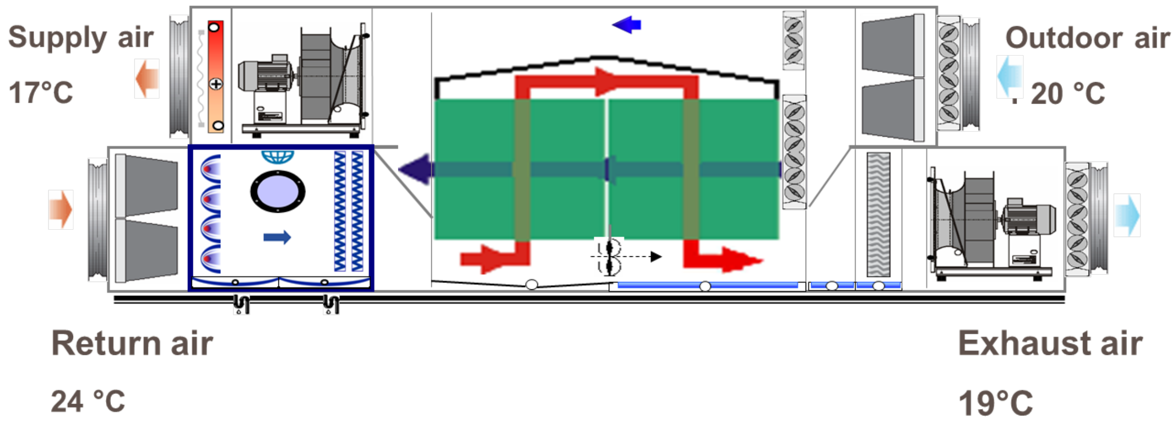


Figure 2.10: Principle of adiabatic cooling [10]

### 2.3.7 Monitoring and evaluation of the energy system

In previous performed research performed by Kauko et al. it is shown that there is often a significant deviation between the measured energy use and the calculated use. This research showed that the calculated energy use is lower than the measured energy use for newer buildings, and vice versa for old buildings. In addition an error of one third in the design of the installed heat rate was estimated due to this deviation. [7]

# 3 Thermal energy supply system description

This chapter describes the basic functioning of the energy system at HiB. First some detailed information the energy system at HiB will be provided. Section 3.1 will explain the design concept and functioning of the energy system at HiB. In Section 3.3 further detailed information on several system components is described. In this section, the relatively complex energy system is translated into a simplified version of the piping and instrumentation diagram. This is necessary in order to understand the operation of the AHACS. Later on in Section 3.4 this simplification helps describing the different possible operation modes of the energy system.

## 3.1 Heating and cooling demand at Bergen University College

In 2014 the campus of the Bergen University College was partially renovated. This resulted in a new energy demand. In addition, SWECO took care of the redesign of the energy system in order for HiB to become more energy efficient, which resulted in the AHACS as it is applied nowadays. As shortly mentioned in Section 2.2.3, the main idea of the energy system design was to avoid energy disposal. Therefore, 'disposed' energy is transferred and stored in order to put it into use in a different place and at a different time, see Figure 3.1. During night the surplus cold is stored in order to supply the the cold whenever de cooling demand is peaking during day. At first it seems odd that the peak cooling load can be higher than the heating peak load, since the total annual heating demand is much higher. A reasonable explanation is related to the fact that buildings are getting better insulated all the time. But most of all educational buildings in general just have a high number of internal loads, e.g. occupants and servers. Especially during summertime this results in an increased cooling peak load. This cooling load consists of solar radiation and high internal loads. While during wintertime, when the heating demand is of great importance, this cooling load lowers down the peak heating load [11].

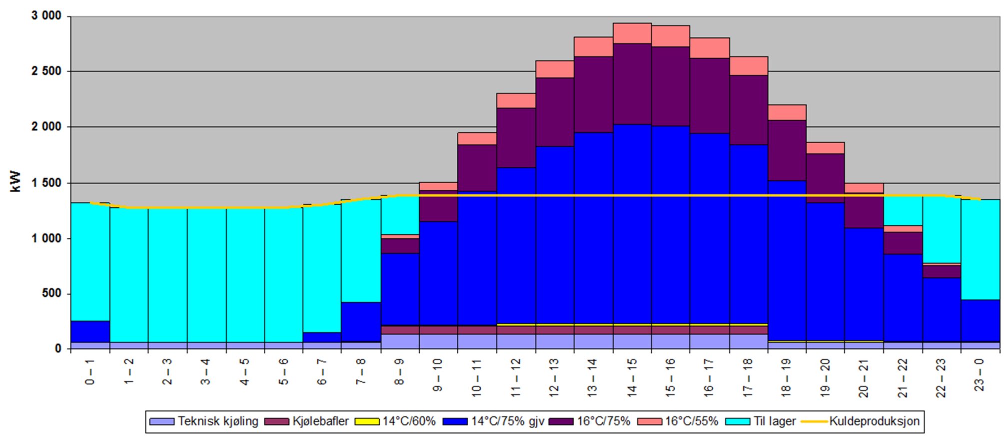


Figure 3.1: Cooling demand distribution over a design day [10]

## 3.2 Overall energy system design

In Section 2.2.3 the basic principal of the thermal energy system at HiB was already explained. This system matches the design steps as described in 2.1. Step 1 and 2 are covered by the renovation, which reduced and dispersed the energy demand at HiB. The HPs provide simultaneously heating and cooling, such that the cooling load of the building is used as a heat source at the evaporator side of the HPs. This assimilates the energy dispersion, and helps spread the load. Step 3 is realized with TES in the form of 81 boreholes and 4 PCM-cold storage tanks. Possible generated surplus energy is stored in borehole system for later use, while the PCM storage accommodates to the daily fluctuations in the cooling demand.

A simplified scheme of the analyzed energy system is given in Figure 3.2. Within this simplification, identical element which are connected parallel are combined into one element. Besides, the measurement devices, bypasses, and the open valves are left out in order make the scheme easy legible. The properties of the system are analysed based on a status report: "Evaluation of PCM-cold-storage at HiB" [11].

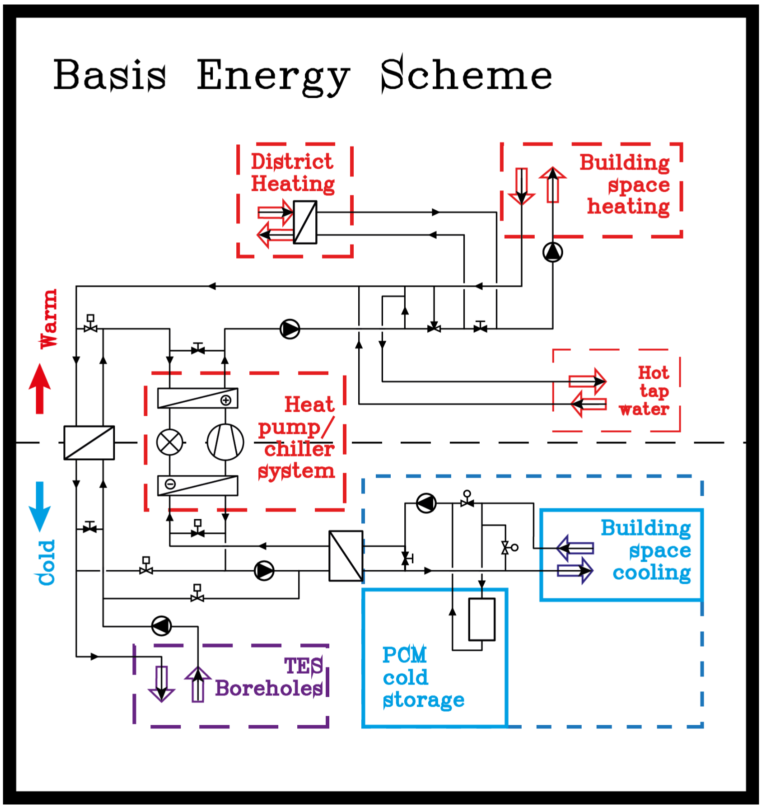


Figure 3.2: A simplified version of the energy scheme of the AHACS at HiB

The HP system covers the heat demand and the DH only provides the peak heating demand. The HP system harvests heat from the the chilled water distribution loop (heat sink for space cooling) and partially from the boreholes (heat supply). When the cooling demand is increasing, the HP system will start operating in cooling mode. In case there is a surplus of heat generated at the condensor side, the heat is stored in the borehole system (heat sink). However, it might appear that the temperatures in the boreholes is low enough to cool down the return temperature far enough in a way that the HP system is not been used. In that case the borehole system will provide free cooling to the chilled water distribution loop. The PCM storage is applied within the chilled water distribution loop. The connections are designed for variable cooling demand. E.g. the PCM-storage can be connected in series to the building returning space cooling at a peaking cooling demand in discharging mode. This way the PCM storage is pre-cooling the returning flow of the space cooling. In case there is no cooling demand, the building space cooling is bypassed to charge the PCM storage.

Figure 3.3 depicts the piping and instrumentation diagram (PID) of the AHACS at HiB. This diagram provides detailed information on the design properties of the entire system, e.g. piping dimensions, designed mass flows and temperatures, capacity rates, energy meters etc. The main part of the energy system are entangled with the red and blue frames namely: DH, building space heating, HPs, TES, building space cooling, and PCM-cold storage. Within the system, energy metering is performed in every part of the system. These energy meters are encircled in Figure 3.3. More extensive metering is performed at the HPs in order to analyse the HP performance into more detail.

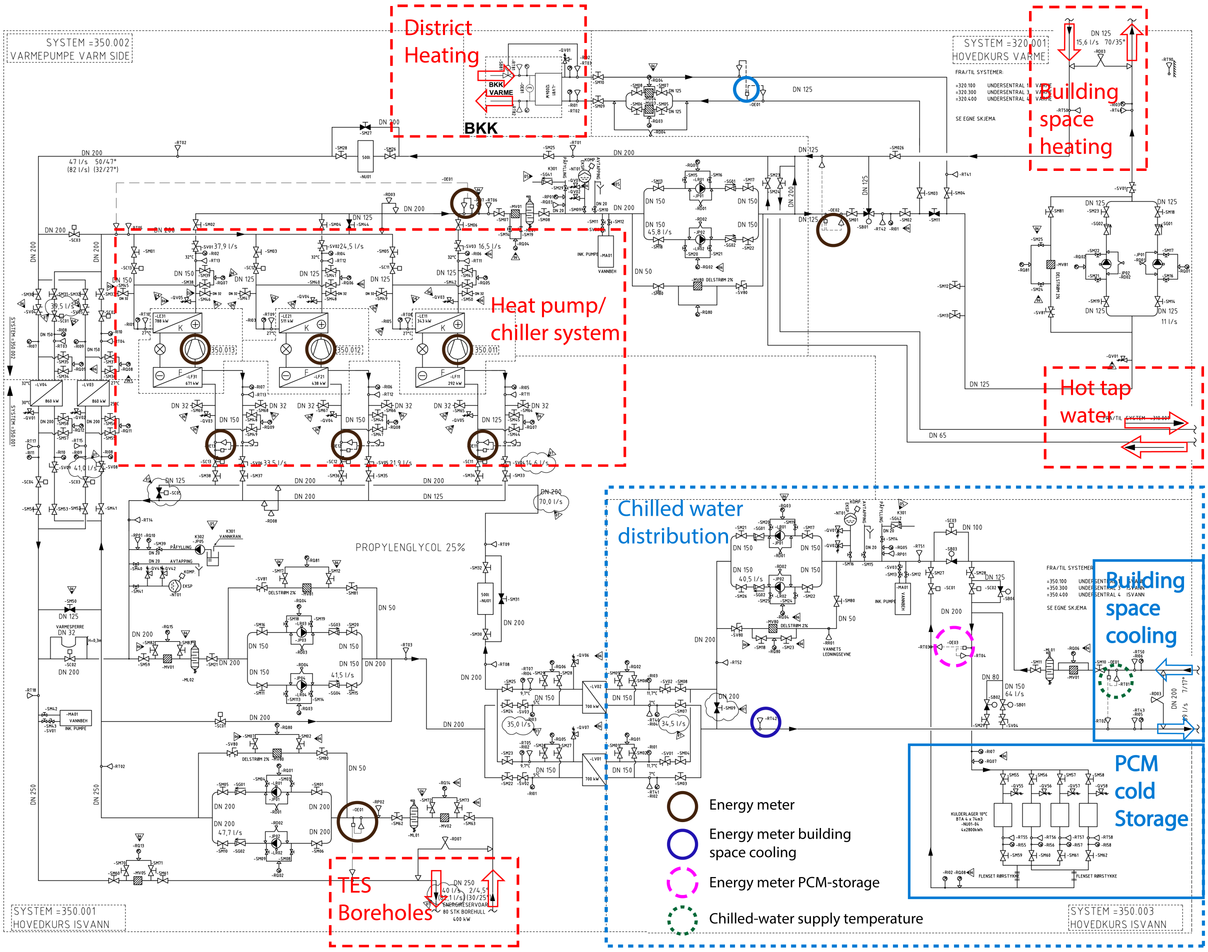


Figure 3.3: Detailed piping and instrumentation diagram of the AHACS at HiB

## 3.3 System description and simplification

The energy system at HiB is basically equipped with the following five elements:

**HP system:** In this specific heating and cooling system at HiB the energy cycle of the HP system is designed as a close loop with ammonia (R717) as the refrigerant. In total three HP's are connected in parallel. The maximal cooling capacity in cooling mode (CM) equals 1.400 $kW$. Whereof the individual cooling capacities for HP 1, 2, and 3 are respectively292 $kW$, 438 $kW$, and 671 $kW$). In heating mode (HM) the the maximal heating capacity is 1.600 $kW$. Whereof the individual heating capacities for HP 1, 2, and 3 are respectively 343 $kW$, 511 $kW$, and 788 $kW$. The total installed power of the compressors is 300$kW$ [10]. The operating temperatures are related to the specific mode the system is running in. The system can run in both HM or CM. In CM the outgoing condenser and evaporator temperature correspond $23°C$ and $5°C$. In HM the outgoing condenser and evaporator temperature correspond $50°C$ and $5°C$. Related to the specific energy demand, the installed variable speed drive (VSD) compressors are able to regulate the capacity down to about 45% of the individual maximal capacity source. This enables the system to run in part load operation [11].

**TES:** The TES system as connected to the AHACS at HiB, consists of 81 boreholes. Each well is about 220 $m$ deep and is distanced 7 $m$ from each other. Overall the boreholes are divided into 9 different groups with each their own supply and return pipelines and separate energy meters to measure the heat flow to and from each connection well. The boreholes serve as heat supply for the HP system in heating mode and function as a heat sink for the condenser in chilling mode if a surplus of heat occurs. The heat sink capacity reaches up to 1.660 $kW$ and whereas the cooling capacity is about 1.400 $kW$. In total the borehole system has a volume of 250 $m^3$. The temperature of the ground is 8-9°C [10].

**PCM cold storage:** The applied PCM based cold storage contains in total 47.000 encapsulated salt-hydrate PCM elements (freezing point 10°C). The FlatICE$^{TM}$ elements (500 x 250 x 32 mm) are stacked within cylindrical tanks. The water is ideally flowing through the tanks and is passing in between the PCM elements via the constructed passages with a large heat exchange surface. The four parallel connected tanks are places underground. The total volume of the tanks is about 228 $m^3$ (single tank volume of 57 $m^3$). This yields a storage capacity of 11.240 $kWh$ (single tank capacity of 2810 $kWh$) [12] and a cooling supply of 1.600 $kW$ for 7 hours. The PCM storage covers the peak cooling load on daily basis. During night the PCM storage is charged, while it it discharged during the day, see Figure 3.1. As it is integrated within the chilled-water distribution loop, the designed installed chiller cooling capacity was reduced with 53% [10].

**DH:** The connection to the district heating covers the peak heating load of the system [10]. The district heating is connected indirectly, meaning that the two systems have physically separated fluid flows. Heat is delivered for space heating at a temperature of 70°C and returns at approximately 35°C according to the design setpoint temperatures.

**Adiabatic cooling:** The evaporative ventilation air cooling system exists of 14 adiabatic cooling aggregates. By means of humidification the exhaust air is reduced in temperature. This enables the exhaust temperature to reach a lower temperature than the supply air. Eventually this needs to be the other way around. Therefore, the same heat exchangers that are being used in the heating period, to transfer heat form the exhaust to supply air, are used to cool down the supply air. This adiabatic cooling effectively reduces the cooling power demand by around 40%.

### 3.4 Energy system operation modes

SINTEF has performed two previous studies upon the AHACS at HiB regarding the cooling system [11] and its PCM storage performance [12]. Several different operation strategies are stated by SWECO, related to the cooling load [11]. Together with some more basic analysis on the AHACS [25], the operations modes are described below as Mode A-D. The division of the modes is based on the cooling load. Some components within the system may operate in two different ways within each mode. This is translated in a version 1 and 2 per mode. Table 2 gives a complete overview of all possible operation modes.

**MODE A-Low cooling demand:** The HP system operates in HM. The generated cold is sufficient to cover up the cooling demand at HiB. Depending on the heat demand and the borehole temperature, the borehole system may be used as heat supply for the HP's or as free-cooling for the chilled water distribution loop. Ideally the PCM storage is fully charged, otherwise the the storage can be charged in parallel to the cold supply.

**MODE B-Moderate cooling demand:** The HP system operates in CM. Generated heat is directly supplied to the college buildings. However, in case there is a surplus of heat generated at the condenser side of the HP's, the borehole system will be used as a heat sink. Ideally the PCM storage is fully charged. Otherwise, the storage can be charged during these conditions as long as the cooling demand in the college buildings will be covered.

**MODE C-High cooling demand:** The HP system operates in CM on full capacity. Along with this the PCM storage is discharged (cooling load$>$ 1400 $kW$ for more than 10 min). The temperature sensor RT51 is controlled with the mass flow through the PCM storage in order to prevent a too fast discharging of the PCM storage. Depending on the heat demand the surplus heat, generated at the condenser side, heat sinks in the borehole system.

**MODE D-PCM storage charging:** The HP system operates in CM. Both the heat and cooling demand are reasonably low(cooling load$<$ 1300 $kW$ for more than 15 min). The borehole system will be used as a heat sink for the heat surplus generated at the condenser side. It is common for the system to run in this mode during night time operation. The night time charging will also be addressed as maintenance charging, this way a fully charged storage can be guarantied.

Table 2: Operation modes, Heat = heat supply, Cool = free cooling, Sink = heat sink, Peak = supply peak heating

| | **Cooling demand** | | | **Heating demand** | | | **Component operation mode** | | | |
|---|---|---|---|---|---|---|---|---|---|---|
| Mode | Low | Moderate | Peak | Low | Moderate | Peak | HP | TES | PCM | DH |
| A1 | x | - | - | - | - | x | HM | Heat | Charge(d) | Peak |
| A2 | x | - | - | - | x | - | HM | Cool | Charge(d) | Peak |
| B | - | x | - | x | - | - | CM | Sink | Charge(d) | Peak |
| C | - | - | x | x | - | - | CM | Sink | Discharge | Peak |
| D | x | - | - | x | - | - | CM | Sink | Charge | Peak |

There was no direct information on the operation strategies related to the heating demand. Therefore it was necessary to track down the possible heat flows during different operation modes. All strategies are observed and the matching energy system modes are translated into several diagrams, see Figure 3.4. It is important to keep track on certain setpoints, in order to understand in what direction the energy is flowing. The simplified energy system, as it was given in Figure 3.2, serves as a basis for all possible modes. The modes, as described by Figure 3.4, will help tracking down the energy flows in certain situations during time.

Both thermal energy and temperature meters installed within the analysed AHACS given by Figure 3.3, help controlling the system. Several important setpoints help describing whether the HP system is running in CM or HM.

**The CM is set if:**

- the temperature difference between the chilled-water supply temperature (350.003RT42) and the borehole system return temperature(350.001RT03) is less than e.g. $0.6K$ and the outdoor temperature exceeds e.g. 15°C for at least 15 minutes, or
- during maintenance charging of the PCM-storage (during night time).

**The HM is set if:**

- the cooling load of the building is reasonably low, that the borehole system supply temperature(350.001RT02) is higher than the chilled-water supply set temperature(350.003RT42), or
- the measured heat supply to the borehole system is less than e.g. $50kW$

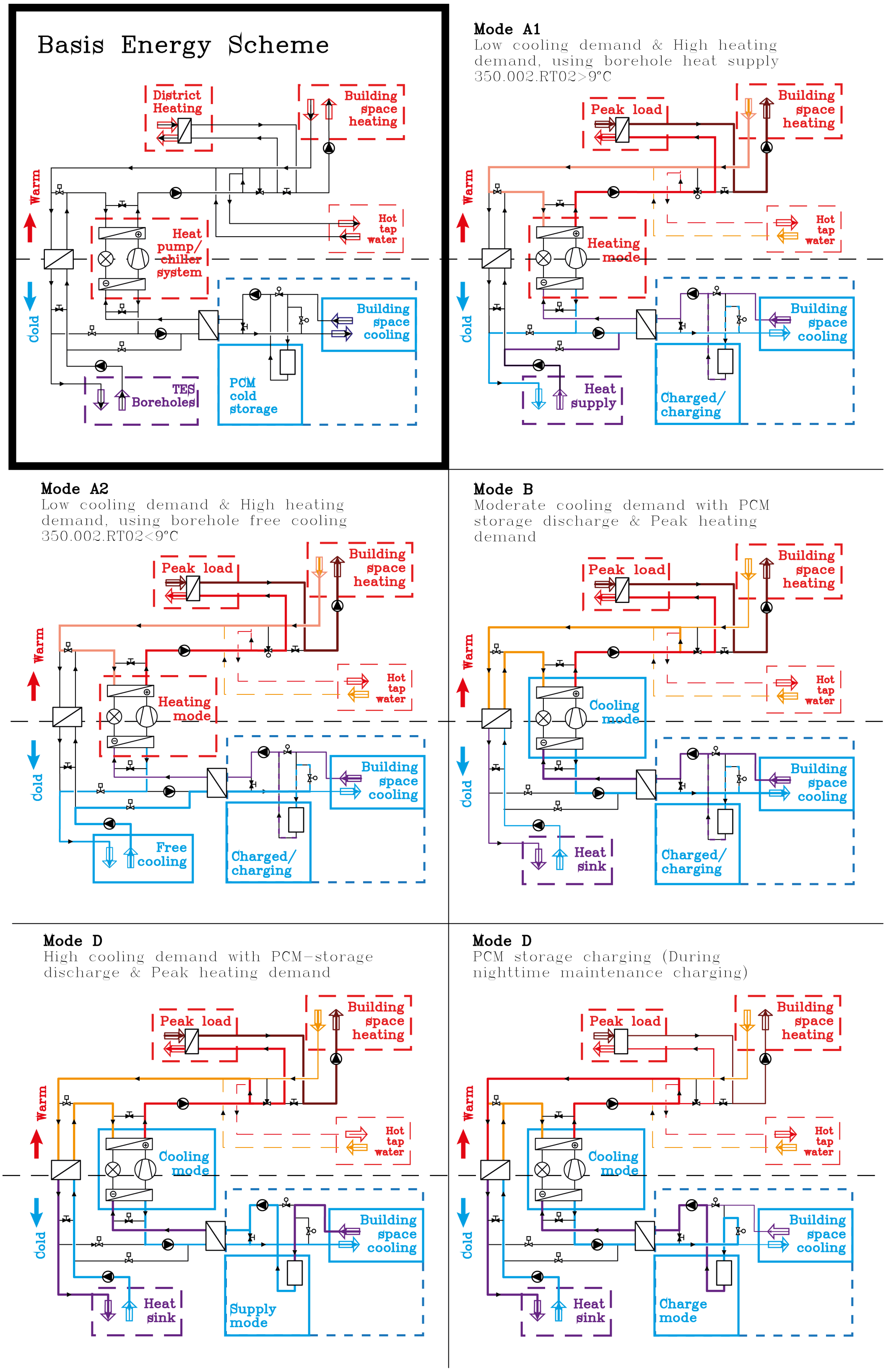




Figure 3.4: Graphical representation of the possible modes of the AHACS at HiB

## 3.5 Energy system regulation

### 3.5.1 Building space heating regulation

By day the building heat supply 320.001.RT40 is regulated based on the outdoor temperature as described in Figure 3.8. By night the temperature curve changes by automatically shifts the curve with $+5°C$ for the outdoor temperature. The time control is set on 5:00 a.m. to 10:00 p.m. for Monday until Friday and 8:00 a.m. to 6:00 p.m. for Saturday and Sunday. The water is preheated by the HP's and the DH lifts the temperature up when necessary during peak time. The connection to the DH is controlled by applying a setpoint temperature which is $1°C$ lower than the aforementioned control curve as described in Figure 3.8.

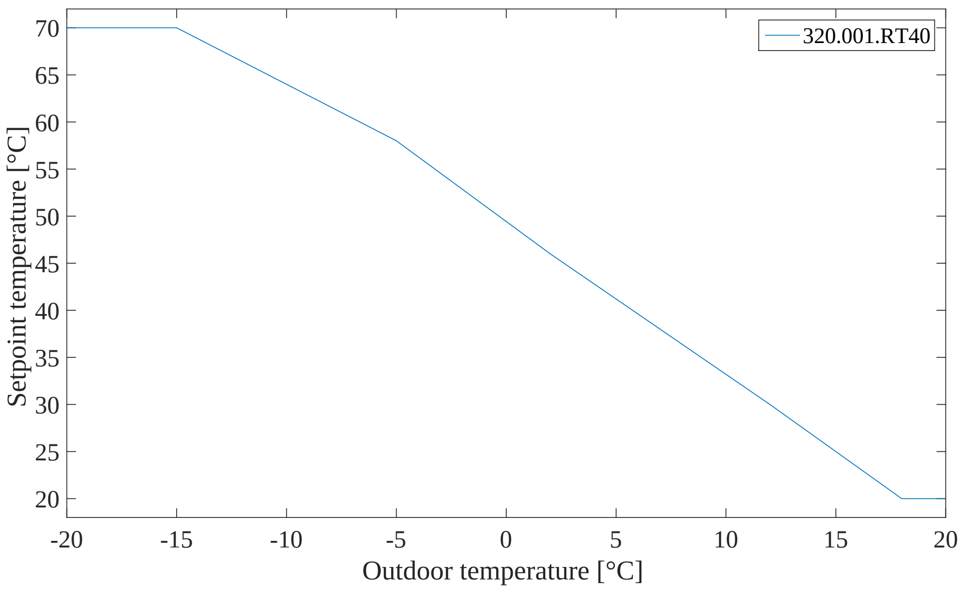


Figure 3.5: Setpoint of the space heating supply temperature as a function of the outdoor temperature, measured by 320.001.RT40

### 3.5.2 Heat pump/chiller system regulation

In the CM and HM there are several different operation strategisch for the HP system. Depending on the actual heating and cooling demand, a combination of all three HP's will be made based on their capacity. For example the HP system is operating in CM 1, meaning only HP 1 is operating. In addition, the cooling demand increases over 270 $kW$, which activates CM 2. Thus HP 1 is shut down, while HP 2 is activated. In Table 3 and 4 further activating and deactivating power setpoints are given. The HP's will be activated or deactivated whenever the cooling or heating demand, in respectively CM and HM, reaches one of these setpoints. Note that the in HM the HP's will never run all at ones. The maximum operation capacity in cooling mode is 1030 $kW$, while this is 1401 $kW$ in heating mode.

Table 3: Five different operation modes for the heat pump/chiller system in cooling mode

| What | 1 | 2 | 3 | 4 | 5 |
|---|---|---|---|---|---|
| Activate [kW] | | 270 | 380 | 590 | 920 |
| Deactivate [kW] | | 235 | 330 | 500 | 720 |
| HP1 | x | - | - | - | x |
| HP2 | - | x | - | x | x |
| HP3 | - | - | x | x | x |
| Evaporator capacity [kW] | 292 | 438 | 671 | 1109 | 1401 |
| Condenser capacity [kW] | 343 | 511 | 788 | 1299 | 1642 |
| Power consumption [kW] | 50 | 74 | 118 | 193 | 243 |

Table 4: Four different operation modes for the heat pump/chiller system in heating mode

| What | 1 | 2 | 3 | 4 |
|---|---|---|---|---|
| Activate [kW] | | 240 | 340 | 480 |
| Deactivate [kW] | | 200 | 290 | 430 |
| HP1 | x | - | - | - |
| HP2 | - | x | - | x |
| HP3 | - | - | x | x |
| Evaporator capacity [kW] | 237 | 356 | 618 | 974 |
| Condenser capacity [kW] | 302 | 453 | 767 | 1220 |
| Power consumption [kW] | 65 | 97 | 153 | 250 |

The setpoint temperature at the condenser side of the HP system is set related to the outdoor temperature. The condenser temperature is measured by temperature meter 350.002.RT06, while the outdoor temperature is measured by 320.001.RT90. The condenser setpoint temperature differs in the CM and HM for the HP system, see Figure 3.6 and 3.7.

Table 5: Specific temperature levels in heat pump/chiller system

| | Cooling mode | | | Heating mode | | |
|---|---|---|---|---|---|---|
| Heat pump | HP1 | HP2 | HP3 | HP1 | HP2 | HP3 |
| Condenser inlet [°C] | 27 | 27 | 27 | 42 | 42 | 46.6 |
| Condenser outlet [°C] | 32 | 32 | 32 | 50 | 50 | 49.2 |
| Evaporator inlet [°C] | 10 | 10 | 10 | 10 | 10 | 7.5 |
| Evaporator outlet [°C] | 5 | 5 | 5 | 5 | 5 | 5 |
| Flow rate condenser $[m^3/h]$ | 58.8 | 87.9 | 136.3 | 52.6 | 78.6 | 140 |
| Flow rate evaporator $[m^3/h]$ | 52.6 | 78.9 | 118.5 | 44.1 | 66.2 | 10 |

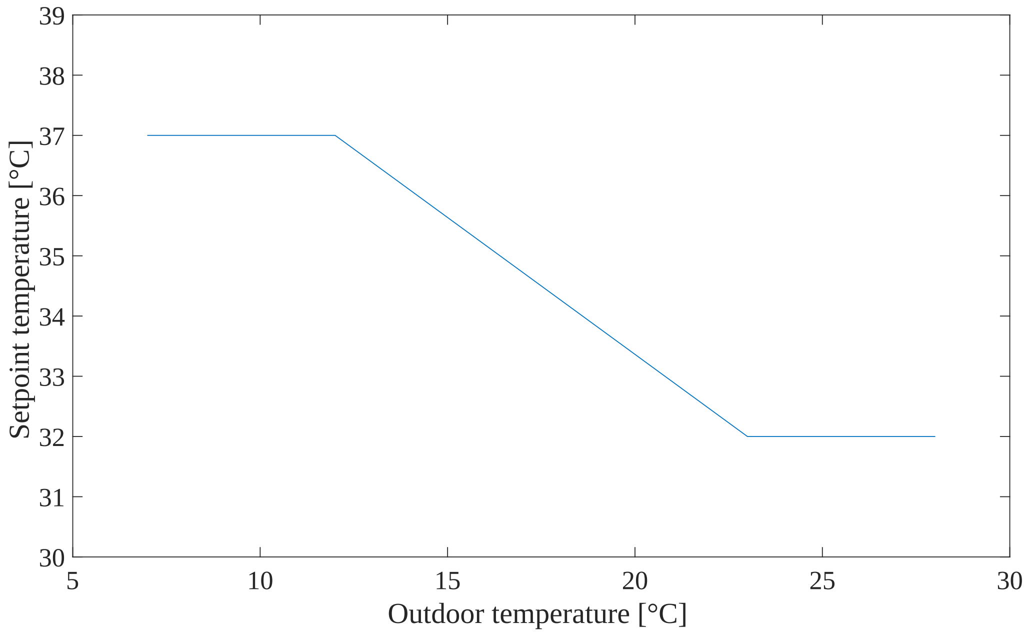


Figure 3.6: Setpoint of the condenser return temperature as a function of the outdoor temperature, measured at the hot side of the heat pumps via 350.002.RT06 when heat pump is in cooling mode

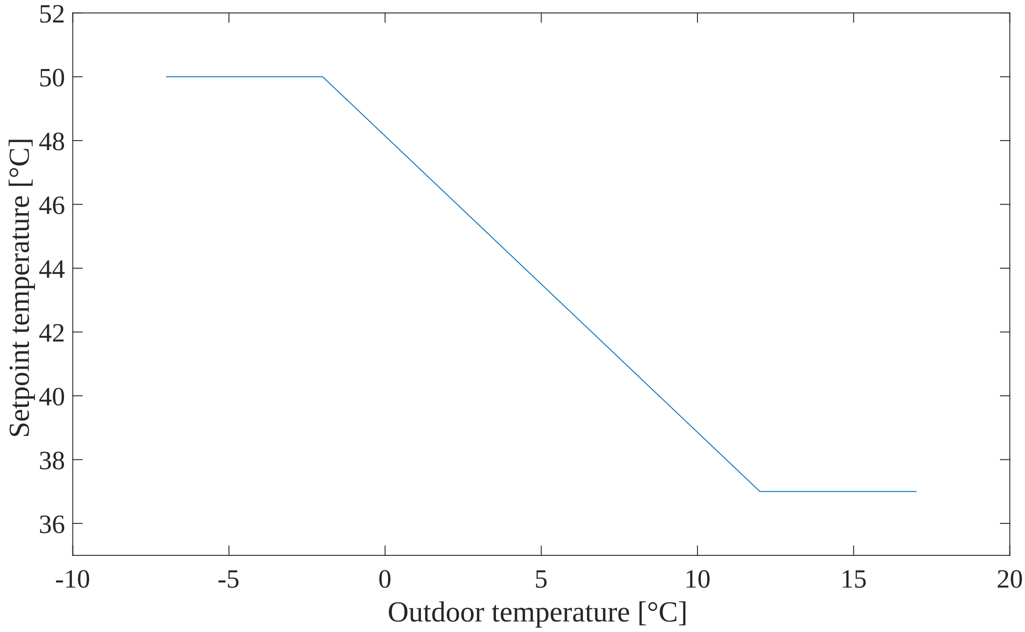


Figure 3.7: Setpoint of the condenser return temperature as a function of the outdoor temperature, measured at the hot side of the heat pumps via 350.002.RT06 when heat pump is in heating mode

### 3.5.3 Cold water distribution regulation

The cold water distribution system (350.003) will deliver ice water for comfort cooling in buildings, to servers and for cooling ventilation. The base cooling load is provided at the evaporator side of the HP system. The peak load is provided by the PCM cold storage. The system also utilizes free cooling from borehole system if the temperature level in the boreholes is lower than the desired ice water temperatures. Design flow and return temperatures are $7°C$ and $17°C$ for the space cooling. The system flow temperature is outdoor compensated to achieve a good cooling and heating factor of heat pumps and to use free cooling from boreholes.

The setpoint temperature of the cold water distribution loop, as well as the setpoint temperature of the supply to the cold distribution loop (system 350.001) given by Figure 3.8. The temperature at the cold water distribution loop is measured by 350.003.RT42. The temperature at the cold supply to the cold distribution loop is measured by 350.001.RT03. The setpoint temperature of this cold supply is always at least 1°C lower than the temperature measured in the cold distribution loop. However, this temperature difference increases to $2.5°C$ over a outdoor temperature increase from $13°C$ to $20.5°C$.

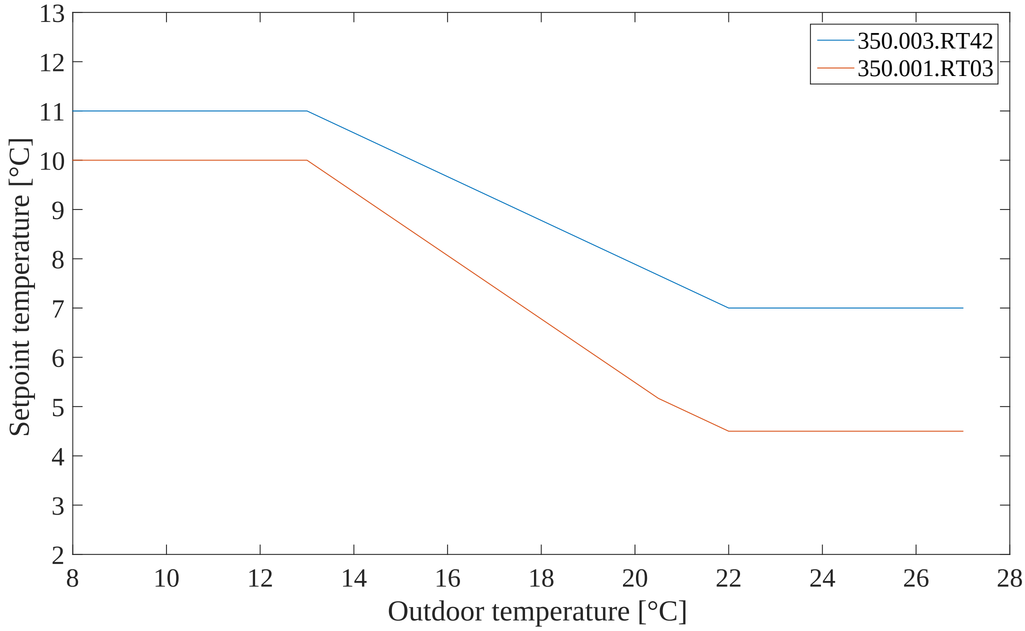


Figure 3.8: Setpoint of the flow temperature as a function of the outdoor temperature, measured at the cold side of the heat pumps via 350.001.RT03 and at the cold distribution loop via 350.003.RT42

PCM storage is activated in case the temperature for the building space cooling supply (350.003.RT42) is lower than 10°C for more tan 8 min or in case all HP's are operating on 100% capacity in cooling mode for at least 10 min. Additionally, the storage will be used as back-up cooling in case all HP's are failing. In case the HP system was running in heating mode the back-up cooling will only be activated in case 350.001.RT03 $> 11°C$.
The PCM discharge is regulated by controlling the return temperature 350.003.RT51, in order to prevent rapid discharge and to prevent that the HP system regulates the discharging. 350.003.RT51 is calculated by Equation 4. This calculation is based on the assumption that the return temperature 350.003.RT50 is approximately $17°C$.

$$RT51W = RT42B + \frac{340}{OE01flowrate} \tag{4}$$

With:

| | | |
|---|---|---|
| RT51W = | Thermal efficiency | [-] |
| RT42B = | Heat supply | $[kWh]$ |
| OE01 = | mass flow rate | $[l/s]$ |

The PCM storage is charged, either when 350.003.OE03 measured a energy discharge over 1.300 $kW$ for more than 15 minutes during the day, or in case the temperature the storage tanks exceeds 10.2°$C$: 350.003.RT55-RT58 $\geq$ 10.2°$C$. During discharging, 350.003.RT42 is determined by adjusting the cold supplied to the cold distribution loop, 350.001.RT03, based on the cold supply 350.003.EO01 as shown in Figure 3.9. The PCM charging is stopped in case 350.003.OE034 $\leq$ 50 $kW$ in 10 minutes time. When the charging is deactivated, 350.003.RT42 will be regulated based on the outdoor temperature again as described in Figure 3.8.

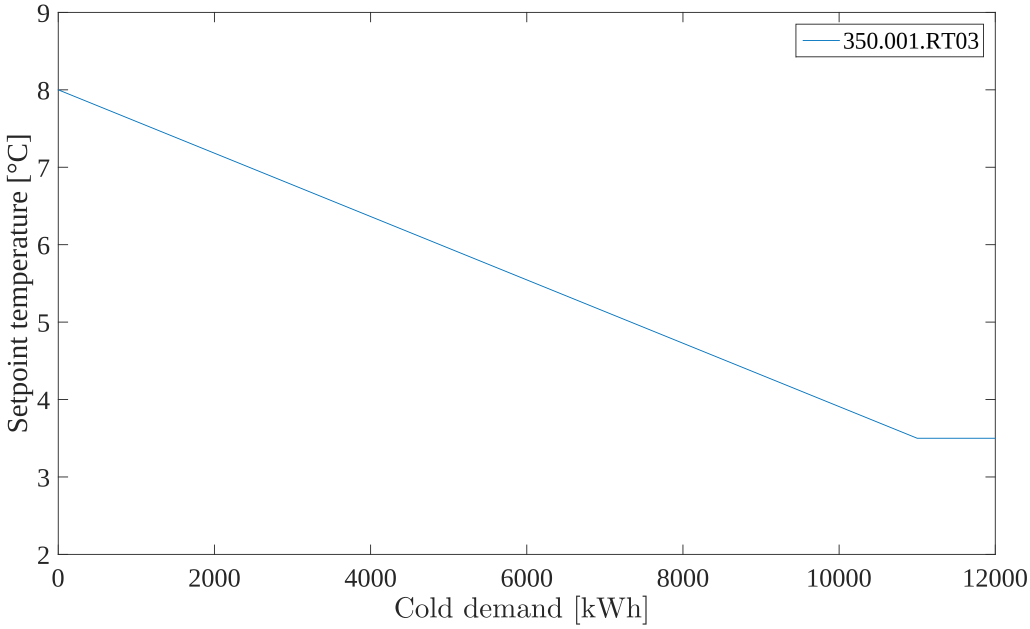


Figure 3.9: Setpoint of the flow temperature 350.001.RT03 as a function of the cold supply, measured by 350.003.EO01

### 3.5.4 Borehole system regulation

During CM the borehole system is loaded in case the is a surplus of heat produced at the condenser side of the HP system. In HM the borehole system supplies heat to the evaporators in case 350.001.RT02 $> 9°C$. In this situation cold from the evaporators partly runs through the borehole and is mixed with the rest of the cold water in order to reach the setpoint temperature 350.001.RT03 of $8.5°C$ for the cold supply to system 350.003. In case 350.001.RT02 $< 9°C$ the borehole system will be used as free cooling. However, free cooling is only applied while the energy output of the boreholes is rather sufficient. This means that the energy measured by 350.003.EO01 should be at least 160 $kW$ or this energy flow should be at least 12 $l/s$.

## 3.6 Energy meters

Within the energy system a lot of measurements are continuously performed, as can be seen in Figure 3.3. The energy meters use ultrasound to measure the flow. The meters have a measurement accuracy following the European standard of Class 2 or 3 (EN1434), which means they have a measuring tolerance of approximately 2% under ideal installation conditions. The unit has a minimum of IP cluster 54 and displays local values for reading. Some sensors need 10 meter of cable. The energy meters are connected to a segment controller via a M-bus and gives updates with real values at least every 45 seconds. A minimum of transferred values are: supply and return temperature with precision of one decimal after comma, flow, power and accumulated energy.

Not only are energy meters controlling the energy system. Depending on the goal of the measurements the data can be logged as well. For the data logging time values are stored for the main temperatures, energy, power, and flow. The scope of the logging data varies a lot. When a period of a year is read from the system, the data is most likely exported with a much bigger time steps than for example reviewing measurements over a period of one specific week. The monitoring system will return accumulated values of the measurements in accordance to the requested period and its conformable time steps.

# 4 Method

This chapter is actually divided in two parts. Section 4.1 describes how the data analysis is performed and which sub-questions of this research are answered. Additionally, Section 4.2 describes how the HP system is analysed up to a greater extend.

## 4.1 Data analysis upon the advanced heating and cooling system

The energy system is analysed based on data provided by SWECO. The data concerns 15 energy measurements within the energy system, over a period from $1^{st}$ of November 2015 until $31^{st}$ of October 2016. The outdoor temperature was measured at the north facade during the same period. The outdoor temperature will help putting the heating and cooling demand into perspective. All energy measurements are given in kWh per day over the given period. See the PID chart in Figure 3.3 for the location of 12 of the 13 energy meters. The hot tap water energy meter is located in the hot water supply system (320.001), which is not visible in Figure 3.3. The energy meters at the borehole system and the PCM storage measure both heat and cold energy. The resulting 15 measurements are described in Table 6.

Table 6: Energy meters

| **Energy meter** | **System component** | **Measured quantity** | **Specifics** |
|---|---|---|---|
| 310.001-OE51 | Hot tap water | Energy consumed | - |
| 320.001-OE01 | District heating | Energy delivered | - |
| 320.001-OE02 | Building space heating | Energy consumed | - |
| 350.002-OE01 | Heat pump | Energy delivered | Condenser total |
| 350.001-OE01 | Borehole system | Energy stored | Heat sink |
| 350.001-OE01 | Borehole system | Energy extracted | Heat supply |
| 350.001-OE11 | Heat pump | Energy delivered | Evaporator HP 1 |
| 350.001-OE12 | Heat pump | Energy delivered | Evaporator HP 2 |
| 350.001-OE13 | Heat pump | Energy delivered | Evaporator HP 3 |
| 350.011, 432.020-RE03 | Heat pump | Energy consumed | Compressor HP 1 |
| 350.012, 432.020-RE04 | Heat pump | Energy consumed | Compressor HP 2 |
| 350.013, 432.020-RE05 | Heat pump | Energy consumed | Compressor HP 3 |
| 350.003-OE01 | Building space cooling | Energy consumed | - |
| 350.003-OE03 | PCM storage | Energy extracted | Discharge |
| 350.003-OE03 | PCM storage | Energy stored | Charge |

The data is analysed based on the following sub-questions:

- **How is the energy use profile of the heating and cooling system?** It is important to know what the building energy usage profile is in the period from $1^{st}$ of November 2015 until $31^{th}$ of October 2016. Data on hot tap water, space heating, and building space cooling is put into perspective related to the outdoor climate. Besides the outdoor temperature, sun radiation might play an important role.

- **Does the heating and cooling system perform as intended?** Basically this can be analysed via the energy balances within the AHACS. The energy balance the HP system, borehole system, and PCM storage are evaluated. In addition, the overal energy balance in the complete AHACS is analysed. Therefore, the overal heat and cold generated and supplied by the AHACS is analyzed.
  Besides the energy balances the performance of the HP/chiller system will be explored into detail.

## 4.2 Heat pump/chiller system analysis

As concluded in Section 2.2.4, the HP is a key element within the energy supply system. In addition to the sub-question *"Does the heating and cooling system perform as intended?"*, the HP system is analysed up to a greater extend. The COP will be evaluated based on Equation 1, along with the different temperatures at the evaporator and condenser side of the HP's. Since there is no data extracted on the temperatures within the HP system, assumptions have been made in order to estimate roughly the performance of the HP system, as described in Section 4.2.1. Eventually these assumptions are applied within a analysis model for the HP system as described in Section 4.2.2.

### 4.2.1 Assumptions upon the heat pump/chiller system

Detailed information on the system operation is given within the functional description of the energy system [26][27]. There is no data available on the different temperatures within the same time interval as the provided energy measurement data. In order to calculate the condenser temperature, it is necessary to make some assumptions. It is assumed that the system temperatures are related to the outdoor temperature as described within the functional description, as depicted in Figure 3.6 and 3.7. At first it is important to approximate for the entire year in which operation mode the HP's are running. Based on the functional description and the fact that only data on the energy meters is available, the easiest assumption is to relate the operations modes to the outdoor temperature. Whenever the outdoor temperature exceeds $15°C$, the cooling mode should be activated. Next, the temperature setpoint described by Figure 3.6 and 3.7 are used to calculate the designed condenser return temperature throughout the year.The mass flow at the condenser side is assumed constant at the designed value of 91.6 $m^3/s$ in cooling mode. In heating mode the similar mass flow is assumed at 52.5 $m^3/s$. Besides that, the condenser supply temperature is assumed to be $5°C$ lower dan the condenser return temperature.

### 4.2.2 Model upon the heat pump/chiller system

The total energy at the condenser side is expressed by means of mass flow and the temperature difference via Equation 5. However, in this situation the $q$ is know as it is measured by energy meter 350.002-OE01 in kWh. Applying the assumptions as described above, the 'real' condenser return temperature can be approximated via Equation 6.

$$q = \dot{m}\rho C_p dT \tag{5}$$

$$T_{cond} = \frac{q}{\dot{m}\rho C_p} + T_{supply} \tag{6}$$

With:

| | | |
|---|---|---|
| $\dot{m} =$ | Mass flow of water | $[m^3/s]$ |
| $\rho =$ | Density of water | $[kg/m^3]$ |
| $C_p =$ | Specific heat capacity | $[J/kg.K]$ |
| $T_{supply} =$ | Condenser supply temperature | $[K]$ |

It is important to realize that this calculation is based on several course assumptions. The mass flow and supply temperature fluctuate a lot in reality. In order to see how this would affect the calculation, both assumptions upon the mass flow and the condenser supply temperature are manually reduced and decreased for five different situations each. In addition, the setpoint temperatures in heating and cooling mode are addressed for five different situations as well. This provides some better insight about whether designed HP system temperatures are properly chosen in the original design or whether they should be changed to suite better to the local climate and the user profile. In Table7 the changes applied to the previous described assumptions are presented, stating whether with what amount the original value is increased or decreased.

### 4.2.3 HP1 and HP2 performance

Since there there was a specification report on all HP's operating in different part loads. It was possible to analyse both HP1 and HP2 into further detail. Based on the HP specifications, see Appendix .2, the COP, carnot efficiency($\epsilon$), and thermal efficiency ($\eta$) are evaluated. Given the data on nominal heating and cooling performances, the temperature levels, electricity demand, and heat production are used to calculated the COP, $\epsilon$, and $\eta$ with Equations 1- 3. In nominal heating and cooling performances the temperature levels in the HP system are according the stated design temperatures in Table 5. The electricity demand and heat production in nominal operation mode is conform Table 8 and 9.

After analysing HP1 and HP2 the measured data in the period from 6 July until 13 July is analysed, while only HP1 and HP2 are operating in this period of time. The main goal is to calculate the primary evaporator temperature $T_L$ and compare it to the nominal design

Table 7: Nominal performances of HP1 based on Appendix .2

| | Cooling mode | | | Heating mode | | |
|---|---|---|---|---|---|---|
| Situation | $\dot{m}$ $[kg/m^3]$ | $T_{supply}$ [K] | Setpoint Tout | $\dot{m}$ $[kg/m^3]$ | $T_{supply}$ [K] | Setpoint Tout |
| M1 | 91.6 | Tset-5 | 12/23 | 52.5+10 | Tset-5 | -2/12 |
| M2 | 91.6-5 | Tset-5 | 12/23 | 52.5+5 | Tset-5 | -2/12 |
| M3 | 91.6-10 | Tset-5 | 12/23 | 52.5 | Tset-5 | -2/12 |
| M4 | 91.6-15 | Tset-5 | 12/23 | 52.5-5 | Tset-5 | -2/12 |
| M5 | 91.6-20 | Tset-5 | 12/23 | 52.5-10 | Tset-5 | -2/12 |
| T1 | 91.6 | Tset-5 | 12/23 | 52.5 | Tset+10 | -2/12 |
| T2 | 91.6 | Tset-10 | 12/23 | 52.5 | Tset+5 | -2/12 |
| T3 | 91.6 | Tset-15 | 12/23 | 52.5 | Tset | -2/12 |
| T4 | 91.6 | Tset-20 | 12/23 | 52.5 | Tset-5 | -2/12 |
| T5 | 91.6 | Tset-25 | 12/23 | 52.5 | Tset-10 | -2/12 |
| M1 | 91.6 | Tset-5 | 15/23 | 52.5 | Tset-5 | -2/15 |
| M2 | 91.6 | Tset-5 | 14/22 | 52.5 | Tset-5 | -3/14 |
| M3 | 91.6 | Tset-5 | 13/21 | 52.5 | Tset-5 | -4/13 |
| M4 | 91.6 | Tset-5 | 12/20 | 52.5 | Tset-5 | -5/12 |
| M5 | 91.6 | Tset-5 | 11/19 | 52.5 | Tset-5 | -6/11 |

Table 8: Nominal performances of HP1 based on Appendix .2

| | Cooling demand | | Heating demand | |
|---|---|---|---|---|
| Partload [%] | Pe [kWh] | Qo [kW] | Pe [kWh] | Qo [kW] |
| 100 | 47.1 | 279.9 | 65.2 | 238.1 |
| 75 | 36.7 | 210.3 | 50.9 | 178.9 |
| 50 | 26.3 | 140.4 | 36.5 | 119.4 |

Table 9: Nominal performances of HP2 based on Appendix .2

| | Cooling demand | | Heating demand | |
|---|---|---|---|---|
| Partload [%] | Pe [kWh] | Qo [kW] | Pe [kWh] | Qo [kW] |
| 100 | 69.6 | 419.6 | 96.8 | 356.9 |
| 83 | 59.1 | 348.8 | 82.3 | 296.7 |
| 67 | 49.3 | 281.9 | 68.7 | 239.7 |
| 50 | 38.9 | 210.6 | 54.2 | 179.0 |
| 33 | 28.5 | 139.1 | – | – |

temperature of the evaporator. This is done by combining Equation 2 and 3 into Equation 7. The thermal efficiency is assumed to be constant, while $T_H$ is based on the outdoor temperature as described by Figure 3.6 and 3.7. The COP is calculated conform Equation 1, by applying the performed measurements in evaporator 1 and 2, in compressor 1 and 2, and at the condenser side.

$$T_L = \frac{T_H * COP}{COP + \eta} \tag{7}$$

With:

| | | |
|---|---|---|
| $T_L =$ | Temperature Low | $[K]$ |
| $T_H =$ | Temperature High | $[K]$ |
| $COP =$ | Coefficient of performance | [-] |
| $\eta =$ | Thermal efficiency | [-] |

# 5 Thermal energy system performance analysis

This chapter is divided in two parts. In the first part, Section 5.1, the analysis on the measured data is described. Additionally in Section 5.2 the HP system is analysed into a greater extend.

## 5.1 Energy measurement analysis

### 5.1.1 General thermal energy demand

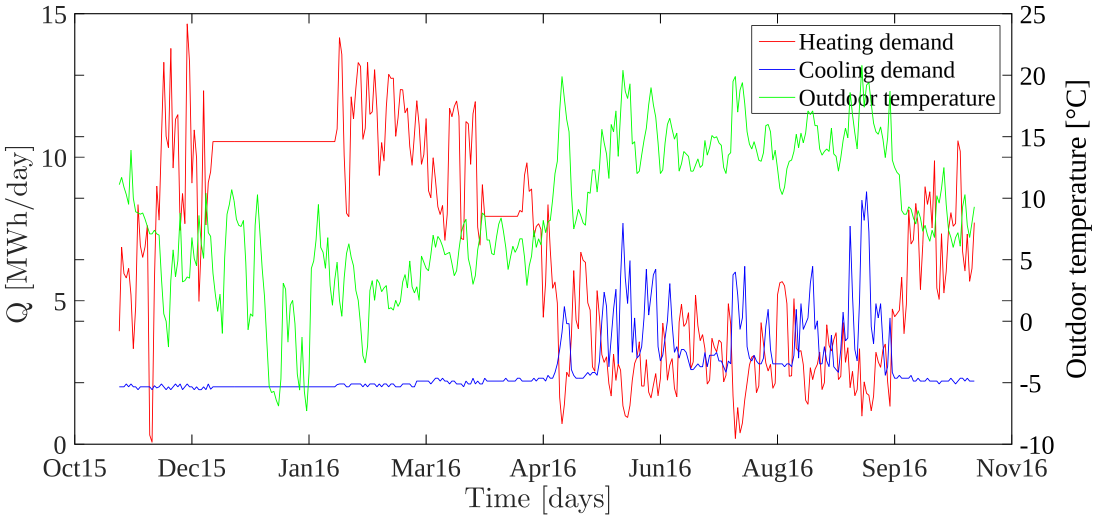


Figure 5.1: Daily building energy usage, heat load measured with 320.001.OE02 and cooling load measured with 350.003.OE03

In Figure 5.1 the yearly overall building energy demand on daily basis and the outdoor temperature is given. Notable are the platforms in the heating and cooling demand around 11 December until 1 February (heating $10500kWh/day$ and cooling $2000kWh/day$) and 5 until 19 April (heating $7900kWh/day$). The stable loads are not matching any other vacation data, therefore it is most assumable that these are errors in the logging system. Seemingly the plateau is an averaged value of data measured just up front and after the measurement error. This might cause deviations in the upcoming data analysis. When necessary these averaged values will be excluded from the analysis.
The annual cooling demand is $1.01GWh$ and the annual heating demand is $2.46GWh$ given over the period November 2015 until November 2016. The annual specific cooling demand is $21.3KWh/m^2.year$ and the annual specific heating demand is $52KWh/m^2.year$. Note that these number might be slightly lower than the real annual demands due the previously described error. Especially the heating demand is might be affected since the heating demand most assumably would be peaking much more in the period around 11 December until 1 February. The

annual heating and cooling demands are in the same order of magnitude as the designed annual cooling and heating demands of the energy system, which were respectively $1.06GWh$ and $2.6GWh$ for annual demands and $22.4kWh/m^2.year$ and $54.9kWh/m^2.year$ for specific annual demands. This Figure shows that the heating demand is peaking during the colder months, September until April. Clearly, the base load of the cooling demand is $2000kWh/day$ all year round, due to a stable cooling load. Probably this is caused by big data rooms which contain computers and servers that need to be constantly up and running. During the warmer months (April until September) the cooling load is showing some higher peaks, conform to the outdoor temperature exceeding $10°C$ in combination with the students occupying the building and most of all the higher solar radiation. However, during July and August the cooling load shows less peaks. This most likely has something to do with the summer vacation, when the building is less occupied. Notable are the platforms in the heating and cooling demand around 11 December until 1 February (heating $10500kWh/day$ and cooling $2000kWh/day$) and 5 until 19 April (heating $7900kWh/day$). The stable loads are not matching any other vacation data, therefore it is most assumable that these are errors in the logging system. Seemingly the plateau is an averaged value of data measured just up front and after the measurement error. This might cause deviations in the upcoming data analysis. When necessary these averaged values will be excluded from the analysis.

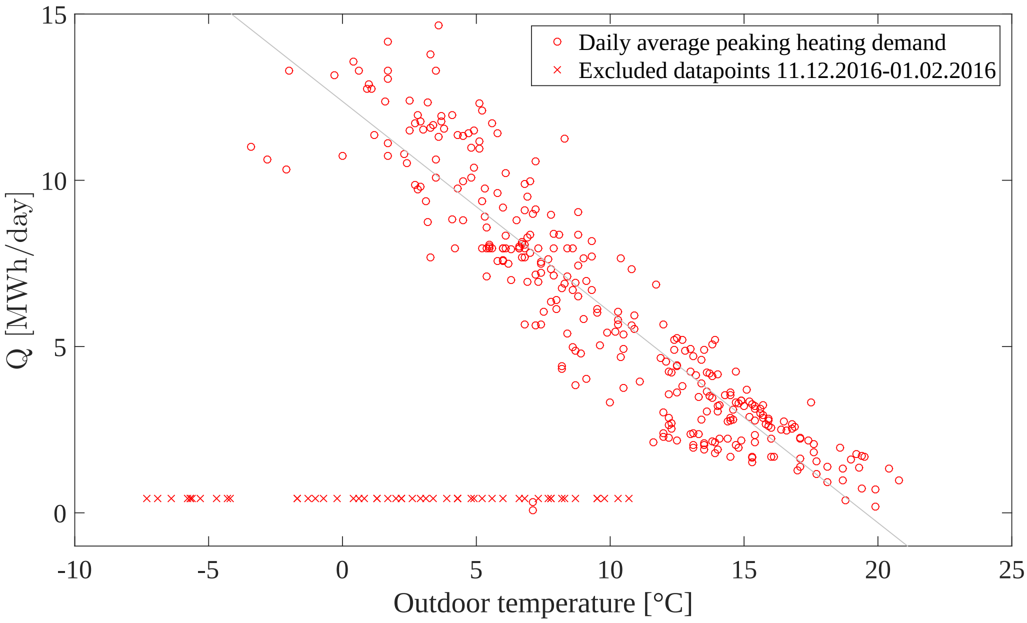


Figure 5.2: Daily heating demand (320.001.OE02) in relation to the outdoor temperature

In Figure 5.2 the daily average peaking heat demand is clearly showing a lineair relation with the outdoor temperature. This lineair relation seems to be more accurate whenever the outdoor temperature is higher, as the data points between the outdoor temperature of $15°C$ and $20°C$ are more densely packed and since these data points show less deviation from the lineair regression line. Within this lineair regression analysis the data points of the period from 11 December until 1 February are left out in order to find a better solution. These excluded data points are plotted as red crosses.

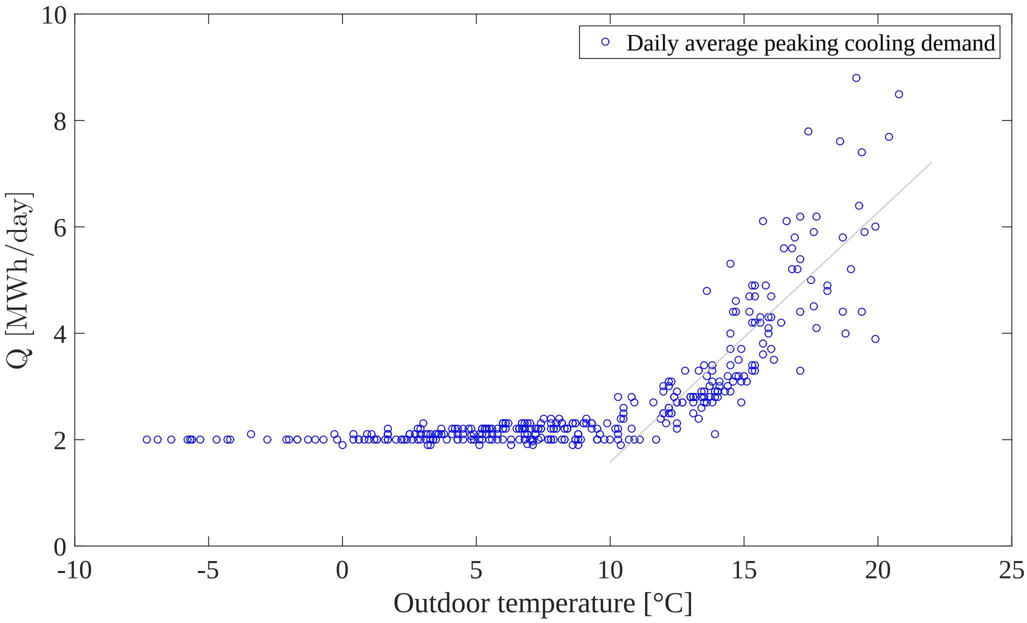


Figure 5.3: Daily cooling demand (350.003.OE03) in relation to the outdoor temperature

In Figure 5.3 it shows that the daily average peaking cooling demand is not related to the outdoor temperature up till it reaches an outdoor temperature of $10°C$. Thereafter, a lineair relation has been discovered between the cooling demand and the outdoor temperature. Whenever the outdoor temperature is exceeding $15°C$ the lineair relation seems to weaken, as the data points are starting to disperse further away from the lineair regression line. This might be caused by solar radiation or an increase in internal loads, e.g. the occupancy level.

In order to calculate the load duration curve, as it is depicted in Figure 5.4, the daily average heating and cooling load is divided by 24 hours. In the cooling load duration curve base load one can clearly extinct the base load of approximately $85kWh$, which is roughly 2/3 of the time the required cooling demand. The cooling load will never drop lower than this base load, in addition the peak cooling load occur less often. The heating load duration curve shows a much bigger spreading of the load. As expected the peak heating demand occurs the least, while the low heat loads occur more often. Around the $450kWh$ a plateau is appearing again. This is caused by the previously described errors in the measurement data.

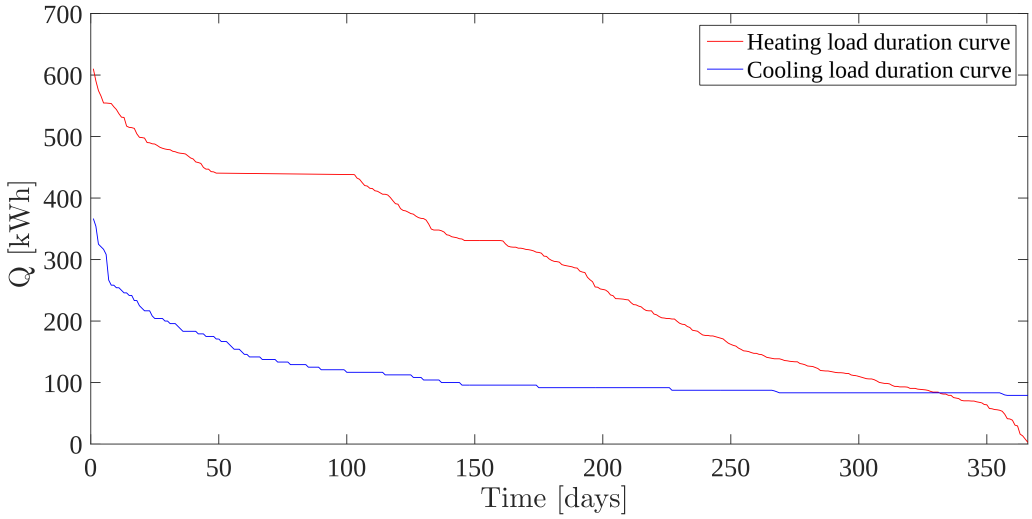


Figure 5.4: Heating and cooling load duration curve

### 5.1.2 Heat supply characteristics

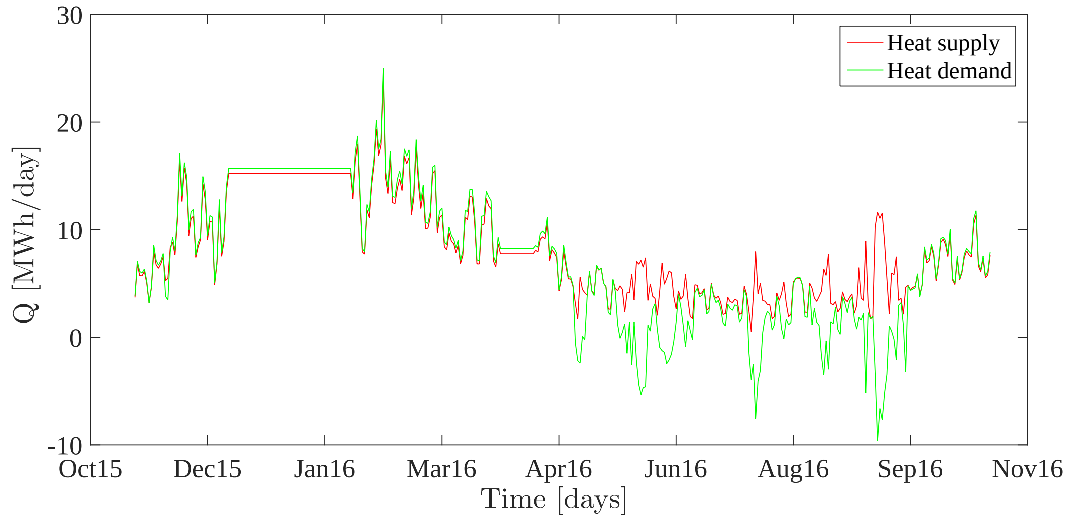


Figure 5.5: Heat supply, consisting of space heating(320.001.OE02), district heating (320.001.OE01), and hot tap water (310.001.OE51), related to the building heat demand (350.002.OE01)

Figure 5.5 shows the heat supplied by the system compared to the heat which is actually delivered to the building. When comparing the annual profile of the supplied and delivered heat, it actually shows a rather equivalent pattern. The measured heat supplied by the energy system is slightly lower than the heat which is actual supplied to the building during winter time. According to SWECO there is a suspicion that the temperature sensor for energy meter 350.002.OE01 is too close to the heat pumps, such that it does not measure an exact mixed water temperature. This means that this measurement is approximately 4% lower.

Within the months April until December the heat supply is peaking, while the heat demand is rather low. If the energy supply system is working correctly, this mismatch in supply and demand should be addressed via seasonal heat storage. In order to see where all heat supplied is coming from, the energy is tracked down from the source in Figure 5.6. The base heat supply is provided by the HP system by supplying heat from the boreholes and the cold distribution loop to the evaporators and electricity from the grid to the compressors. The peak heat supply is supplied by the DH. The red line represents the actual heat demand minus the heat that is rejected into the boreholes. During heating period the real heat demand and supply show a perfect agreement. The energy mismatch in the period from April until September is clearly counteracted by the boreholes. The negatives energy peaks mean that there is heat stored in the boreholes since the demand of the building is low.

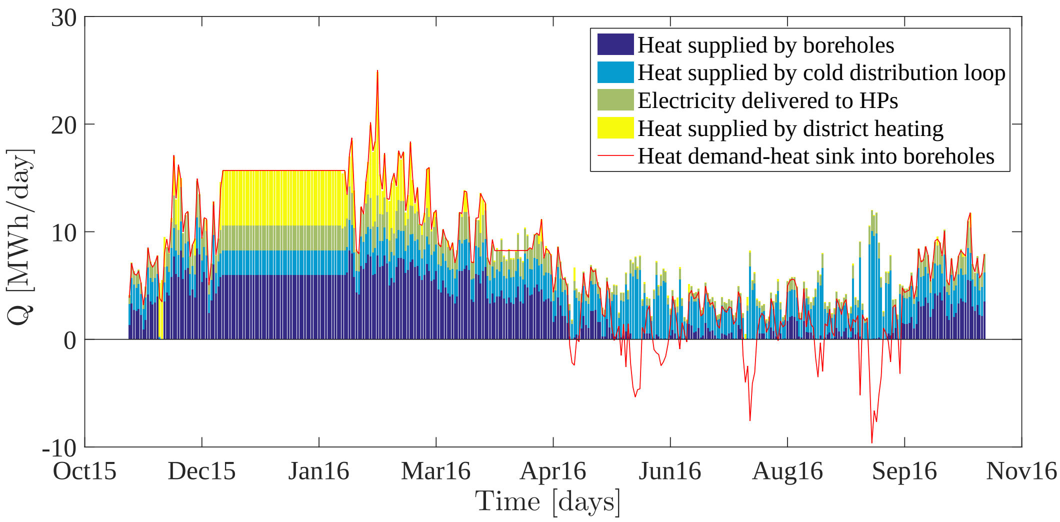


Figure 5.6: Heat supply, consisting of energy supplied by the boreholes (350.001.OE01), the cold distribution loop(350.001.OE11-OE13 minus 350.001.OE01), the electricity grid(432.020.RE02-RE05) and, the DH (320.001.OE01), related to the heat demand (350.002.OE01) minus the heat supplied to the boreholes (350.001.OE01)

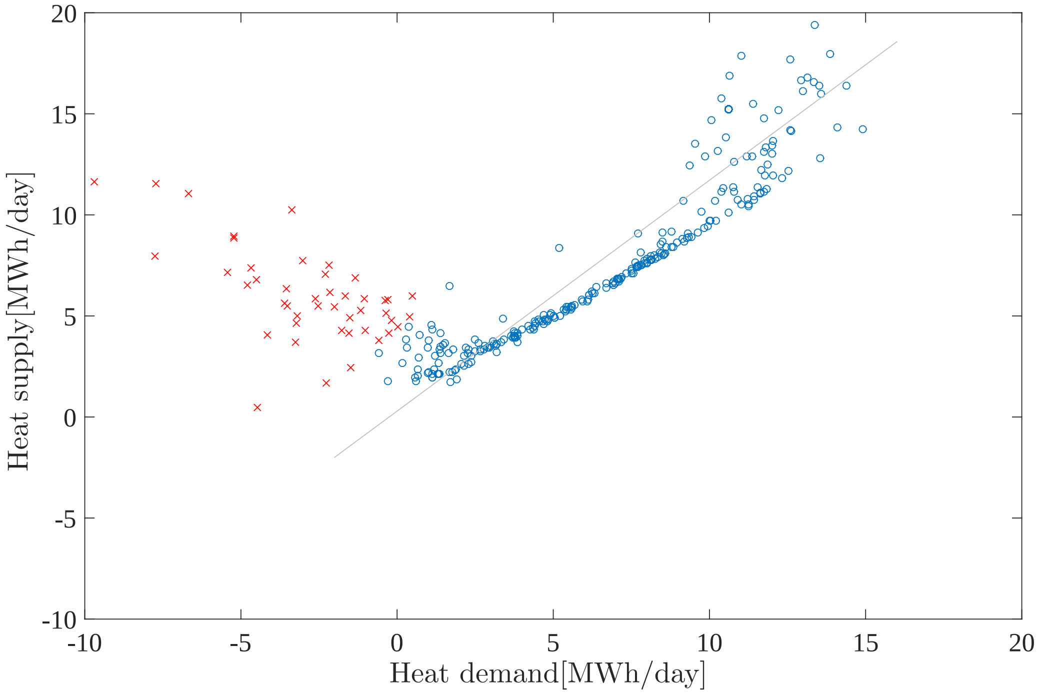


Figure 5.7: Heat supply, consisting of heat supplied by the boreholes (350.001.OE01), the cold distribution loop(350.001.OE11-OE13 minus 350.001.OE01), the electricity grid(432.020.RE02-RE05) and, the DH (320.001.OE01), related to the heat demand (350.002.OE01) minus the heat supplied to the boreholes (350.001.OE01), based on least sum of squares method

A lineair relation between the real heat demand (350.001.EO01) and the heat supply is found in Figure 5.7. The heat supply is calculated based on Equation 8.

$$\dot{Q}_{supply} = \dot{Q}_{BHout} + \dot{Q}_{Colddistr.} + P_{el} + \dot{Q}_{DHout} - \dot{Q}_{BHin} \tag{8}$$

In order to approximate the lineair regression line, the data points which correspond to the negative real heat demand are excluded. Those data points are represented by the red crosses within Figure 5.7. In case the real heat demand is in between $2 - 10 MWh/day$, the demand and supply seem to show a perfect lineair relation. Clearly the heat supply rises above the heat demand whenever the heat demand is peaking or in case there is no heat demand.

### 5.1.3 Cold supply characteristics

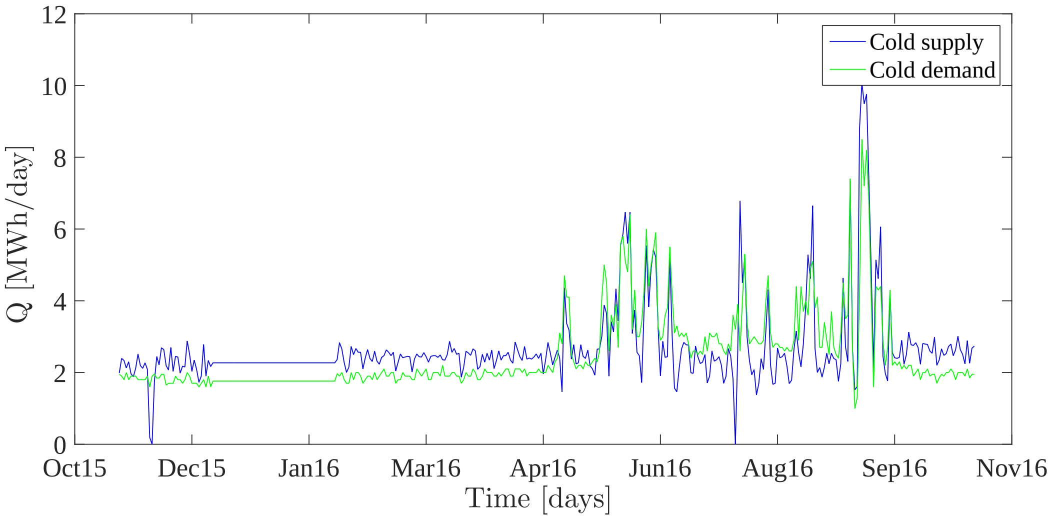


Figure 5.8: Cold supply, consisting of cold extracted form PCM storage (350.003.OE03) and generated by the HP system(350.001.OE11-OE13), related to the building space cooling demand (350.003.OE01)

Figure 5.1 showed a base cooling load of $2MWh/day$. The cooling load is analysed in more detail in Figure 5.8. In Figure 5.9 the cold source supply is tracked down. As both graphs in Figure 5.1 and 5.9 show, the cooling load is peaking from april until September. During this time of the year the HP's are running in cooling mode, since the cold supply is peaking. Upon checking Figure 5.1, the cooling demand is peaking whenever the outdoor temperature is exceeding $10°C$. Clearly the PCM storage supplies cold all year round. However, when the cooling load is peaking, the PCM discharge is peaking as well. Overall the cold demand seems to be lower than the real cold supplied by the energy system. The relation between the cold supply and demand is further analysed in Figure 5.10.

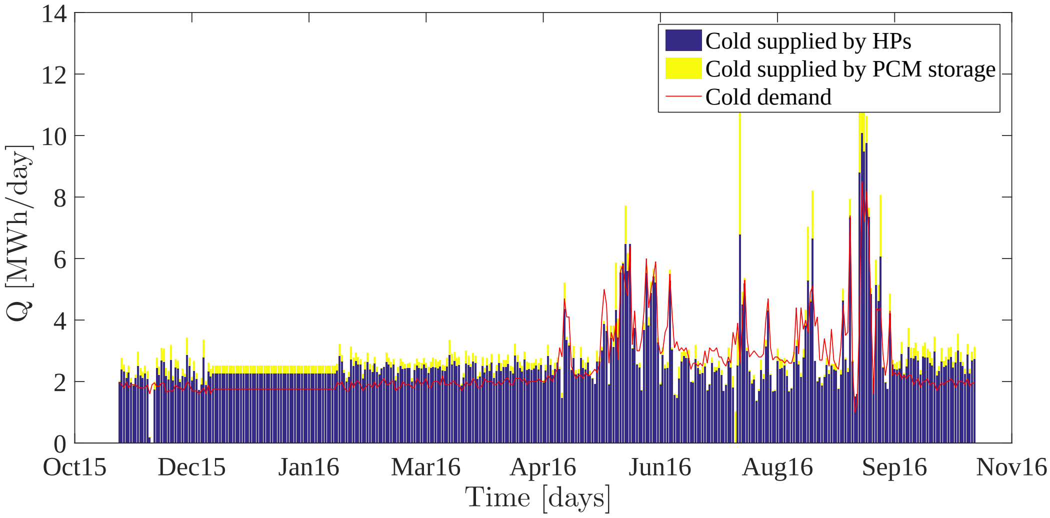


Figure 5.9: Cold supply, consisting of cold extracted form PCM storage (350.003.OE03) and generated by the HP system (350.001.OE11-OE13), related to the building space cooling demand (350.003.OE01) minus the cold stored in the PCM storage (350.003.OE03)

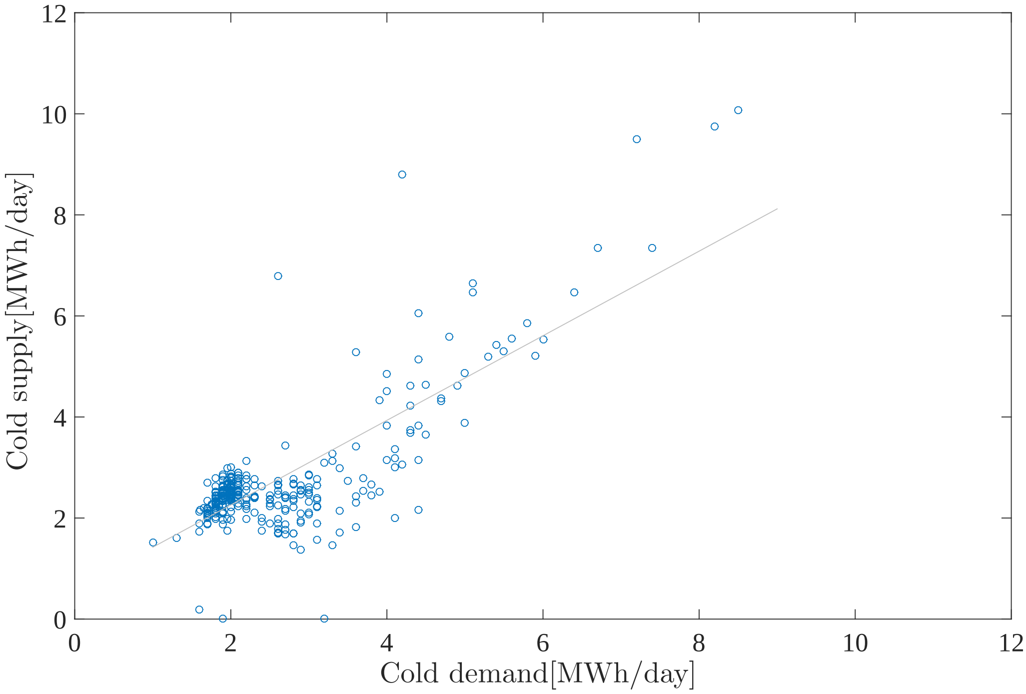


Figure 5.10: Cold supply, consisting of cold extracted form PCM storage (350.003.OE03) and generated by the HP system (350.001.OE11-OE13), related to the building space cooling demand (350.003.OE01) minus the cold stored in the PCM storage (350.003.OE03), based on least sum of squares method

Figure 5.10 gives the lineair relation between actual heat demand of the building compared to the heat supplied by the energy system. Due to the base load of $2MWh/day$ which is often occurring, a lot of data point are clustered at that point. Since there are less data point for the peak cooling load, the data points are deviating to an increasing extend from the lineair regression line as the cooling load is higher than te base load. The lineair regression between the cold supply and demand therefore is not that strong.

### 5.1.4 PCM cold storage energy characteristics

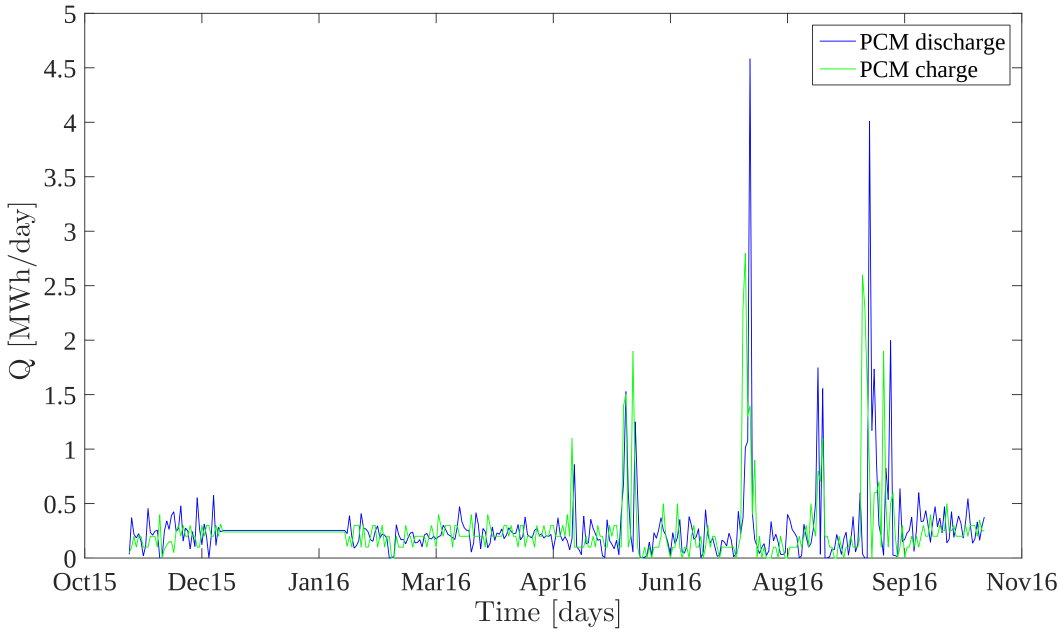


Figure 5.11: PCM cold storage charged and discharged energy during the year(350.003.OE03)

It is of great importance that the PCM storage is in balance. As can be seen in Figure 5.11 the measured energy charged and discharged is in the same order of magnitude. The PCM cold storage is peaking around $4.5 MWh/day$. However, the maximum capacity of the PCM storage is approximately $11 MWh$. Thus not even half of the capacity is been used any day during the year. When the absolute difference between the total amount of discharged and charged energy during the year is compared there is been found a difference of 5.6%. In total the PCM storage is charged $94 MWh/year$, while the storage is $100 MWh/year$ discharged. Also there is more energy discharged than there is been charged. Thus, there is a small mismatch in energy within the PCM storage. As expected Figure 5.12 shows that there is a rather bad relation between the cold stored and extracted from and to the PCM storage. Seemingly the cold extracted is often higher than the cold stored during one day. Now it is a good thing that the PCM storage has a maximum capacity of approximately $11 MWh$. This way the PCM storage will still be able to supply the required cold, while it is been charged during the time when the PCM storage is supplying less cold.

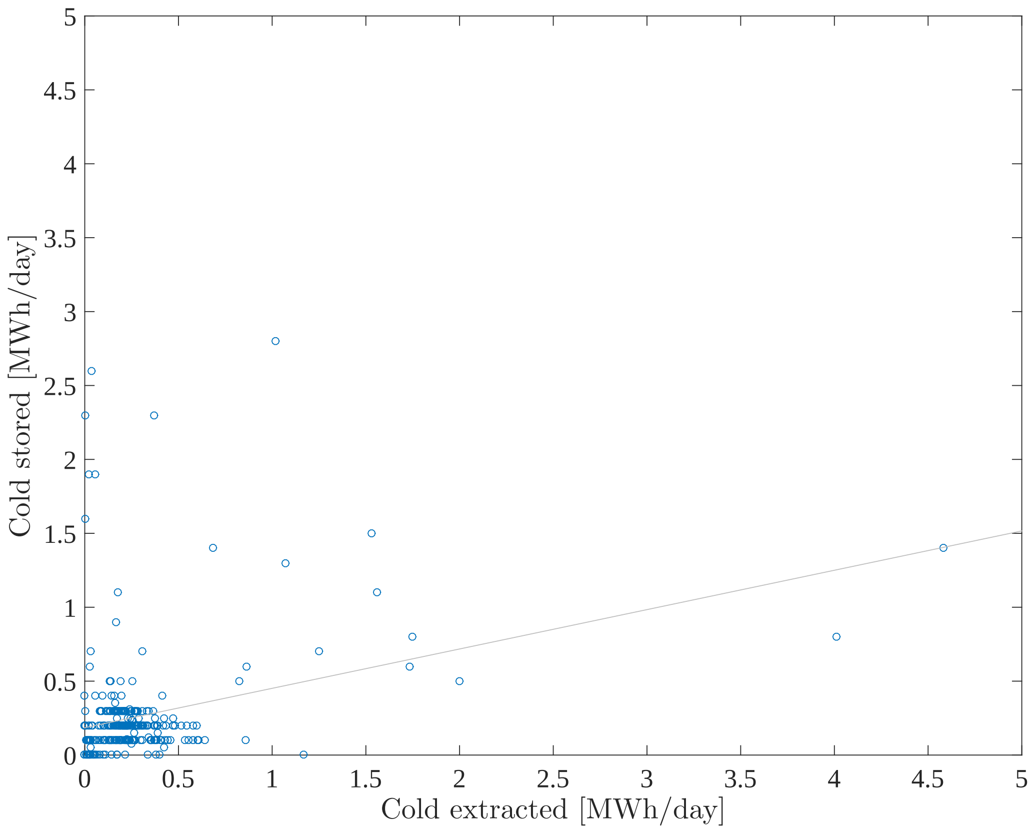


Figure 5.12: Relation between PCM cold storage charged and discharged energy (350.003.OE03), based on least sum of squares method

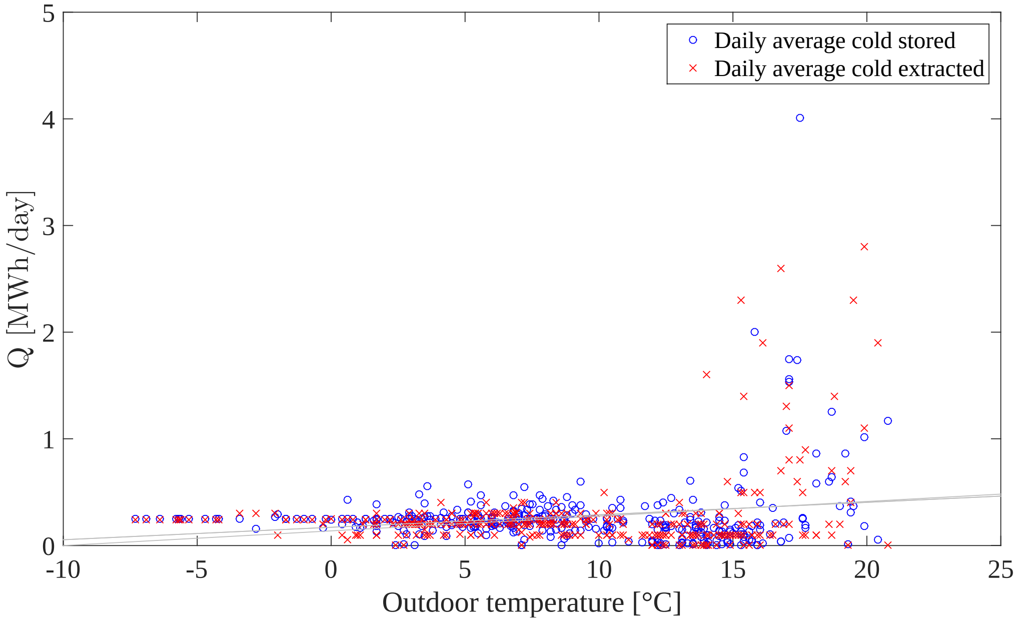


Figure 5.13: PCM cold storage charged and discharged energy (350.003.OE03) related to the outdoor temperature

In Figure 5.13 it becomes clear that there is not really a clear relation between the daily average cold stored in and extracted from the PCM storage. At least until an outdoor temperature of $15°C$ both charged and discharged energy is rather constant. When the outdoor temperature exceeds $15°C$, the charged and discharged energy seems to be peaking randomly. At this same time the building space cooling demand is peaking and the HP system will operate in cooling mode. It seems that fluctuating peak cold demand during this time of the year is responsible for the sudden peaks in Figure 5.13. The HP system simply just has a hard time supplying the required cold demand. Every time the cold distribution supply temperature is lower than $10°C$ for at least 10 min. the PCM storage discharge will be activated.

### 5.1.5 Borehole park energy characteristics

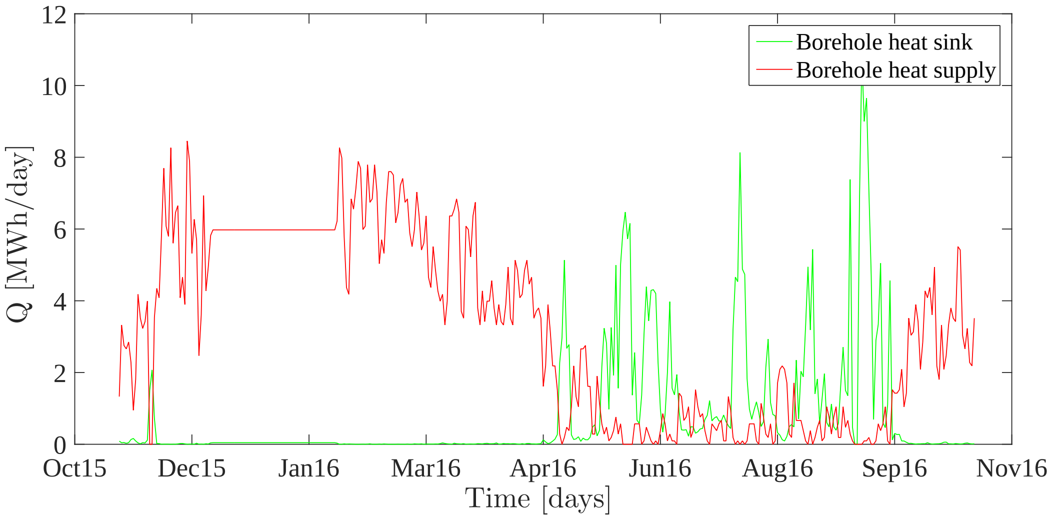


Figure 5.14: Borehole system heat rejection and extraction during the year (350.001.OE01)

Figure 5.14 shows the heat rejection and extraction to and from the borehole system. This figure displays a rather important matter, which was already discussed in Paragraph 2.3.4 regarding borehole systems. The heat which stored into the ground during summer period, will never cover the heat which is extracted during winter. This might reduces the soil temperature and will result in a reduced energy efficiency over time of the AHACS. Depending on the heat flowing from the surrounding ground towards the boreholes, the soil temperature might still stay constant. Upon checking the relation between heat stored and extracted from and to the borehole system in Figure 5.15 a reasonable, however weak, relation is been discovered. Since the borehole system functions mainly as seasonal storage, it is a logical outcome that heat extraction and storage is most likely not happening at the same time. So ideally the data points are laying on the x-axis and y-axis only, something which is showing of in Figure 5.15. Still there is more heat extracted from the borehole system. Therefore, most data point are laying on the x-axis in Figure 5.15. In total $1171MWh$ is extracted from the boreholes system, while only $304MWh$ is rejected to the borehole system in the analysed period. Meaning that only $1/4^{th}$ of the extracted heat from the borehole system is recovered by the energy system itself.

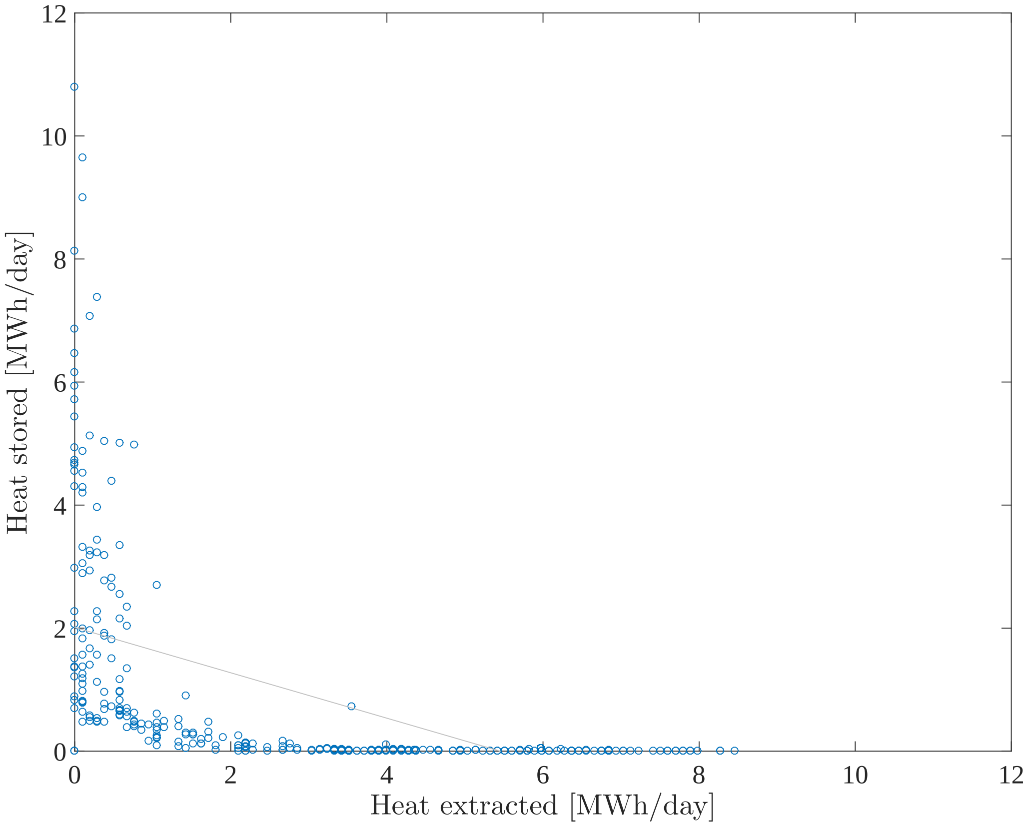


Figure 5.15: Borehole system heat rejection compared to heat extraction during the year (350.001.OE01), based on least sum of squares method

### 5.1.6 Heat pump/chiller system energy characteristics

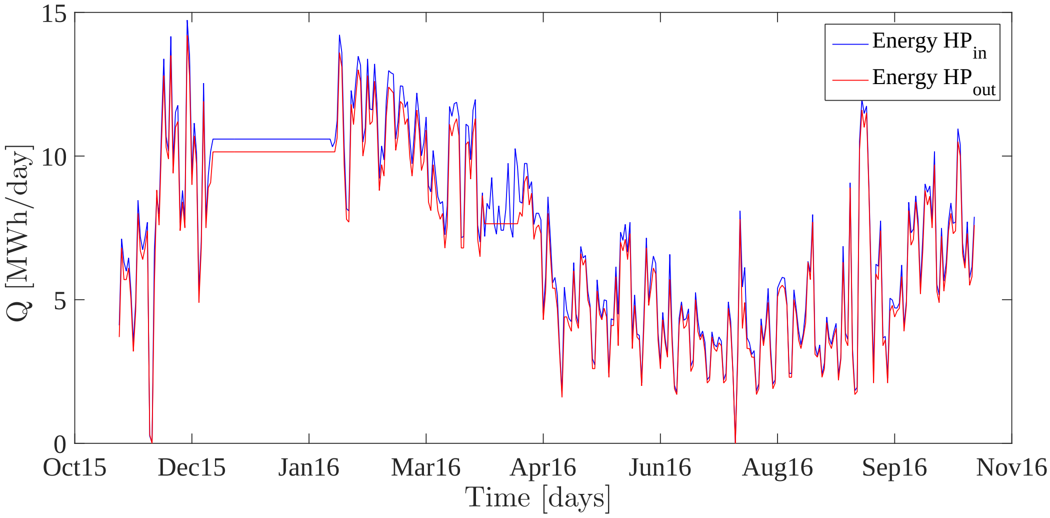


Figure 5.16: Energy in-(350.001.OE11-OE13 plus 432.020.RE02-RE05) and output in the heat pump/chiller system(350.001.OE01)

In Figure 5.16 the energy in- and output within the HP system are compared. The energy input consists out of the heat delivered to the evaporators (350.001.OE11-OE13) plus the electricity delivered to the compressors (432.020.RE02-RE05). The energy output is the heat supplied by the condenser(350.001.OE01). Overall the HP system seems to be balanced. In order to get better insight in the energy balance of the HP system, the lineair relation between energy in- and output is evaluated in Figure 5.17. From the figure, it can be concluded that the energy in- and output is showing a strong lineair relation. Meaning the HP system is operating correctly. If the HP system is actually performing as required, or if it should be optimized in a different way compared to the current HP system design can be read in the next Section 5.2.

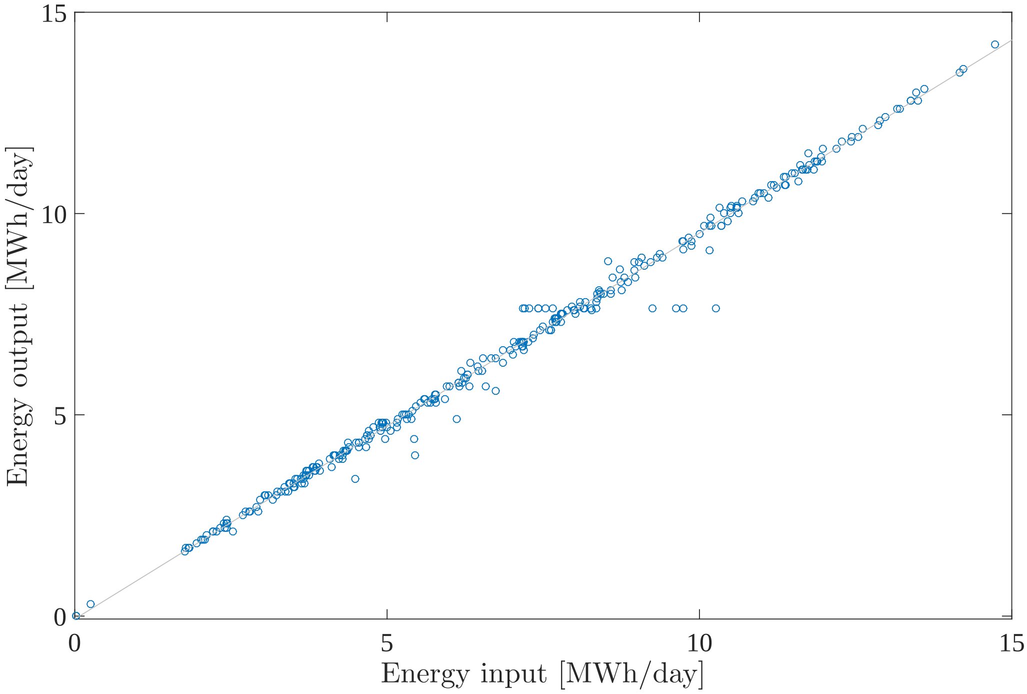


Figure 5.17: Energy input(350.001.OE11-OE13 plus 432.020.RE02-RE05) compared to the energy output in the heat pump/chiller system(350.001.OE01), based on least sum of squares method

## 5.2 Heat pump analysis

### 5.2.1 Heat pump temperature level

As explained before, the condenser temperature in the HP system is set based on the setpoint as displayed in Figure 3.6 and 3.7. Based on the measured condenser energy, the condenser temperature is calculated as explained in Section 4.2.2. This temperature is approximated on the assumptions as described in Section 4.2.1. The calculated condenser temperature is compared to the condenser setpoint temperature over the complete year, taken the different operation modes into account, see Figure 5.18. Overall the calculated condenser temperature is higher than the setpoint temperatures. Especially during winter, the condenser temperature seems to exceed the designed setpoint temperature to a far extend.

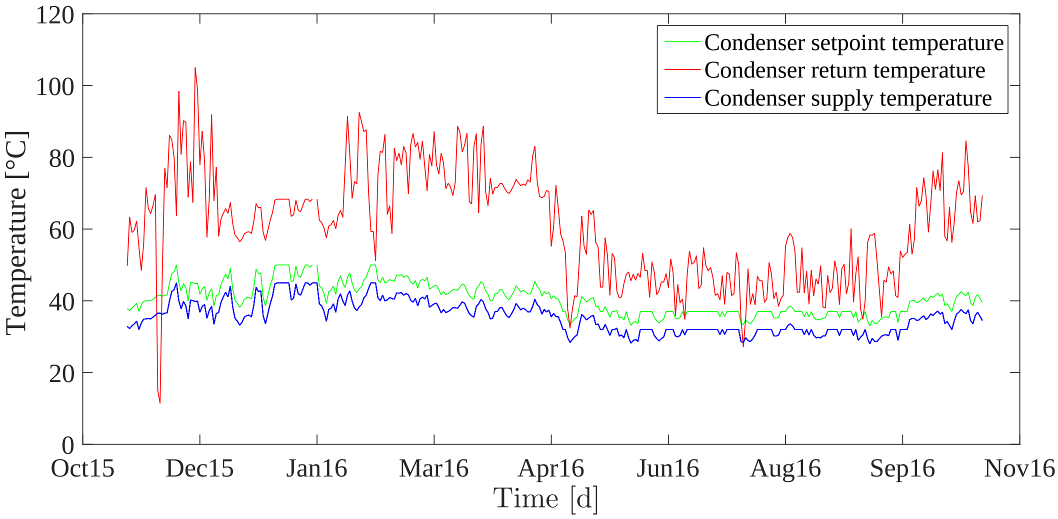


Figure 5.18: The setpoint temperature compared to the 'real' condenser return temperature plotted together with the assumed condenser supply temperature

### 5.2.2 Heat pump temperature level sensitivity

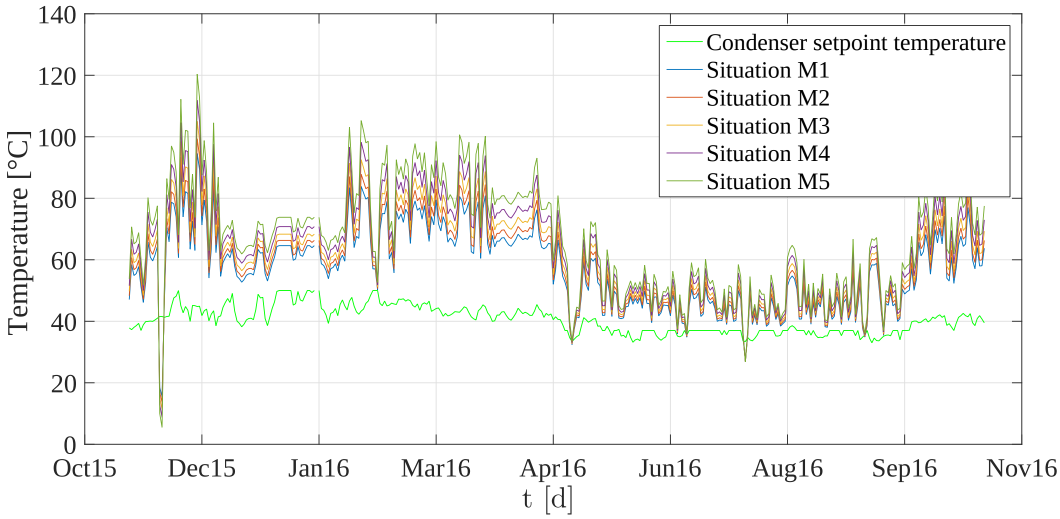


Figure 5.19: Variable mass flow in condensor in heating and cooling mode

Figure 5.19 shows 5 different situation wherein the mass flow varies. In order to understand the figure all five situations will be shortly commented. The original assumption of the mass flow is altered in step difference of $5m^3/s$. Starting with the first situation (the blue line), the mass flow in heating mode is kept the same. Whereas, the mass flow in cooling mode is increased with $10m^3/s$. In the four successive situations the mass flow is decreased with $5m^3/s$ each step. Meaning that in the second situation (orange line) the mass flow in heating mode is $5m^3/s$ lower and the mass flow in cooling mode is $5m^3/s$ higher compared to in the base case.
A decrease of the mass flow results in a decrease of the calculated condenser return temperature. However the further the mass flow decreases the less the return temperature decreases relative to previous mass flow changes. In cooling mode the change of mass flow seemingly does not affect the return temperature of the condenser that much. However, for the heating mode the new return temperature is visibly more affected.

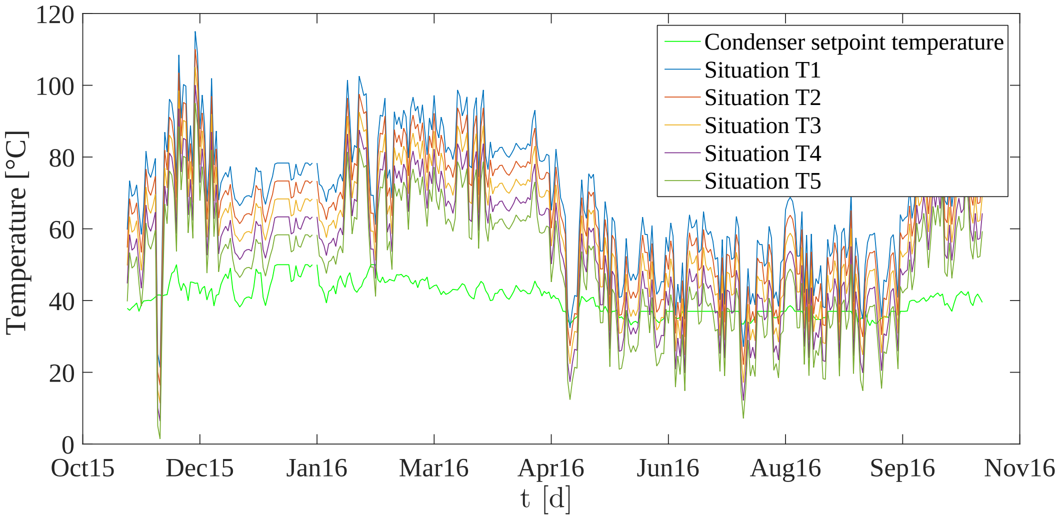


Figure 5.20: Variable condensor supply temperature in heating and cooling mode

Figure 5.20 shows 5 different situation wherein the supply temperature to the condenser varies. The same approach is applied as in the former Figure 5.19. This time only the supply temperature of the condenser is altered compared to the base case. The first situation describes the condenser return temperature in case of a supply temperature equal to the base case in heating mode and $+10°C$ in cooling mode. In the four successive situation the supply temperature is decreased with $5°C$ each step.

Both in heating and cooling mode the condenser return temperature is equally declining with every temperature step. Still the heating demand is deviating from the setpoint temperature to a great extend. In cooling mode it seems favorable to decrease the condenser supply temperature with $5°C$, in order to correspond to the condenser setpoint temperature.

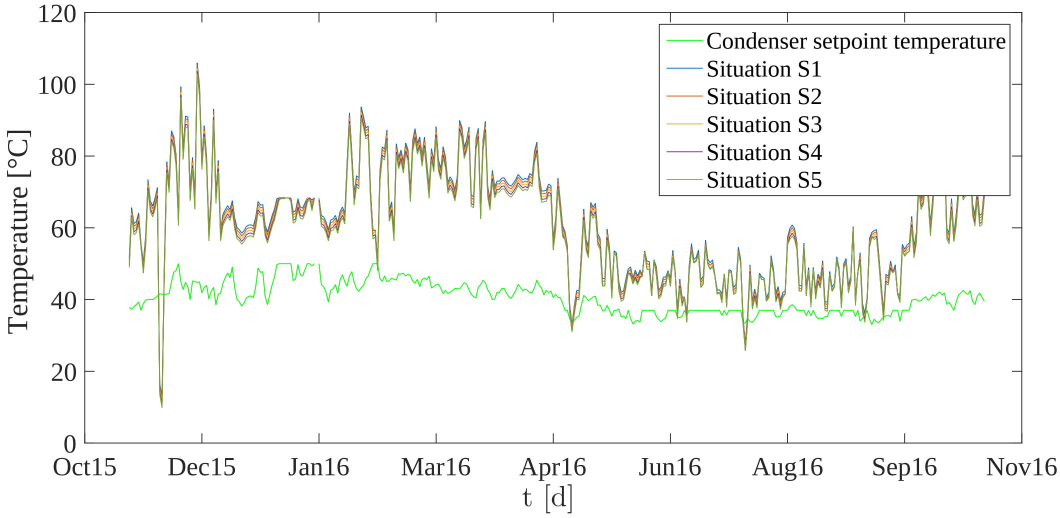


Figure 5.21: Changed condensor setpoint temperature in four different situations

Seemingly the supply temperature at the condenser side of the HP's should be lower during heating mode. Originally this one is designed for $32°C$

### 5.2.3 HP1 and HP2 performance

The designed performances of HP1 and HP2 in nominal heating and cooling mode are depicted in Figure 5.22- 5.25. From Figure 5.22 and 5.23 it can be concluded that the COP is independ from the part load it is operating in. While the carnot efficiency $\epsilon$ is slightly increasing when the part load is increasing. Upon checking the thermal efficiency of both HP1 and HP2, the resulting thermal efficiency is relatively constant, compared to the increasing heat production in Figure 5.24 and 5.25. This way the assumption of a constant thermal efficiency is proven right. The thermal efficiency per operating mode is given in Table 10. Note that the COP and $\epsilon$ are both higher for a heat pump in CM, when the temperature setpoint levels are lower.

Table 10: Nominal performances of HP2 based on Appendix .2

| | **HP1** | | **HP2** | | **Average** | |
|---|---|---|---|---|---|---|
| | CM | HM | CM | HM | CM | HM |
| $\eta_c$ | 0.65 | 0.4 | 0.66 | 0.4 | 0.65 | 0.4 |
| $\eta_h$ | 1.2 | 0.8 | 1.2 | 0.8 | 1.2 | 0.8 |

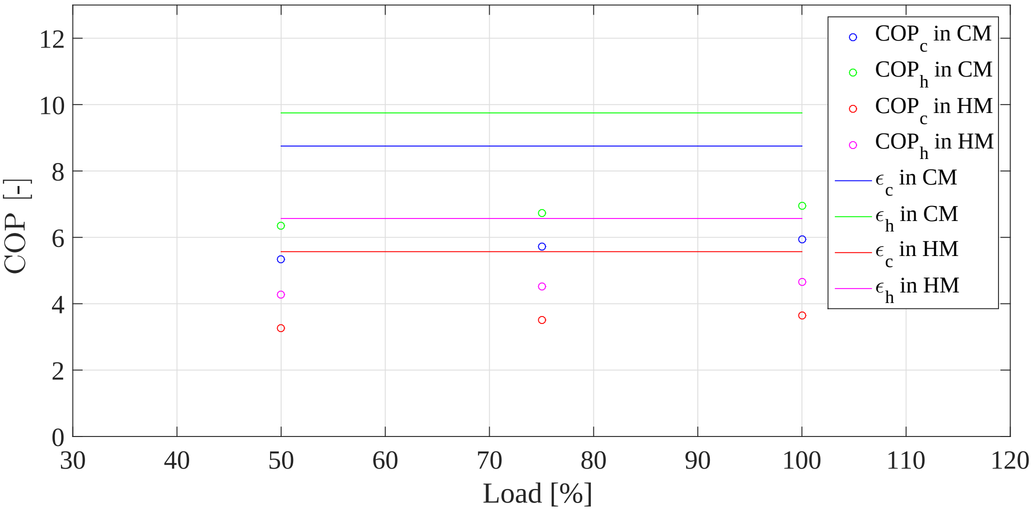


Figure 5.22: COP and $\epsilon$ of heat pump 1 based on heat pump specifications, see Appendix .2

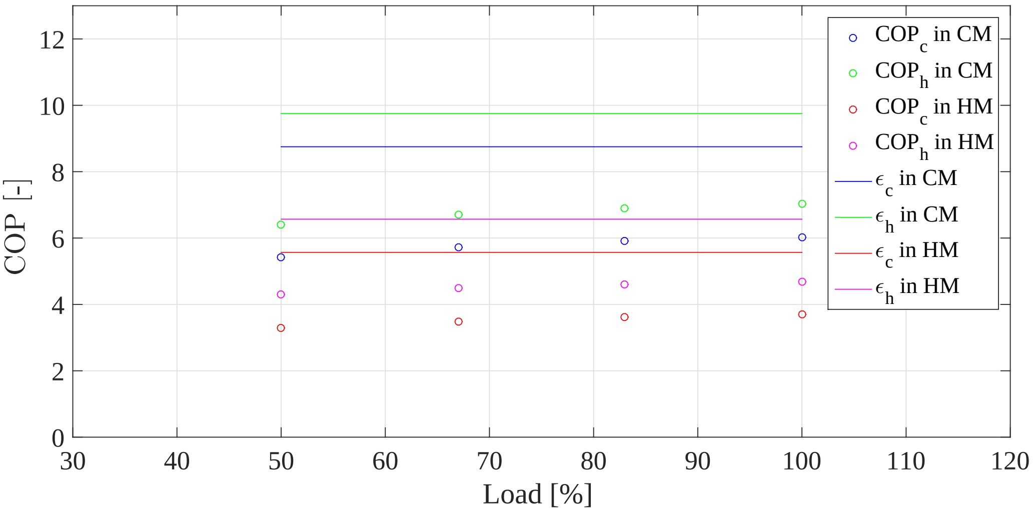


Figure 5.23: COP and $\epsilon$ of heat pump 2 based on heat pump specifications, see Appendix .2

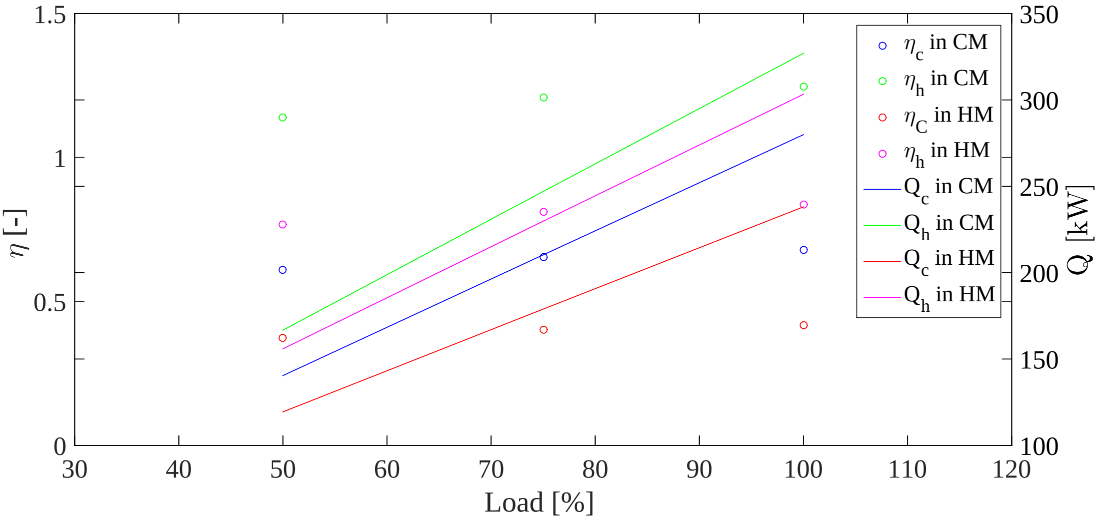


Figure 5.24: Q and $\eta$ of heat pump 1 based on heat pump specifications, see Appendix .2

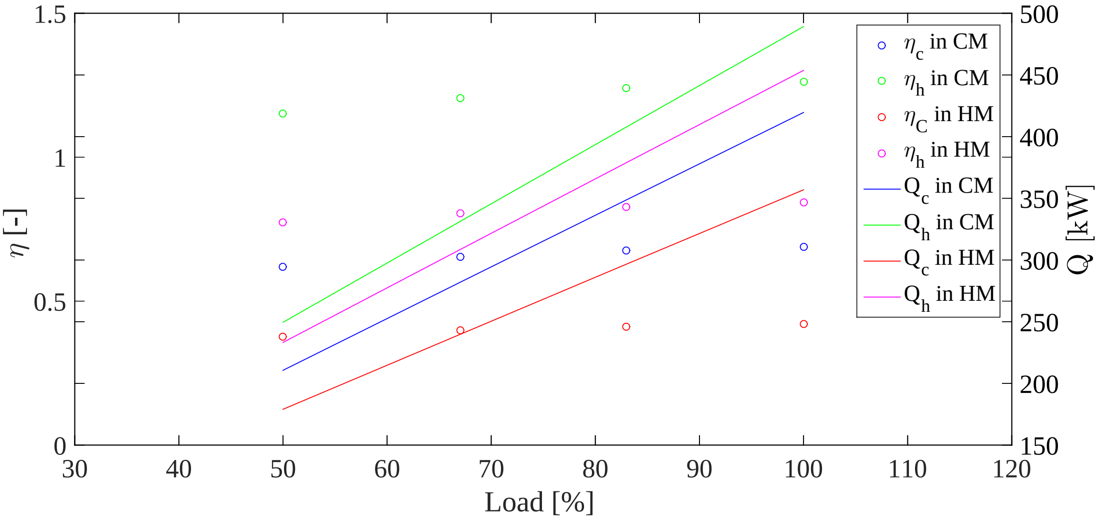


Figure 5.25: Q and $\eta$ of heat pump 2 based on heat pump specifications, see Appendix .2

In addition the HP performance in the period from 6 July until 13 July is analysed, see Figure 5.26- 5.28. Figure 5.26 shows the $T_H$ and $T_L$ based on the method as described in Section 4.2.3 and $T_H$ approximated in accordance with Figure 5.18. The real value for $T_H$ should lay somewhere in between these two values. Since the $T_H$ affects the carnot efficiency, the ratio of COP with carnot efficiency is evaluated for both the expected design value $T_H$ and the approximated $T_H$. The calculated $T_L$ is most of the time exceeding the designed temperature level of $2.5°C$, even the maximum designed temperature of $7°C$ is exceeded.

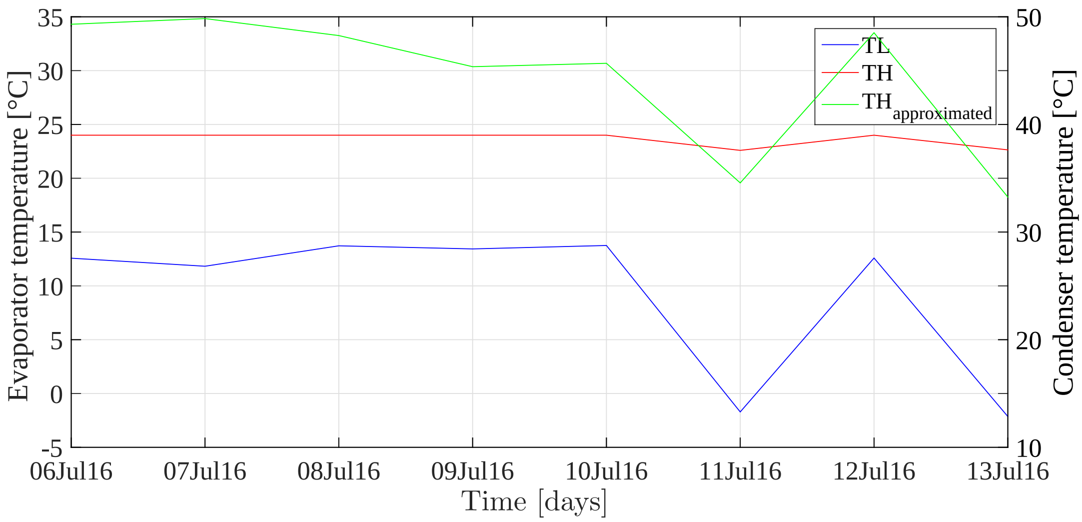


Figure 5.26: Calculated $T_L$ and $T_H$ based on design values and approximated real value over the period 06.07.2016-13.07.2016

Figure 5.27 shows the relation between the ratio of COP with carnot efficiency for heating compared to $T_H$. A higher ratio means that the HP performance is operating closer to the most optimal efficiency. Seemingly the performance of the HP is dropping significantly when $T_H$ is getting higher than $38°C$. Since the approximated condenser temperature over the entire year was already concluded to be higher than the designed values, it is suspectable that the HP system at the heating side is not running at its most optimal performance level.

The same analysis is performed at the cooling side of the HP system. Figure 5.28 shows the relation between the ratio of COP with carnot efficiency for cooling compared to $T_L$. Note that overal the cooling process is operating with less thermal efficient in comparison to the the heating process. The cooling process has a thermal efficiency between 0.4 and 0.55 and the heating process has a thermal efficiency between 0.75 and 0.95. As expected, the cooling performance of the HP is dropping significantly at the higher $T_L$ temperatures.

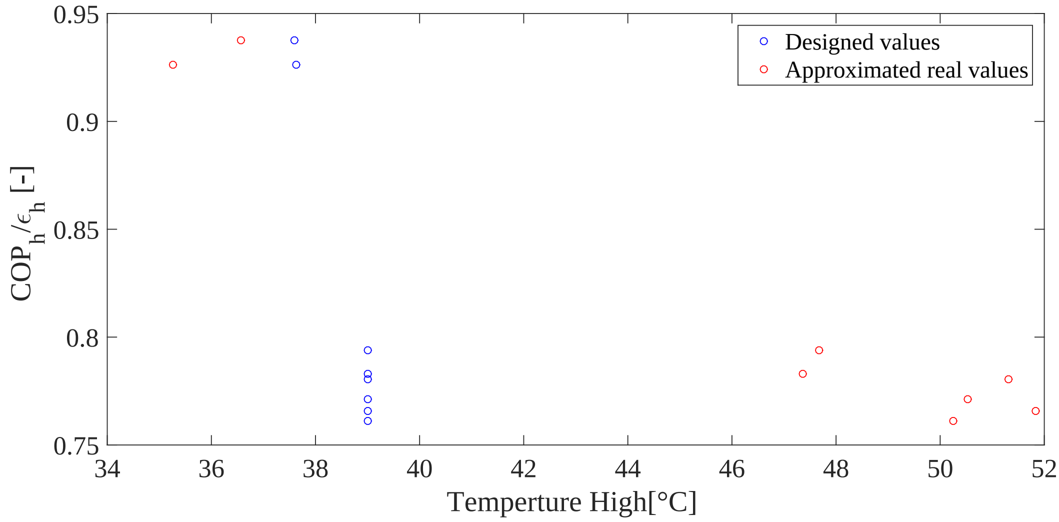


Figure 5.27: $COP_H/\epsilon_H$ compared to $T_H$ over the period 06.07.2016-13.07.2016 for both the designed values as the approximated real values

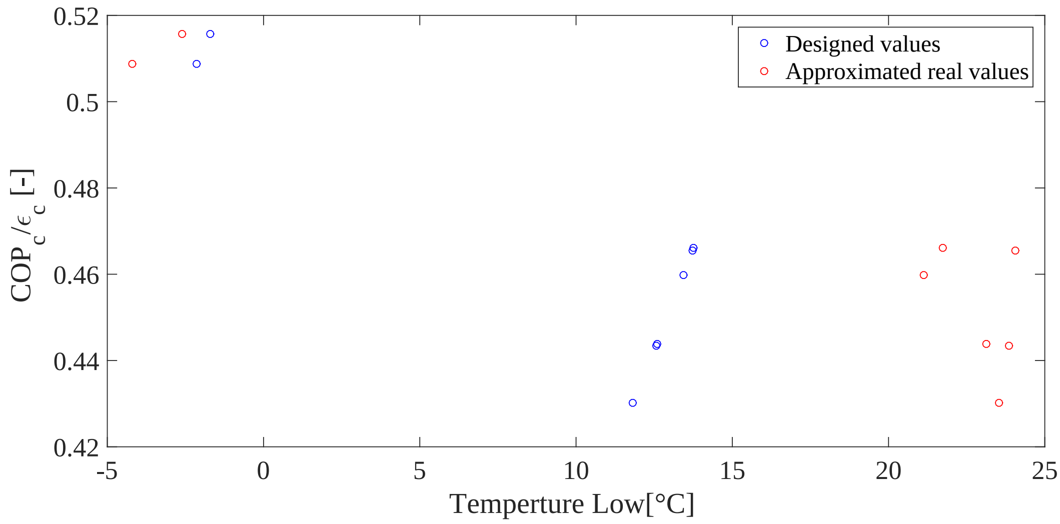


Figure 5.28: $COP_C/\epsilon_C$ compared to $T_L$ over the period 06.07.2016-13.07.2016 for both the designed values as the approximated real values

### 5.2.4 Heat pump performance

Heat pump heating and cooling performance is measured by its COP, as described in Section 2.3.2. Dar stated earlier research that the COP for the HP system equals 4.2 overall [10]. As discussed in Paragraph 2.3.2 the COP is related to the effective energy output and the additional energy input. The average COP of all three enumerated HP's is calculated for the whole year around for both cooling and heating, given Figure 5.29. On yearly bases this results in an average COP of 4.7 for heating and 4.0 for cooling. In addition the carnot efficiencies, for the cold and the heat provided, are depicted in Figure 5.29. The carnot efficiency is based on the assumption that the constant value of the thermal efficiency $\eta$ also counts for HP3. Note that the COP for cooling is relatively lower compared to the carnot efficiency. The COP for heating is matching the carnot efficiency to a much greater extend.

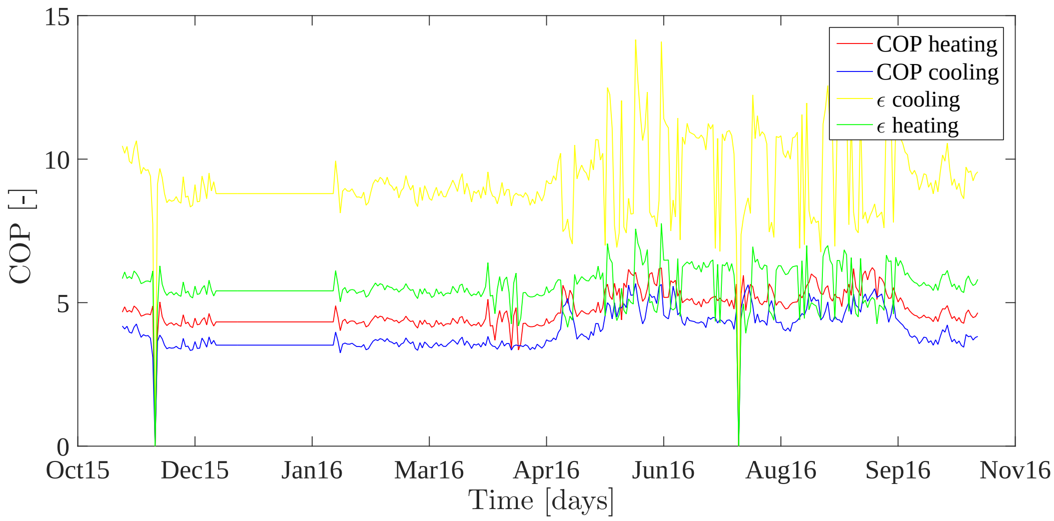


Figure 5.29: Average COP for both cooling and heating mode of the heat pump/chiller system

# 6 Discussion

In between the periods 11 December until 1 February and 5 until 19 April the measured data shows a significant error. This affects the performed energy analysis over the heating period. At several points within the data analysis, these measurement errors were excluded e.g. to find the real lineair relation of the heating demand compared to the outdoor temperature. Upon checking with the data provider, the error in the first period was appearing due to a upgrade failure in the energy monitoring system.

The provided data only gives energy in $kWh$ per day over the period from $1^{st}$ of November 2015 until $31^{st}$ of October 2016. This means that daily fluctuation in the heat and cold demand and supply by different system components was not able to be analysed. Apart from that, minor errors within the measurement devices might affect the current analysis. The energy meters are provided for class 2, this means a measuring tolerance of approximately 2% under ideal installation conditions. One abnormal measurement error occurs in energy meter 350.002.OE01. Apparently this meter is places too close to the heat pump, such that it does not measure an exact mixed water temperature. This leads to an measurement error of 4% instead. In theory the measured condenser heat (350.002.OE01) should measure the same value as the heat transmitted to the 320.001.OE02 in heating mode operation. However, one senses that energy meter 320.001.OE02 measures slightly higher energy than the energy meter 350.002.OE01.

Due to time constraints of the project, it was not possible to analyse the energy system performance into as much detail as wanted. For further research the imbalance of the borehole system should be investigated. Since it is important for the complete energy system that the soil temperature is constant in order to maintain the efficiency of the complete energy system. In order to investigate this, more measurements should be applied within the soil surrounding the boreholes.

# 7 Conclusion

*How is the energy use profile of the heating and cooling system?*
The annual heating demand is $2.460MWh$. The annual cooling demand is $1.010MWh$. Which is in line with the actual designed annual heating and cooling demand. The heating demand is peaking in the cold winter months, while the cooling is peaking in the warmer summer months when the outdoor temperature is exceeding $10°C$. The base load of the cooling demand is $2MWh/day$.

There is a strong lineair relation between the outdoor temperature and the heating heating demand. In case the outdoor temperature is increasing, the heat demand in linearly decreasing. Until an outdoor temperature of $10°C$, the cooling demand is not related to the outdoor temperature. In case the outdoor temperature is exceeding $10°C$, the cooling demand shows a lineair relation to the outdoor temperature. However this relation is seemingly less strong than the relation between the heat demand and the outdoor temperature, the cooling demand is linearly increasing when the outdoor temperature is increasing.

*Does the heating and cooling system perform as intended?*
In the warmer months April until September, the cooling load is peaking. At this time of the year the energy system generates surplus heat. $1171MWh$ of surplus heat is stored in boreholes. Overall this happens in case the energy system is running in cooling mode. Apart from the moments at which the system generates a surplus of heat, the energy system shows a strong lineair relation between the real heat demand and the actual supplied heat. Thus the heat supply is rather accurate. The lineair relation between the actual cold demand and the cold supply is seemingly weaker. Meaning that the cold supply is less accurate than the heat supply.

The PCM cold storage is annually $94MWh$ charged, while it is $100MWh$ discharged. This means there is an imbalance of approximately 5.6%. This seems rather acceptable. The PCM cold storage charged and discharged energy is only partly related to the outdoor temperature. This weak lineair relation is applicable whenever the outdoor temperature is exceeding $15°C$. In this state, the HP system is most likely running in cooling mode and cooling load most likely peaking. Seemingly the supply temperature in the cold distribution is rather instable in this state, which causes the need for the PCM storage to provide additional cold.

Since $1171MWh$ heat is yearly extracted from the borehole system, while only $304MWh$ is rejected, the borehole system is in great imbalanced. This might lead to a soil temperature drop, and subsequently an efficiency drop.

The energy input and output of the HP system shows a strong lineair relation. Meaning that the HP system is operation correctly. The yearly averaged COP for heating is 4.7. The yearly averaged COP for cooling is 4.0. Seemingly the temperature levels at both evaporator and condenser side seem to be exceeding the designed values.

*What potential optimization possibilities do exist for the advanced heating and cooling system that is used at HiB?*
The HP system analysis gave an indication upon the temperature levels of the system. Seemingly the designed evaporator temperature of $2.5°C$ is quite easily exceeded. These higher evaporator temperature might be the cause of the relatively low COP for cooling. Therefore it is interesting to investigate how this temperature can be declined. Is it a solution to speed up the mass flow in such a way that the evaporator supply temperature drops. Or is it for example possible to decrease the heat extracted from the borehole system in order to keep the evaporator supply temperature down? This last option might also help balancing the heat extraction and rejection from the boreholes.

As well as the evaporator temperature, the condenser temperature should be brought back to a lower value in order to improve the energy efficiency of the HP system. In combination with trying to restore the balance in the borehole system, it would be interesting to see whether the more heat can be extracted from the space heating return temperature in order to realize a lower condenser supply temperature. In a small notification on the COP and $\epsilon$ of HP1 and HP2, it was stated that these values were higher in CM. This is related to the lower temperature setpoint levels at the condenser side. In terms of energy efficiency therefore it would be better to run the HP system in CM more often. Since the HP system is now only operating in CM during night for maintenance charging or in case the outdoor temperature is exceeding $15°C$, and the outdoor temperature is fairly little exceeding that temperature, the HP system is most often operating in HM. In combination with the fact that the HP system is over-dimensioned for the heating supply, it would be interesting to find out if the setpoint for activating the CM can be adapted to a lower activation temperature. However this will only be relevant in case it is managed to increase the COP for cooling as mentioned above. Since the COP for heating is better than for cooling for the current operating system.

# References

[1] MOPAE, "White paper on norway's energy policy: Power for change," 2016.

[2] Statistisk and Sentralbyra, "Energy balance, 2015, preliminary figures," 2015.

[3] N. Djuric, V. Novakovic, and F. Frydenlund, "Improved measurements for better decision on heat recovery solutions with heat pumps," *International Journal of Refrigeration*, vol. 35, no. 6, pp. 1558–1569, 2012.

[4] N. Djuric, V. Novakovic, and F. Frydenlund, "Performance estimation and documentation of an integrated energy supply solution," *Energy Procedia*, 2011.

[5] O. Stavset and H. Kauko, "Energy use in non-residential buildings - possibilities for smart energy solutions," Tech. Rep. 1.1, SINTEF Energy Research, 2015.

[6] S. Altomonte, P. Rutherford, and R. Wilson, "Human factors in the design of sustainable built environments," *Intelligent Buildings International*, vol. 7, no. 4, pp. 224–241, 2015.

[7] H. Kauko, O. Stavset, M. Bantle, and N. Nord, "Energy use in norwegian non-residential buildings: building regulations, calculations and measurements," 2015.

[8] I. F. Nordang, "Analyse av varme- kjølesystemet ved powerhouse kjørbo," tech. rep., Norges teknisk-naturvitenskapelige universitet Institutt for energi- og prosessteknikk, 2015.

[9] I. F. Nordang, "Analysis of the thermal energy supply system at powerhouse kjørbo, sandvika," tech. rep., Norwegian University of Science and Technology, 2014.

[10] U. Dar, "Høgskolen i bergen energisentral," 27 November 2014 2014.

[11] C. Schlemminger, M. J. Alonso, U. Dar, E. Gronnesby, and I. Claussen, "Evaluation of pcm-cold-storage at hib," 2015.

[12] M. Jokiel, "Development and performance analysis of an object oriented model for phase change mateiral thermal storage," tech. rep., SINTEF Energy Research NTNU Department of Thermal Energy, 01-07-2016 2016.

[13] C. P. 10.3, "Wolfram demonstratrions project," 2015.

[14] S. R. Turns, *Thermodynamics: Concepts and Applications.* Cambridge University Press, 2006.

[15] G. Lorentzen, "The use of natural refrigerants: a complete solution to the cfc/hcfc predicament," *International Journal of Refrigeration*, vol. 18, no. 3, pp. 190–197, 1995.

[16] R. K. Ambs and T. G. Kiessel, "Geothermal heat exchanger and heat pump circuit," 1998.

[17] Z. Ure, MCIBSE, MASHRAE, M. R, and MIIR, "Phase change material (pcm) based energy storage materials and global application examples," 2013.

[18] X. Q. Zhai, X. L. Wang, T. Wang, and R. Z. Wang, "A review on phase change cold storage in air-conditioning system: Materials and applications," *Renewable and Sustainable Energy Reviews*, vol. 22, pp. 108–120, 2013.

[19] B. Welsch, W. Rühaak, D. O. Schulte, K. Bär, and I. Sass, "Characteristics of medium deep borehole thermal energy storage," *International Journal of Energy Research*, vol. 40, no. 13, pp. 1855–1868, 2016.

[20] X. Q. Zhai, M. Qu, X. Yu, Y. Yang, and R. Z. Wang, "A review for the applications and integrated approaches of ground-coupled heat pump systems," *Renewable and Sustainable Energy Reviews*, vol. 15, no. 6, pp. 3133–3140, 2011.

[21] W. Wu, T. You, B. Wang, W. Shi, and X. Li, "Evaluation of ground source absorption heat pumps combined with borehole free cooling," *Energy Conversion and Management*, vol. 79, pp. 334–343, 2014.

[22] Z. Zhou, S. Wu, T. Du, G. Chen, Z. Zhang, J. Zuo, and Q. He, "The energy-saving effects of ground-coupled heat pump system integrated with borehole free cooling: A study in china," *Applied Energy*, vol. 182, pp. 9–19, 2016.

[23] IDEA, "About district energy: What is district energy?," Accesed: 22-10-2016.

[24] S. B. Riffat, H. A. Shehata, A. T. Howarth, and P. S. Doherty, "Novel evaporative air cooler," *International Journal of Ambient Energy*, vol. 21, no. 2, pp. 97–108, 2000.

[25] O. Stavset and H. Kauko, "Energy use in non-residential buildings -possibilities for smart energy solutions," tech. rep., SINTEF, 05-02-2015 2015.

[26] SWECO, "Funksjonsbeskrivelse, 320.001 hovedkurs varme," 2015.

[27] SWECO, "Funksjonsbeskrivelse, 350.001- 350.003 energicentral ve," tech. rep., 2015.

# Appendices

## .1 Hydronic system symbols

As can be seen from Figure .1, there are a lot of different types of valves and system elements. Each type of valve has its own functionality. A black valve means that it is closed most of the time. When and how to open or close a valve depends on the control system. For example a valve can be manually opened or closed hand operated via a plug or automatically pressure driven. For this last option the pressure controlling device is connected into the middle of the valve. In case some hydraulic characteristics of the flow are measured within the valve, a measurement device is connected to the center of the valve. Loss from the valves several different measurements are able to be performed within the system as well. This is done both in serie as parallel to the mass flow. Related to these measurements, the retrieved data can be translated into a signal to modify the system mode and thereby control the energy flow.

There are six system elements frequently applied within the energy supply system at HiB. Together the four elements; condensor, compressor, evaporator, and expansion valve form the heat pump/chiller system. Two other returning elements are the pump and the heat exchanger.

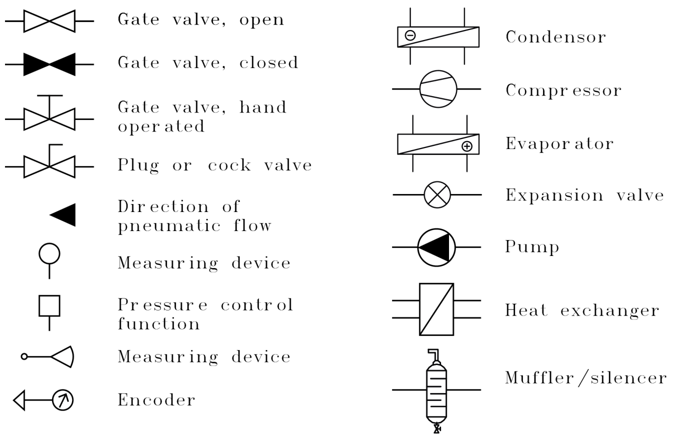


Figure .1: Legend of the applied symbols in the energy system scheme

## .2 Heat pump/chiller system specifications

### Heat pump 1

# Technical Specification

## Pos. 1] 1 x Chiller Type FX GC PP 260 NH3 variable speed drive

### ● Technical details

Survey of technical details

| | | | |
|---|---|---|---|
| Mode of operation | : | Cooling | Heating |
| Rated speed | : | 725-1600 min-1 | 725-1470 $min^{-1}$ |
| Refrigeration capacity acc. to EN 12900 and DIN 8976 | : | 292 kW | 237 kW |
| Power consumption | : | 50,2 kW | 65.2 kW |
| Condenser rating | : | 342,2 kW | 302.2 kW |
| Type sec. refrigerant | : | Propylene Glycol 30% | |
| Sec. refrigerant inlet | : | 10 °C | 10 °C |
| Sec. refrigerant outlet | : | 5 °C | 5 °C |
| Sec. refrigerant outlet min. / max. | : | 2 °C / 10 °C | - |
| Type cooling/heating medium | : | Water | |
| Cooling/heating medium inlet | : | 27 °C | 42 °C |
| Cooling/heating medium outlet | : | 32 °C | 50 °C |
| Heating medium outlet min/max | : | - | 30 °C / 50 °C |
| Flow rate evaporator | : | 52,6 $m^3/h$, constant flow | 44.1 $m^3/h$, constant flow |
| Flow rate condenser | : | 58,8 $m^3/h$, constant flow | 52.6 $m^3/h$, constant flow |

The following values for dimensions, weights and charges are preliminary. Final binding data according to the latest version of the general drawing only.

| | | |
|---|---|---|
| Length approx. | : | **3100 mm (without power panel, measurements of the power panel: height=2100mm,width=1200mm,depth=600mm)** |
| Width approx. | : | **1600 mm without spring elements, with spring elements=1800mm** |
| Height approx. | : | **2200 mm** |
| Refrigerant charge approx | : | 37 kg |
| Oil charge approx | : | 12 l |
| Operating weight approx | : | **4200 kg** |

### ● Package

| | | |
|---|---|---|
| Grasso Ammonia-Liquid Chiller Type | : | FX GC PP 260 NH3 |
| Description | : | Ammonia liquid Chiller with reciprocating compressor, evaporator and condenser in execution as plate type heat exchanger, as a compact, complete factory packaged unit, ready for connection on site, dismounted for transport |
| Compressor Configuration | : | Reciprocating compressor Grasso 410, open-type execution with multi-stage capacity control by cylinder offloading. Available part load steps in %: 50/75/100. The applicable part load steps depend on the operating conditions. The compressor is equipped with integrated gas suction filter, solenoid valves for capacity control, oil heater, suction and discharge oil filters, back-pressure independent overflow valve and partially loaded start. |
| Compressor type | : | Grasso 410 |
| Design pressure chiller | : | 25 bar |
| Type liquid separator | : | horizontal |
| Valves on suction side | : | Stop valve(s) on suction side |
| Valves on discharge side | : | Stop valve(s) on discharge side |
| Wiring | | |
| Painting | : | Protective paint system S 2.15 acc. to EN ISO 12944-5 for environmental conditions C2 acc. to EN ISO 12944-2. Designed for machine room temperatures between 5°C and 40°C. |
| Color | : | RAL 5014 pigeon blue (standard) |
| Insulation type | : | Suction pipe and liquid separator insulated with PUR and coated with Aluminium sheets. The Insulation is designed for 20°C machine |

room temperature and 70% humidity.

Control unit

| | | |
|---|---|---|
| Controller type | : | Chiller control GSC (216 SER) with TP 605 CQ 5,7" color graphic display with Windows CE© and capacity control via the secondary refrigerant (cooling mode) and switchable with an external signal from the costumer to the capacity control via the heating outlet temperature (heating mode) . Limitations: suction pressure, condenser pressure, motor current. 11 different operating modes available, incl. auto, remote, service etc. Main functions of the PLC: 1. Control of secondary refrigerant inlet resp. outlet temperature 2. Electronic unit protection and record of operating hours 3. Release contacts for secondary refrigerant pump and condenser system 4. Operating information, all values of analogue inputs were displayed 5. Failure information shown as text on the display and indicated by an information lamp 6. Potential-free status report of the unit (unit ready, unit in operation, multiple fault).7. data logging function and trend report |
| Controller Display | : | Display separate arranged in panel door |
| Controller arrangement | : | Integrated in power panel |
| Controller communication | : | Modbus TCP, acc. Grasso description |
| Display language | : | Norwegian |
| Pressure sensors | : | Standard sensors |
| Number of pressure sensors: | : | 3 |
| Mounting of pressure sensors | : | in tube |
| Number of temperature sensors: | : | 4 |
| Additional temperature sensors | : | none |
| Selection flow switch secondary refrigerant | : | Mechanical flow switch, delivered loose |
| Selection flow switch cooling medium | : | without flow switch |

Motor, manufacturer ABB

| | | |
|---|---|---|
| Motor type | : | Low voltage motor IP 55 |
| Number of motors | : | 1 |
| Type of construction | : | IMB 3 |
| Number of poles | : | 4 |
| Degree of protection | : | IP 55 |
| Drive motor rating | : | 90 kW |
| Voltage | : | 3 x 400 V ± 5% / 50 Hz |
| Frequency | : | 50 Hz |
| Switch on mode | : | Variable speed drive (VSD), brand for frequence inverter is Danfoss |
| Type of Power Supply | : | Power Panel, IP 54 protection, complete wired and tested, main switch, emergency switch, contactors for oil heater, thermal over current release and safety fuses, power fuses, control transformer with double control safety, primary and secondary, 24 V AC current supply |
| Cable entry point | : | at the bottom with cables in Aluminium |
| Type of net | : | TN-L1,L2,L3;N+PE |

Evaporator

| | | |
|---|---|---|
| Design Pressure Evaporator | : | 16 bar |

Plate heat-exchanger of modular semi welded design; medium ports are completed with flanges and counter flanges.

| | | |
|---|---|---|
| Cassette material evaporator | : | AISI 304 |
| Pressure drop | : | 30,2 kPa |

Drip tray evaporator

Condenser

| | | |
|---|---|---|
| Design Pressure Condenser | : | 25 bar |

Plate heat-exchanger of modular semi welded design; medium ports are completed with flanges and counter flanges.

| | | |
|---|---|---|
| Cassette material condenser | : | AISI 316 |

| | | |
|---|---|---|
| Pressure drop | : | 28 kPa |
| Safety devices | | |
| Type | : | Double safety valve with change over valve |
| Safety valve(s) acc. to PED | : | 1 |
| Number of overflow valves | : | 1 |
| Approval and documentation | | |
| Approval for Chiller Unit | : | Work's Certificate, Certificate of Conformity acc. to Machines Directive 98/37/EG, Certificate of Conformity acc. to Pressure Equipment Directive (PED) 97/23/EG. Calculation and manufacturing acc. to AD 2000 and EN 378, module H1. |
| Approval pressure equipment | : | Certificate of Conformity acc. to Pressure Equipment Directive (PED) 97/23/EG. Calculation and manufacturing acc. to AD 2000 and EN 378. |
| Non destructive Testing | : | 10 % non destructive welding test acc. to EN 1435 |
| Documentation consisting of | : | Documentation and CD-ROM consisting of |
| Language of the documentation | : | English/Norwegian (PED related language) |
| Sets of documentation | : | 2 |
| *** Options (included in price) *** | | |
| -Spring Elements | | |
| -Remote adjustable set point | | |
| -Quick shut off valves | | |
| -additional option 1 | : | Insulation of the warm side with mineral wool / Aluminium |
| -additional option 2 | : | Trip tray under the complete chiller |
| -additional option 3 | : | Sequence control module |
| -additional option 4 | : | TAG-Numbers for control panel, acc. Grasso Standard, for explanation the connection between MODBUS and CTS-system |
| -additional option 5 | : | Energy management system, manufacturer Janitza, type UMG 96S, with interface MODBUS RTU |
| -additional option 6 | : | Additional display in the front of the power panel for showing pressures and temperatures |

## ● Exclusions

| | | |
|---|---|---|
| Exclusion from scope of supply | : | Foundations, reassembling onsite, pipes on water side, Spare parts and special tools, Refrigerant and lubricating oil, wiring between the chillers for the sequence control, performance test and start up, everything what is not especially mentioned. |

# 200 kW

- Komp: 1500 o/min
- Ydelse: 280 kW v. $^{2.5}/_{34}$ °
- Kond. Ydelse: 377 kW – " –

200kW

GEA

Refrigeration Division

GCPP 260

Nominal cooling

Pos. 1.

**GEA Grasso GmbH**
Holzhauser Straße 165
13509 Berlin
Germany
Phone: +49 (0)30 - 43 592 6
Fax: +49 (0)30 - 43 592 777
E-mail: info@grasso.de
Website: www.grasso-global.com

## Comsel - Grasso Compressor Selection Software

| | |
|---|---|
| Print date/time | 13-07-2011 . 12:13 |
| Program version | 3.10.00 Build 00 Valid until 31.12.2011 |

TECHNICAL DATA (Standard package)

| | | |
|---|---|---|
| Reciprocating compressor package | 1 x Grasso 410 | |
| Refrigerant | $NH_3$ | |
| Speed | 1500 | (/min) |
| Rotation frequency | 50 | (Hz) |
| Evap. temp. | 2,5 | (°C) |
| Superheat | 0,0 | (K) |
| Superheat useful | 0,0 | (K) |
| Cond. temp. | 34,0 | (°C) |
| Subcooling | 0,0 | (K) |
| Power consumption | 47,1 | (kW) |
| Refrigerating capacity | 279,9 | (kW) |
| COP = Qo/Pe | 5,95 | (-) |
| Oil separator | OS4 | |
| Possible steps | 50/75/100 | (%) |

10/5°C

27/32°C

| Partload [%] | Cyl. [-] | Pe [kW] | Qo [kW] |
|---|---|---|---|
| 100 | 4 | 47,1 | 279,9 |
| 75 | 3 | 36,7 | 210,3 |
| 50 | 2 | 26,3 | 140,4 |

| | | | | | |
|---|---|---|---|---|---|
| Quotation number | : 2011018433-1 | Customer | : GEA Grasso GmbH | TLC Version | : 3.1.23.Prof |
| Item number | : 1 | Project | : Hoyskolen Bergen | | |
| Version number | : 1 | Calculator | : Reichardt | | |
| Section name | : 1 | Date | : 21.09.2011 | | |
| Inquiry item | : Pos. 1 | Candidate | : Kandidat0125 | | |

| | | |
|---|---|---|
| Media | :Ammonia Gravity | PROP.GLYCOL 30% |
| Evaporating temperature | [°C]:2,50 | |
| Inlet pressure | [bara]:4,73 | |
| Temperature In-->Out | [°C]:2,50 --> 2,50 | 10,00 --> 5,00 |
| Mass flow rate (Vapor/Overall) | [kg/h]:790,0 / 908,5 | 51295,3 |
| Volumetric flow rate | [m³/h]:208,845 | 49,513 |

| | | |
|---|---|---|
| Density | [kg/m³]: | 1036,00 |
| Specific heat capacity | [J/kg K]: | 3865,0 |
| Heat conductivity | [W/m K]: | 0,455 |
| Dyn. Viscosity | [m Pa s]: | 5,799 |

| | | |
|---|---|---|
| Heat load | [kW]: | 275,000 |
| Direction of flow | : | Cocurrent flow |
| Log. Temperature difference | [°C]: | 4,55 |
| Heat transfer surface | [m²]: | 26,792 |
| Number of plates Installed/Maximum | : | 102 / 117 |
| k-value (Real) / Theoretic | [W/m²*K]: | 2255,4 / 2535,0 |
| Excess surface | [%]: | 12,40 |
| Fouling resistance | [m² K/W]: | 0,00005 |

| | | |
|---|---|---|
| No.of passes x (No.of gap) | :1 x 50 PHSH | 1 x 50 SHPH |
| Port velocity In/Out | [m/s]:0,051 / 7,386 | 1,753 / 1,749 |
| Gap velocity | [m/s]: | SHPH: 0,248 |
| Pressure loss Calculated | [bar]:0,010 | 0,323 |

| | | |
|---|---|---|
| Working temperature Min./Max. | [°C]:0,00 / 40,00 | 0,00 / 40,00 |
| Design temperature Min./Max. | [°C]:0,00 / 40,00 | 0,00 / 40,00 |
| Working pressure Min./Max. | [barg]:0,00 / 4,55 | 0,00 / 6,00 |
| Design pressure Min./Max. | [barg]:0,00 / 16,00 | 0,00 / 16,00 |
| Testing pressure | [barg]:17,60 | 20,00 |
| Content | [l]:40,411 | 40,411 |

| | | |
|---|---|---|
| Plate material / Plate thickness | [mm]:1.4301 ( AISI 304) / 0,6 | |
| Ring gasket | :CR-LT | Laser welded |
| Field gasket | :Laser welded | CR-LT |
| Gasket fixing | :Clip on (glueless) | Clip on (glueless) |

| | |
|---|---|
| Apparatus name | :ThermoLine TL0250 TCGL - 750 |
| Pressure vessel code / Design code | :PED 97 / 23 /EC module H1 / AD-Merkblatt 2000 |
| Weight Empty/Filled | [kg]:714 / 781 |
| Length x Width x Height / Initial dimen. | [mm]:750,0 x 550,0 x 1140,0 / 359,6 - 355,4 |
| Frame material | :1.0570 / painted RAL5018 |

Remark

| Pos | IN/OUT | Media | Temp | Type | Code | Form | DN | PN | Material |
|---|---|---|---|---|---|---|---|---|---|
| K1 | Out | PROP.GLYCOL 30% | 5,00 | Stud bolts | DIN 2501 | C | 100 | 16 | EPDM-NT |
| K2 | Out | Ammonia | 2,50 | Stud bolts | DIN 2501 | N | 100 | 40 | 1.0038 |
| K3 | In | Ammonia | 2,50 | Stud bolts | DIN 2501 | N | 100 | 40 | 1.0038 |
| K4 | In | PROP.GLYCOL 30% | 10,00 | Stud bolts | DIN 2501 | C | 100 | 16 | EPDM-NT |
| D1 | | | | | | | | | |
| D2 | | | | | | | | | |
| D3 | Out | Oil drainage | 2,50 | Welding neck flange | DIN 2635 | N | 40 | 40 | 1.0460 |
| D4 | | | | | | | | | |

| | | | | | |
|---|---|---|---|---|---|
| Quotation number | : 2011018433-1 | Customer | : GEA Grasso GmbH | TLC Version | : 3.1.23.Prof |
| Item number | : 2 | Project | : Hoyskolen Bergen | | |
| Version number | : 1 | Calculator | : Reichardt | | |
| Section name | : Nominal cooling | Date | : 20.09.2011 | | |
| Inquiry item | : Pos. 2 | Candidate | : Kandidat0112 | | |

| | | | |
|---|---|---|---|
| Media | | :Water | Ammonia |
| Condensation temperature | [°C]: | | 34,00 |
| Inlet pressure | [bara]: | | 13,14 |
| Temperature In-->Out | [°C]: | 27,00 --> 32,00 | 130,00 --> 34,00 |
| Mass flow rate (Vapor/Overall) | [kg/h]: | 54777,9 | 817,9 |
| Volumetric flow rate | [m³/h]: | 55,029 | 120,389 |

| | | |
|---|---|---|
| Density | [kg/m³]: | 995,43 |
| Specific heat capacity | [J/kg K]: | 4219,7 |
| Heat conductivity | [W/m K]: | 0,617 |
| Dyn. Viscosity | [m Pa s]: | 0,788 |

| | | |
|---|---|---|
| Heat load | [kW]: | 321,000 |
| Direction of flow | : | Counter flow |
| Log. Temperature difference | [°C]: | 4,73 |
| Heat transfer surface | [m²]: | 17,049 |
| Number of plates Installed/Maximum | : | 65 / 93 |
| k-value (Real) / Theoretic | [W/m²*K]: | 3184,2 / 3585,4 |
| Excess surface | [%]: | 12,60 |
| Fouling resistance | [m² K/W]: | 0,00004 |

| | | | |
|---|---|---|---|
| No.of passes x (No.of gap) | : | 1 x 32 SHSH | 1 x 32 SHSH |
| Port velocity In/Out | [m/s]: | 1,945 / 1,948 | 4,258 / 0,049 |
| Gap velocity | [m/s]: | SHSH: 0,337 | |
| Pressure loss Calculated | [bar]: | 0,246 | 0,007 |

| | | | |
|---|---|---|---|
| Working temperature Min./Max. | [°C]: | 0,00 / 32,00 | 0,00 / 130,00 |
| Design temperature Min./Max. | [°C]: | 0,00 / 130,00 | 0,00 / 135,00 |
| Working pressure Min./Max. | [barg]: | 0,00 / 6,00 | 0,00 / 23,00 |
| Design pressure Min./Max. | [barg]: | 0,00 / 10,00 | 0,00 / 25,00 |
| Testing pressure | [barg]: | 12,50 | 27,50 |
| Content | [l]: | 32,998 | 32,998 |

| | | | |
|---|---|---|---|
| Plate material / Plate thickness | [mm]: | 1.4404 (AISI 316L) / 0,6 | |
| Ring gasket | : | Laser welded | CR-HT |
| Field gasket | : | CR-HT | Laser welded |
| Gasket fixing | : | Clip on (glueless) | Clip on (glueless) |

| | | |
|---|---|---|
| Apparatus name | : | ThermoLine TL0250 TDGL - 750 |
| Pressure vessel code / Design code | : | PED 97 / 23 /EC module H1 / AD-Merkblatt 2000 |
| Weight Empty/Filled | [kg]: | 683 / 735 |
| Length x Width x Height / Initial dimen. | [mm]: | 750,0 x 550,0 x 1140,0 / 279,5 - 279,5 |
| Frame material | : | 1.0570 / painted RAL5018 |

Remark

| Pos | IN/OUT | Media | Temp | Type | Code | Form | DN | PN | Material |
|---|---|---|---|---|---|---|---|---|---|
| K1 | Out | Water | 32,00 | Stud bolts | DIN 2501 | C | 100 | 40 | EPDM-NT |
| K2 | In | Ammonia | 130,00 | Stud bolts | DIN 2501 | N | 100 | 40 | 1.0038 |
| K3 | Out | Ammonia | 34,00 | Stud bolts | DIN 2501 | N | 100 | 40 | 1.0038 |
| K4 | In | Water | 27,00 | Stud bolts | DIN 2501 | C | 100 | 40 | EPDM-NT |
| D1 | | | | | | | | | |
| D2 | | | | | | | | | |
| D3 | | | | | | | | | |
| D4 | | | | | | | | | |

# 200 kw

- komp: 1710 %/min

- Ytelse: 315 kw v $^{2,5}/_{34°c}$

- Kond Ytelse: ≈ 370 kw -"-

Refrigeration Division

**GEA Grasso GmbH**

Holzhauser Straße 165
13509 Berlin
Germany
Phone: +49 (0)30 - 43 592 6
Fax: +49 (0)30 - 43 592 777
E-mail: info@grasso.de
Website: www.grasso-global.com

**Comsel - Grasso Compressor Selection Software**

| | | |
|---|---|---|
| Print date/time | 22-09-2011 . 11:37 | |
| Program version | 3.12.00 Build 01 Valid until 31.12.2011 | |

| | | |
|---|---|---|
| TECHNICAL DATA (Agilium package) | | |
| Reciprocating compressor package | 1 x Grasso 410 | |
| Refrigerant | $NH_3$ | |
| Speed | 1800 | (/min) |
| Rotation frequency | 50 | (Hz) |
| Evap. temp. | 2,5 | (°C) |
| Superheat | 0,0 | (K) |
| Superheat useful | 0,0 | (K) |
| Cond. temp. | 34,0 | (°C) |
| Subcooling | 0,0 | (K) |
| Power consumption | 56,9 | (kW) |
| Refrigerating capacity | 331,9 | (kW) |
| COP = Qo/Pe | 5,83 | (-) |
| Oil separator | OS4 | |
| Possible steps | 25/33/40/50/60/70/80/90/100 | (%) |

| Partload [%] | Speed (Cyl.) [/min] ([-]) | Pe [kW] | Qo [kW] |
|---|---|---|---|
| 100 | 1800 (4) | 56,9 | 331,9 |
| 90 | 1620 (4) | 50,9 | 300,8 |
| 80 | 1440 (4) | 45,2 | 269,3 |
| 70 | 1260 (4) | 39,5 | 237,3 |
| 60 | 1080 (4) | 34,0 | 204,8 |
| 50 | 900 (4) | 28,5 | 171,8 |
| 40 | 720 (4) | 23,0 | 138,3 |
| 33 | 600 (4) | 19,3 | 115,7 |
| 25 | 600 (3) | 15,1 | 86,8 |

1710 $^0$/min ≙ 315 kW

| | | | | | |
|---|---|---|---|---|---|
| Quotation number | : 2011018433-1 | Customer | : GEA Grasso GmbH | TLC Version | : 3.1.23.Prof |
| Item number | : 1 | Project | : Hoyskolen Bergen | | |
| Version number | : 1 | Calculator | : Reichardt | | |
| Section name | : 1 | Date | : 21.09.2011 | | |
| Inquiry item | : Pos. 1 | Candidate | : Kandidat0123 | | |

thermowave Gesellschaft für Wärmetechnik mbH

| | | | |
|---|---|---|---|
| Media | | :Ammonia Gravity | PROP.GLYCOL 30% |
| Evaporating temperature | [°C]: | 2,50 | |
| Inlet pressure | [bara]: | 4,73 | |
| Temperature In-->Out | [°C]: | 2,50 --> 2,50 | 10,00 --> 5,00 |
| Mass flow rate (Vapor/Overall) | [kg/h]: | 904,9 / 1040,6 | 58756,5 |
| Volumetric flow rate | [m³/h]: | 239,222 | 56,715 |

| | | | |
|---|---|---|---|
| Density | [kg/m³]: | | 1036,00 |
| Specific heat capacity | [J/kg K]: | | 3865,0 |
| Heat conductivity | [W/m K]: | | 0,455 |
| Dyn. Viscosity | [m Pa s]: | | 5,799 |

| | | |
|---|---|---|
| Heat load | [kW]: | 315,000 |
| Direction of flow | : | Cocurrent flow |
| Log. Temperature difference | [°C]: | 4,55 |
| Heat transfer surface | [m²]: | 26,792 |
| Number of plates Installed/Maximum | : | 102 / 117 |
| k-value (Real) / Theoretic | [W/m²*K]: | 2583,4 / 2758,7 |
| Excess surface | [%]: | 6,80 |
| Fouling resistance | [m² K/W]: | 0,00002 |

| | | | |
|---|---|---|---|
| No.of passes x (No.of gap) | : | 1 x 50 PHSH | 1 x 50 SHPH |
| Port velocity In/Out | [m/s]: | 0,058 / 8,461 | 2,008 / 2,004 |
| Gap velocity | [m/s]: | | SHPH: 0,284 |
| Pressure loss Calculated | [bar]: | 0,013 | 0,398 |

| | | | |
|---|---|---|---|
| Working temperature Min./Max. | [°C]: | 0,00 / 40,00 | 0,00 / 40,00 |
| Design temperature Min./Max. | [°C]: | 0,00 / 40,00 | 0,00 / 40,00 |
| Working pressure Min./Max. | [barg]: | 0,00 / 4,55 | 0,00 / 6,00 |
| Design pressure Min./Max. | [barg]: | 0,00 / 16,00 | 0,00 / 16,00 |
| Testing pressure | [barg]: | 17,60 | 20,00 |
| Content | [l]: | 40,411 | 40,411 |

| | | | |
|---|---|---|---|
| Plate material / Plate thickness | [mm]: | 1.4301 ( AISI 304) / 0,6 | |
| Ring gasket | : | CR-LT | Laser welded |
| Field gasket | : | Laser welded | CR-LT |
| Gasket fixing | : | Clip on (glueless) | Clip on (glueless) |

| | | |
|---|---|---|
| Apparatus name | : | ThermoLine TL0250 TCGL - 750 |
| Pressure vessel code / Design code | : | PED 97 / 23 /EC module H1 / AD-Merkblatt 2000 |
| Weight Empty/Filled | [kg]: | 714 / 781 |
| Length x Width x Height / Initial dimen. | [mm]: | 750,0 x 550,0 x 1140,0 / 359,6 - 355,4 |
| Frame material | : | 1.0570 / painted RAL5018 |

Remark

| Pos | IN/OUT | Media | Temp | Type | Code | Form | DN | PN | Material |
|---|---|---|---|---|---|---|---|---|---|
| K1 | Out | PROP.GLYCOL 30% | 5,00 | Stud bolts | DIN 2501 | C | 100 | 16 | EPDM-NT |
| K2 | Out | Ammonia | 2,50 | Stud bolts | DIN 2501 | N | 100 | 40 | 1.0038 |
| K3 | In | Ammonia | 2,50 | Stud bolts | DIN 2501 | N | 100 | 40 | 1.0038 |
| K4 | In | PROP.GLYCOL 30% | 10,00 | Stud bolts | DIN 2501 | C | 100 | 16 | EPDM-NT |
| D1 | | | | | | | | | |
| D2 | | | | | | | | | |
| D3 | Out | Oil drainage | 2,50 | Welding neck flange | DIN 2635 | N | 40 | 40 | 1.0460 |
| D4 | | | | | | | | | |

**Heat pump 2**

## Pos. 2] 1 x Chiller Type FX GC PP 400 NH3 variable speed drive

- **Technical details**

| | | | |
|---|---|---|---|
| Survey of technical details | | | |
| Mode of operation | | Cooling | Heating |
| Rated speed | : | 725-1600 min-1 | 725-1470 $min^{-1}$ |
| Refrigeration capacity acc. to EN 12900 and DIN 8976 | : | 438,0 kW | 356 kW |
| Power consumption | : | 74,5 kW | 96.8 kW |
| Condenser rating | : | 512,5 kW | 453 kW |
| Type sec. refrigerant | : | Propylene Glycol 30% | |
| Sec. refrigerant inlet | : | 10 °C | 10 °C |
| Sec. refrigerant outlet | : | 5 °C | 5 °C |
| Sec. refrigerant outlet min. / max. | | 2 °C / 10 °C | - |
| Type cooling/heating medium | : | Water | |
| Cooling/heating medium inlet | : | 27 °C | 42 °C |
| Cooling/heating medium outlet | : | 32 °C | 50 °C |
| Heating medium outlet min/max | : | - | 30 °C / 50 °C |
| Flow rate evaporator | : | 78,9 $m^3/h$, constant flow | 66.2 $m^3/h$, constant flow |
| Flow rate condenser | : | 87,9 $m^3/h$, constant flow | 78.6 $m^3/h$, constant flow |

The following values for dimensions, weights and charges are preliminary. Final binding data according to the latest version of the general drawing only.

| | | |
|---|---|---|
| Length approx. | : | **3750 mm, (without power panel, measurements of the power panel: height=2100mm, width=1200mm,depth=600mm)** |
| Width approx. | : | **1600 mm without spring elements, with spring elements=1800mm** |
| Height approx. | : | **2290 mm** |
| Refrigerant charge approx. | : | 42 kg |
| Oil charge approx. | : | 15 l |
| Operating weight approx. | : | **5200 kg** |

- **Package**

| | | |
|---|---|---|
| Grasso Ammonia-Liquid Chiller Type | : | FX GC PP 400 NH3 |
| Description | : | Ammonia liquid Chiller with reciprocating compressor, evaporator and condenser in execution as plate type heat exchanger, as a compact, complete factory packaged unit, ready for connection on site, dismounted for transport |
| Compressor Configuration | : | Reciprocating compressor Grasso 610, open-type execution with multi-stage capacity control by cylinder offloading. Available part load steps in %: 50/67/83/100. The applicable part load steps depend on the operating conditions. The compressor is equipped with integrated gas suction filter, solenoid valves for capacity control, oil heater, suction and discharge oil filters, back-pressure independent overflow valve and partially loaded start. |
| Compressor type | : | Grasso 610 |
| Design pressure chiller | : | 25 bar |
| Type liquid separator | : | horizontal |
| Valves on suction side | : | Stop valve(s) on suction side |
| Valves on discharge side | : | Stop valve(s) on discharge side |
| Wiring | | |
| Painting: | : | Protective paint system S 2.15 acc. to EN ISO 12944-5 for environmental conditions C2 acc. to EN ISO 12944-2. Designed for machine room temperatures between 5°C and 40°C. |
| Color | : | RAL 5014 pigeon blue (standard) |
| Insulation type | : | Suction pipe and liquid separator insulated with PUR and coated with Aluminium sheets. The Insulation is designed for 20°C machine room temperature and 70% humidity. |
| Control unit | | |

| | | |
|---|---|---|
| Controller type | : | Chiller control GSC (216 SER) with TP 605 CQ 5,7" color graphic display with Windows CE© and capacity control via the secondary refrigerant (cooling mode) and switchable with an external signal from the costumer to the capacity control via the heating outlet temperature (heating mode). Limitations: suction pressure, condenser pressure, motor current. 11 different operating modes available, incl. auto, remote, service etc. Main functions of the PLC: 1. Control of secondary refrigerant inlet resp. outlet temperature 2. Electronic unit protection and record of operating hours 3. Release contacts for secondary refrigerant pump and condenser system 4. Operating information, all values of analogue inputs were displayed 5. Failure information shown as text on the display and indicated by an information lamp 6. Potential-free status report of the unit (unit ready, unit in operation, multiple fault).7. data logging function and trend report |
| Controller Display | : | Display separate arranged in panel door |
| Controller arrangement | : | Integrated in power panel |
| Controller communication | : | Modbus TCP, acc. Grasso description |
| Display language | : | Norwegian |
| Pressure sensors | : | Standard sensors |
| Number of pressure sensors: | : | 3 |
| Mounting of pressure sensors | : | in tube |
| Number of temperature sensors: | : | 4 |
| Additional temperature sensors | : | none |
| Selection flow switch secondary refrigerant | : | Mechanical flow switch, delivered loose |
| Selection flow switch cooling medium | : | without flow switch |
| Motor, manufacturer ABB | | |
| Motor type | : | Low voltage motor IP 55 |
| Number of motors | : | 1 |
| Type of construction | : | IMB 3 |
| Number of poles | : | 4 |
| Degree of protection | : | IP55 |
| Drive motor rating | : | 132 kW |
| Voltage | : | 3 x 400 V ± 5% / 50 Hz |
| Frequency | : | 50 Hz |
| Switch on mode | : | Variable speed drive (VSD), brand for frequence inverter is Danfoss |
| Type of Power Supply: | : | Power Panel, IP 54 protection, complete wired and tested, main switch, emergency switch, contactors for oil heater, thermal over current release and safety fuses, power fuses, control transformer with double control safety, primary and secondary, 24 V AC current supply |
| Cable entry point | : | at the bottom with cables in Aluminium |
| Type of net | : | **TN-L1,L2,L3;N+PE** |

Evaporator

| | | |
|---|---|---|
| Design Pressure Evaporator | : | 16 bar |

Plate heat-exchanger of modular semi welded design; medium ports are completed with flanges and counter flanges.

| | | |
|---|---|---|
| Cassette material evaporator | : | AISI 304 |
| Pressure drop | : | 33,6 kPa |

Drip tray evaporator

Condenser

| | | |
|---|---|---|
| Design Pressure Condenser | : | 25 bar |

Plate heat-exchanger of modular semi welded design; medium ports are completed with flanges and counter flanges.

| | | |
|---|---|---|
| Cassette material condenser | : | AISI 316 |
| Pressure drop | : | 30,6 kPa |

Safety devices

| | |
|---|---|
| Type | : Double safety valve with change over valve |
| Safety valve(s) acc. to PED | : 1 |
| Number of overflow valves | : 1 |
| Approval and documentation | |
| Approval for Chiller Unit | : Work's Certificate, Certificate of Conformity acc. to Machines Directive 98/37/EG, Certificate of Conformity acc. to Pressure Equipment Directive (PED) 97/23/EG. Calculation and manufacturing acc. to AD 2000 and EN 378, module H1. |
| Approval pressure equipment | : Certificate of Conformity acc. to Pressure Equipment Directive (PED) 97/23/EG. Calculation and manufacturing acc. to AD 2000 and EN 378. |
| Non destructive Testing | : 10 % non destructive welding test acc. to EN 1435 |
| Documentation consisting of | : Documentation and CD-ROM consisting of |
| Language of the documentation | : English/Norwegian (PED related language) |
| Sets of documentation | : 2 |
| *** Options (included in price) *** | |
| -Spring Elements | |
| -Remote adjustable set point | |
| -Quick shut off valves | |
| -additional option 1 | : Insulation of the warm side with mineralwool / Aluminium |
| -additional option 2 | : Trip tray under the chiller |
| -additional option 3 | : Sequence control module |
| -additional option 4 | : TAG-Numbers for control panel, acc. Grasso Standard, for explanation the connection between MODBUS and CTS-system |
| -additional option 5 | : Energy management system, manufacturer Janitza, type UMG 96S, with interface MODBUS RTU |
| -additional option 6 | : Additional display in the front of the power panel showing pressures and temperatures |

## ● Exclusions

| | |
|---|---|
| Exclusion from scope of supply | : Foundations, reassembling onsite, pipes on water side, Spare parts and special tools, Refrigerant and lubricating oil, wiring between the chillers for the sequence control, performance test and start up, everything what is not especially mentioned |

200kW

GEA

Refrigeration Division

GCPP 260

Pos. 1.

Nominal cooling

**GEA Grasso GmbH**

Holzhauser Straße 165
13509 Berlin
Germany
Phone: +49 (0)30 - 43 592 6
Fax: +49 (0)30 - 43 592 777
E-mail: info@grasso.de
Website: www.grasso-global.com

## Comsel - Grasso Compressor Selection Software

| | |
|---|---|
| Print date/time | 13-07-2011 . 12:13 |
| Program version | 3.10.00 Build 00 Valid until 31.12.2011 |

| TECHNICAL DATA (Standard package) | | | |
|---|---|---|---|
| Reciprocating compressor package | 1 x Grasso 410 | | |
| Refrigerant | $NH_3$ | | |
| Speed | 1500 | (/min) | |
| Rotation frequency | 50 | (Hz) | |
| Evap. temp. | 2,5 | (°C) | 10/5°C |
| Superheat | 0,0 | (K) | |
| Superheat useful | 0,0 | (K) | |
| Cond. temp. | 34,0 | (°C) | |
| Subcooling | 0,0 | (K) | 27/32°C |
| Power consumption | 47,1 | (kW) | |
| Refrigerating capacity | 279,9 | (kW) | |
| COP = Qo/Pe | 5,95 | (-) | |
| Oil separator | OS4 | | |
| Possible steps | 50/75/100 | (%) | |

| Partload [%] | Cyl. [-] | Pe [kW] | Qo [kW] |
|---|---|---|---|
| 100 | 4 | 47,1 | 279,9 |
| 75 | 3 | 36,7 | 210,3 |
| 50 | 2 | 26,3 | 140,4 |

200kW

GEA

Refrigeration Division

GCKK 260

Pos..
1

Cooling
min. coolant

**GEA Grasso GmbH**

Holzhauser Straße 165
13509 Berlin
Germany
Phone: +49 (0)30 - 43 592 6
Fax: +49 (0)30 - 43 592 777
E-mail: info@grasso.de
Website: www.grasso-global.com

## Comsel - Grasso Compressor Selection Software

| | |
|---|---|
| Print date/time | 13-07-2011 . 12:13 |
| Program version | 3.10.00 Build 00 Valid until 31.12.2011 |

TECHNICAL DATA (Standard package)

| | | |
|---|---|---|
| Reciprocating compressor package | 1 x Grasso 410 | |
| Refrigerant | $NH_3$ | |
| Speed | 1500 | (/min) |
| Rotation frequency | 50 | (Hz) |
| Evap. temp. | -1,0 | (°C) |
| Superheat | 0,0 | (K) |
| Superheat useful | 0,0 | (K) |
| Cond. temp. | 34,0 | (°C) |
| Subcooling | 0,0 | (K) |
| Power consumption | 46,5 | (kW) |
| Refrigerating capacity | 241,2 | (kW) |
| COP = Qo/Pe | 5,19 | (-) |
| Oil separator | OS4 | |
| Possible steps | 50/75/100 | (%) |

| Partload [%] | Cyl. [-] | Pe [kW] | Qo [kW] |
|---|---|---|---|
| 100 | 4 | 46,5 | 241,2 |
| 75 | 3 | 36,2 | 181,2 |
| 50 | 2 | 26,0 | 121,0 |

GEA

Refrigeration Division

GC PP 260

200kW

Pos. 1.

Cooling

max. coolant

**GEA Grasso GmbH**

Holzhauser Straße 165
13509 Berlin
Germany
Phone: +49 (0)30 - 43 592 6
Fax: +49 (0)30 - 43 592 777
E-mail: info@grasso.de
Website: www.grasso-global.com

## Comsel - Grasso Compressor Selection Software

| | | |
|---|---|---|
| Print date/time | 13-07-2011 . 12:14 | |
| Program version | 3.10.00 Build 00 Valid until 31.12.2011 | |
| TECHNICAL DATA (Standard package) | | |
| Reciprocating compressor package | 1 x Grasso 410 | |
| Refrigerant | $NH_3$ | |
| Speed | 1500 | (/min) |
| Rotation frequency | 50 | (Hz) |
| Evap. temp. | 7,0 | (°C) |
| Superheat | 0,0 | (K) |
| Superheat useful | 0,0 | (K) |
| Cond. temp. | 34,0 | (°C) |
| Subcooling | 0,0 | (K) |
| Power consumption | 46,8 | (kW) |
| Refrigerating capacity | 335,5 | (kW) |
| COP = Qo/Pe | 7,16 | (-) |
| Oil separator | OS4 | |
| Possible steps | 50/75/100 | (%) |

| Partload [%] | Cyl. [-] | Pe [kW] | Qo [kW] |
|---|---|---|---|
| 100 | 4 | 46,8 | 335,5 |
| 75 | 3 | 36,5 | 252,2 |
| 50 | 2 | 26,2 | 168,4 |

GEA
Refrigeration Division

6C PP 260

200kW

Heating

Nominal

Pos. 1.

**GEA Grasso GmbH**
Holzhauser Straße 165
13509 Berlin
Germany
Phone: +49 (0)30 - 43 592 6
Fax: +49 (0)30 - 43 592 777
E-mail: info@grasso.de
Website: www.grasso-global.com

## Comsel - Grasso Compressor Selection Software

Print date/time 13-07-2011 . 12:15
Program version 3.10.00 Build 00 Valid until 31.12.2011

TECHNICAL DATA (Standard package)
Reciprocating compressor package 1 x Grasso 410
Refrigerant $NH_3$
Speed 1500 (/min)
Rotation frequency 50 (Hz)

Evap. temp. 2,5 (°C) 10/5 °C
Superheat 0,0 (K)
Superheat useful 0,0 (K)
Cond. temp. 52,0 (°C)
Subcooling 0,0 (K)

Power consumption 65,2 (kW)
Refrigerating capacity 238,1 (kW) 42/50 °C
COP = Qo/Pe 3,65 (-)

Oil separator OS3
Possible steps 50/75/100 (%)

| Partload [%] | Cyl. [-] | Pe [kW] | Qo [kW] |
|---|---|---|---|
| 100 | 4 | 65,2 | 238,1 |
| 75 | 3 | 50,9 | 178,9 |
| 50 | 2 | 36,5 | 119,4 |

200kW

GCKK260

Heating

Liq. outlet

Pos.

1.

Refrigeration Division

**GEA Grasso GmbH**
Holzhauser Straße 165
13509 Berlin
Germany
Phone: +49 (0)30 - 43 592 6
Fax: +49 (0)30 - 43 592 777
E-mail: info@grasso.de
Website: www.grasso-global.com

**Comsel - Grasso Compressor Selection Software**

| | |
|---|---|
| Print date/time | 13-07-2011 . 12:16 |
| Program version | 3.10.00 Build 00 Valid until 31.12.2011 |

TECHNICAL DATA (Standard package)

| | | |
|---|---|---|
| Reciprocating compressor package | 1 x Grasso 410 | |
| Refrigerant | $NH_3$ | |
| Speed | 1500 | (/min) |
| Rotation frequency | 50 | (Hz) |
| | | |
| Evap. temp. | 2,5 | (°C) |
| Superheat | 0,0 | (K) |
| Superheat useful | 0,0 | (K) |
| Cond. temp. | 33,0 | (°C) |
| Subcooling | 0,0 | (K) |
| | | |
| Power consumption | 46,0 | (kW) |
| Refrigerating capacity | 282,3 | (kW) |
| COP = Qo/Pe | 6,14 | (-) |
| | | |
| Oil separator | OS4 | |
| Possible steps | 50/75/100 | (%) |

15°C

130°C

| Partload [%] | Cyl. [-] | Pe [kW] | Qo [kW] |
|---|---|---|---|
| 100 | 4 | 46,0 | 282,3 |
| 75 | 3 | 35,8 | 212,2 |
| 50 | 2 | 25,7 | 141,7 |

GC PF 400 400kW

Cooling Nominal

Refrigeration Division

Pos. 2.

**GEA Grasso GmbH**

Holzhauser Straße 165
13509 Berlin
Germany
Phone: +49 (0)30 - 43 592 6
Fax: +49 (0)30 - 43 592 777
E-mail: info@grasso.de
Website: www.grasso-global.com

## Comsel - Grasso Compressor Selection Software

Print date/time 13-07-2011 . 12:21
Program version 3.10.00 Build 00 Valid until 31.12.2011

| | | |
|---|---|---|
| TECHNICAL DATA (Standard package) | | |
| Reciprocating compressor package | 1 x Grasso 610 | |
| Refrigerant | $NH_3$ | |
| Speed | 1500 | (/min) |
| Rotation frequency | 50 | (Hz) |
| | | |
| Evap. temp. | 2,5 | (°C) 10/5°C |
| Superheat | 0,0 | (K) |
| Superheat useful | 0,0 | (K) |
| Cond. temp. | 34,0 | (°C) 27/32°C |
| Subcooling | 0,0 | (K) |
| | | |
| Power consumption | 69,6 | (kW) |
| Refrigerating capacity | 419,6 | (kW) |
| COP = Qo/Pe | 6,03 | (-) |
| | | |
| Oil separator | OS5 | |
| Possible steps | 33/50/67/83/100 | (%) |

| Partload [%] | Cyl. [-] | Pe [kW] | Qo [kW] |
|---|---|---|---|
| 100 | 6 | 69,6 | 419,6 |
| 83 | 5 | 59,1 | 348,8 |
| 67 | 4 | 49,3 | 281,9 |
| 50 | 3 | 38,9 | 210,6 |
| 33 | 2 | 28,5 | 139,1 |

GCYP 400

400 kW

Cooling

min. coolant

Pos. 2.

Refrigeration Division

**GEA Grasso GmbH**
Holzhauser Straße 165
13509 Berlin
Germany
Phone: +49 (0)30 - 43 592 6
Fax: +49 (0)30 - 43 592 777
E-mail: info@grasso.de
Website: www.grasso-global.com

**Comsel - Grasso Compressor Selection Software**

| | |
|---|---|
| Print date/time | 13-07-2011 . 12:22 |
| Program version | 3.10.00 Build 00 Valid until 31.12.2011 |

TECHNICAL DATA (Standard package)

| | | |
|---|---|---|
| Reciprocating compressor package | 1 x Grasso 610 | |
| Refrigerant | $NH_3$ | |
| Speed | 1500 | (/min) |
| Rotation frequency | 50 | (Hz) |
| Evap. temp. | -1,0 | (°C) |
| Superheat | 0,0 | (K) |
| Superheat useful | 0,0 | (K) |
| Cond. temp. | 34,0 | (°C) |
| Subcooling | 0,0 | (K) |
| Power consumption | 68,7 | (kW) |
| Refrigerating capacity | 361,6 | (kW) |
| COP = Qo/Pe | 5,27 | (-) |
| Oil separator | OS4 | |
| Possible steps | 33/50/67/83/100 | (%) |

| Partload [%] | Cyl. [-] | Pe [kW] | Qo [kW] |
|---|---|---|---|
| 100 | 6 | 68,7 | 361,6 |
| 83 | 5 | 58,4 | 300,6 |
| 67 | 4 | 48,7 | 242,9 |
| 50 | 3 | 38,5 | 181,5 |
| 33 | 2 | 28,2 | 119,8 |

GEA

Refrigeration Division

Pos. 2.

GCPP 400

cooling

max. coolant

400kW

**GEA Grasso GmbH**

Holzhauser Straße 165
13509 Berlin
Germany
Phone: +49 (0)30 - 43 592 6
Fax: +49 (0)30 - 43 592 777
E-mail: info@grasso.de
Website: www.grasso-global.com

**Comsel - Grasso Compressor Selection Software**

| | |
|---|---|
| Print date/time | 13-07-2011 . 12:22 |
| Program version | 3.10.00 Build 00 Valid until 31.12.2011 |

| TECHNICAL DATA (Standard package) | | |
|---|---|---|
| Reciprocating compressor package | 1 x Grasso 610 | |
| Refrigerant | NH3 | |
| Speed | 1500 | (/min) |
| Rotation frequency | 50 | (Hz) |
| | | |
| Evap. temp. | 7,0 | (°C) |
| Superheat | 0,0 | (K) |
| Superheat useful | 0,0 | (K) |
| Cond. temp. | 34,0 | (°C) |
| Subcooling | 0,0 | (K) |
| | | |
| Power consumption | 69,2 | (kW) |
| Refrigerating capacity | 503,1 | (kW) |
| COP = Qo/Pe | 7,27 | (-) |
| | | |
| Oil separator | OS5 | |
| Possible steps | 33/50/67/83/100 | (%) |

| Partload [%] | Cyl. [-] | Pe [kW] | Qo [kW] |
|---|---|---|---|
| 100 | 6 | 69,2 | 503,1 |
| 83 | 5 | 58,8 | 418,2 |
| 67 | 4 | 49,1 | 338,0 |
| 50 | 3 | 38,7 | 252,5 |
| 33 | 2 | 28,4 | 166,8 |

GC PP 400 400kW

Pos. 2.

Heating nominal

Refrigeration Division

**GEA Grasso GmbH**
Holzhauser Straße 165
13509 Berlin
Germany
Phone: +49 (0)30 - 43 592 6
Fax: +49 (0)30 - 43 592 777
E-mail: info@grasso.de
Website: www.grasso-global.com

## Comsel - Grasso Compressor Selection Software

| | |
|---|---|
| Print date/time | 13-07-2011 . 12:23 |
| Program version | 3.10.00 Build 00 Valid until 31.12.2011 |

| TECHNICAL DATA (Standard package) | | |
|---|---|---|
| Reciprocating compressor package | 1 x Grasso 610 | |
| Refrigerant | $NH_3$ | |
| Speed | 1500 | (/min) |
| Rotation frequency | 50 | (Hz) |
| Evap. temp. | 2,5 | (°C) |
| Superheat | 0,0 | (K) |
| Superheat useful | 0,0 | (K) |
| Cond. temp. | 52,0 | (°C) |
| Subcooling | 0,0 | (K) |
| Power consumption | 96,8 | (kW) |
| Refrigerating capacity | 356,9 | (kW) |
| COP = Qo/Pe | 3,69 | (-) |
| Oil separator | OS4 | |
| Possible steps | 50/67/83/100 | (%) |

10/5 °C

42/50 °C

| Partload [%] | Cyl. [-] | Pe [kW] | Qo [kW] |
|---|---|---|---|
| 100 | 6 | 96,8 | 356,9 |
| 83 | 5 | 82,3 | 296,7 |
| 67 | 4 | 68,7 | 239,7 |
| 50 | 3 | 54,2 | 179,0 |
| 33 | 2 | -- | -- |

GCPP 400 400kW

Refrigeration Division

Pos. 2.

Heating min. outlet

**GEA Grasso GmbH**
Holzhauser Straße 165
13509 Berlin
Germany
Phone: +49 (0)30 - 43 592 6
Fax: +49 (0)30 - 43 592 777
E-mail: info@grasso.de
Website: www.grasso-global.com

## Comsel - Grasso Compressor Selection Software

| | |
|---|---|
| Print date/time | 13-07-2011 . 12:23 |
| Program version | 3.10.00 Build 00 Valid until 31.12.2011 |

| | | |
|---|---|---|
| TECHNICAL DATA (Standard package) | | |
| Reciprocating compressor package | 1 x Grasso 610 | |
| Refrigerant | $NH_3$ | |
| Speed | 1500 | (/min) |
| Rotation frequency | 50 | (Hz) |
| Evap. temp. | 2,5 | (°C) |
| Superheat | 0,0 | (K) |
| Superheat useful | 0,0 | (K) |
| Cond. temp. | 33,0 | (°C) |
| Subcooling | 0,0 | (K) |
| Power consumption | 67,9 | (kW) |
| Refrigerating capacity | 423,3 | (kW) |
| COP = Qo/Pe | 6,23 | (-) |
| Oil separator | OS5 | |
| Possible steps | 33/50/67/83/100 | (%) |

15°C

130°C

| Partload [%] | Cyl. [-] | Pe [kW] | Qo [kW] |
|---|---|---|---|
| 100 | 6 | 67,9 | 423,3 |
| 83 | 5 | 57,7 | 351,9 |
| 67 | 4 | 48,2 | 284,4 |
| 50 | 3 | 38,0 | 212,5 |
| 33 | 2 | 27,8 | 140,3 |

**Heat pump 3**

# Sabroe

## Refrigeration Plant Computation

**Version 21.06**

| | | | | | |
|---|---|---|---|---|---|
| File | : 255662Q_108_sommer | Ref | : CMAD | Page : | 1 |
| Date | : 2011/09/12 | Time | : 14.12.33 | | |
| User | : JCI - HOLME - YROE SALES | | | | |
| Prog | : COMP1/104509 | Print | : MIE ver. 8.0.6001.18702 | | |

## SINGLE STAGE COMPRESSOR

| | | | | | |
|---|---|---|---|---|---|
| compressor type | SMC 108 E VSD | | refrigerant | R 717 | |
| number of compressors | 1.00 | | evaporating temperature | 1.6 | deg.C |
| compressor load | 100.0 | % | condensing temperature | 33.5 | deg.C |
| drive shaft speed | 1500.0 | RPM (list) | total suction superheat | 0.0 | K |
| no. of working cylinders: | 8 | | suction line superheat | 0.0 | K |
| drive type | direct | | total liquid subcooling | 0.6 | K |
| suction line loss | 0.6 | K | | | |
| discharge line loss | 0.0 | K | | | |

| | | | | | |
|---|---|---|---|---|---|
| total cooling capacity | 671.1 | kW | total shaft power req. | 117.7 | kW |
| | | | drive shaft torque | 749. | Nm |
| total heating capacity | 788. | kW | cooling cap./shaft power ratio | 5.70 | |
| | | | cooling cap./line power ratio | 5.47 | |

| | |
|---|---|
| equipment for head cooling | water |
| equipment for oil cooling | water |

| | | | |
|---|---|---|---|
| motor: | Leroy/141kW/400V/50Hz/IP55/315MR | | |
| start-up: | VSD | | |
| motor eff. | 0.958 | motor line power cons. | 122.8 kW |
| | | coupling type. | CFA-30/90 |

operating conditions:

| | | | | | |
|---|---|---|---|---|---|
| suction pressure | 4.45 | bar_a | discharge pressure | 12.92 | bar_a |
| suction temperature | 0.96 | deg.C | discharge temperature | 92.70 | deg.C |
| suction specific volume | 0.2795 | m3/kg | disch. temp. at min. load | 103.32 | deg.C |
| enthalpy difference (ref.) | 1109.72 | kJ/kg | discharge specific volume | 0.1296 | m3/kg |
| suction side mass flow | 0.6047 | kg/s | condenser subcooled liquid density | 590.9 | kg/m3 |
| swept volume | 678.6 | m3/h | evaporator saturated liquid density | 636.4 | kg/m3 |
| cover cooling water flow | 0.6 | m3/h | pressure ratio (p2/p1) | 2.90 | |
| cover cooling pressure loss | 17.15 | kPa | | | |

errors and warnings:
NB: no sound level computation - motor data error or data not def.
NB: At certain VSD frequencies, resonance vibrations may occur.
NB: Skipping limited frequency ranges may be necessary.
NB: All data valid for factory built VSD unit only !
NB: Sound computation "box" with non-standard dimensions.
NB: External motor cooling or oversize motor may be necessary
NB: design limits check OK

Full load performance data for chillers and other refrigeration systems are according to ISO-R916.
Measurement tolerances according to ISO-917.
Data subject to change without notice.

# Sabroe

## Refrigeration Plant Computation

**Version 21.06**

| | | | | | |
|---|---|---|---|---|---|
| File | : 255662Q_108_sommer | Ref | : CMAD | Page : | 2 |
| Date | : 2011/09/12 | Time | : 14.12.33 | | |
| User | : JCI - HOLME - YROE SALES | | | | |
| Prog | : COMP1/104509 | Print | : MIE ver. 8.0.6001.18702 | | |

EVAPORATOR

| | | | | | |
|---|---|---|---|---|---|
| evaporator type | ESRD 702001 | | number of evaporators | 1.00 | |
| primary side: | | | | | |
| primary refrigerant | R-717 | | total capacity | 671.1 | kW |
| evaporating temperature | 1.6 | deg.C | mean temperature diff. | 5.55 | K |
| | | | fouling factor | 0.000035 | m2.K/W |
| inlet velocity - prim. side | 4.20 | m/s | outlet velocity - prim. side | 12.09 | m/s |
| secondary side: | | | | | |
| secondary refrigerant (204) PROPYLENE_GLYCOL | | | percentage by weight | 25.0 | % |
| inlet temperature | 10.0 | deg.C | freezing temperature | -10.4 | deg.C |
| outlet temperature | 5.0 | deg.C | total flow | 118.5 | m3/h |
| pressure loss | 20.9 | kPa | | | |
| velocity | 1.73 | m/s | | | |
| density | 1024.5 | kg/m3 | specific heat capacity | 3.981 | kJ/kg.K |
| dynamic viscosity | 3.841 | Cpoise | thermal conductivity | 0.479 | W/m.K |
| inlet velocity - sec. side | 1.83 | m/s | outlet velocity - sec. side | 1.83 | m/s |
| min. wall temperature | 3.2 | deg.C | | | |
| | | | secondary side pass number | 1 | |
| built-in liquid separator performance: | | | separator speed | 0.22 | m/s |
| separator pressure loss | 0.0 | K | velocity ratio (cmax/cgas) | 1.56 | |
| special PHE output: | | | | | |
| no. of cassettes and type | 1*200 MG | | service transfer coefficient | 1494.9 | W/m2K |
| design/rating mode | rating | | clean transfer coefficient | 1655.4 | W/m2K |
| plate material | AISI-316 | | refrigerant pressure loss | 0.17 | mbg |
| plate thickness | 0.6 | mm | margin | 5.00 | % |
| max. pressure loss sec. side | 10.00 | mbg | available liquid head | 0.40 | mbg |
| primary side connection - in/out | 1/1 | | quality of vapour | 0.85 | |
| secondary side connection - in/out | 2/2 | | excessive area | 0.00 | % |
| hot side channel pressure loss | 19.2 | kPa | | | |
| cold side channel pressure loss | 0.25 | mbg | | | |

errors and warnings:
NB: suitable for closed systems only (dp-channel < 2.9 mbg.)
NB: nucleate boiling multiplier automatically disabled

Full load performance data for chillers and other refrigeration systems are according to ISO-R916.
Measurement tolerances according to ISO-917.
Data subject to change without notice.

# Sabroe

## Refrigeration Plant Computation

**Version 21.06**

| | | | | | |
|---|---|---|---|---|---|
| File | : 255662Q_108_sommer | Ref | : CMAD | Page : | 3 |
| Date | : 2011/09/12 | Time | : 14.12.33 | | |
| User | : JCI - HOLME - YROE SALES | | | | |
| Prog | : COMP1/104509 | Print | : MIE ver. 8.0.6001.18702 | | |

### CONDENSER

| | | | | | |
|---|---|---|---|---|---|
| condenser type | CRRD 802001 | | number of condensers | 1.00 | |
| primary side: | | | | | |
| primary refrigerant | R-717 | | total capacity | 788.0 | kW |
| condensing temperature | 33.5 | deg.C | mean temperature diff. | 3.20 | K |
| condenser liquid subcooling | 0.6 | K | | | |
| | | | fouling factor | 0.000020 | m2.K/W |
| secondary side: | | | | | |
| secondary refrigerant (200) WATER | | | | | |
| inlet temperature | 27.0 | deg.C | | | |
| outlet temperature | 32.0 | deg.C | total flow | 136.3 | m3/h |
| pressure loss | 22.6 | kPa | | | |
| velocity | 1.99 | m/s | | | |
| density | 995.8 | kg/m3 | specific heat capacity | 4.181 | kJ/kg.K |
| dynamic viscosity | 0.808 | Cpoise | thermal conductivity | 0.614 | W/m.K |
| inlet velocity - sec. side | 2.10 | m/s | outlet velocity - sec. side | 2.10 | m/s |
| special PHE output: | | | | | |
| no. of cassettes and type | 1*200 MG | | service transfer coefficient | 3105.5 | W/m2K |
| design/rating mode | rating | | clean transfer coefficient | 3479.2 | W/m2K |
| plate material | AISI-316 | | refrigerant pressure loss | 0.02 | mbg |
| plate thickness | 0.6 | mm | margin | 5.00 | % |
| max. pressure loss sec. side | 10.00 | mbg | | | |
| primary side connection - in/out | 1/1 | | superheated vapour temp. | 92.70 | deg.C |
| secondary side connection - in/out | 2/2 | | excessive area | 0.00 | % |
| hot side channel pressure loss | 0.02 | mbg | | | |
| cold side channel pressure loss | 19.7 | kPa | | | |

errors and warnings:
NB: suitable for closed systems only (dp-channel < 3.0 mbg.)

# Sabroe

## Refrigeration Plant Computation

Version 21.06

| | | | | | | | |
|---|---|---|---|---|---|---|---|
| File | : | 255662Q_108_sommer | Ref | : | CMAD | Page : | 4 |
| Date | : | 2011/09/12 | Time | : | 14.12.33 | | |
| User | : | JCI - HOLME - YROE SALES | | | | | |
| Prog | : | COMP1/104509 | Print | : | MIE ver. 8.0.6001.18702 | | |

**ChillPAC UNIT DATA - ChillPAC108EV-C**

| | | |
|---|---|---|
| plant load percentage | 100.0 | % |
| plant cooling capacity | 671.1 | kW |
| plant heating capacity | 788.0 | kW |
| totalt shaft power consumption | 117.7 | kW |
| total line power consumption | 122.8 | kW |
| capacity/shaft power ratio | 5.70 | |
| capacity/line power ratio | 5.47 | |

| | | |
|---|---|---|
| chiller unit approx. length | 4.84 | m |
| chiller unit exact width | 1.00 | m |
| chiller unit approx. height | 2.00 | m |
| unit approx. operating weight | 5525. | kg |
| unit approx. refrigerant charge | 51. | kg |
| unit approx. evaporator brine/water charge | 80. | kg |
| unit approx. condensor water charge | 80. | kg |
| number of vibration dampers | 6 | |
| chiller unit expansion valve | 1 x HFI-060FD | |
| unit expansion valve load | 61.5 | % |

errors and warnings:

# Sabroe

## Refrigeration Plant Computation

**Version 21.06**

| | | | | | | | |
|---|---|---|---|---|---|---|---|
| File | : | 255662Q_108_HP | Ref | : | CMAD | Page : | 1 |
| Date | : | 2011/09/12 | Time | : | 14.21.02 | | |
| User | : | JCI - HOLME - YROE SALES | | | | | |
| Prog | : | COMP1/104509 | Print | : | MIE ver. 8.0.6001.18702 | | |

## SINGLE STAGE COMPRESSOR

| | | | | | |
|---|---|---|---|---|---|
| compressor type | SMC 108 E VSD | | refrigerant | R 717 | |
| number of compressors | 1.00 | | evaporating temperature | 3.1 | deg.C |
| compressor load | 55.0 | % | condensing temperature | 49.9 | deg.C |
| drive shaft speed | 825.0 | RPM (list) | total suction superheat | 0.0 | K |
| no. of working cylinders: | 8 | | suction line superheat | 0.0 | K |
| drive type | direct | | total liquid subcooling | 0.0 | K |
| suction line loss | 0.6 | K | | | |
| discharge line loss | 0.0 | K | | | |

| | | | | | |
|---|---|---|---|---|---|
| total cooling capacity | 340.6 | kW | total shaft power req. | 84.0 | kW |
| | | | drive shaft torque | 973. | Nm |
| total heating capacity | 422. | kW | cooling cap./shaft power ratio | 4.05 | |
| | | | cooling cap./line power ratio | 3.87 | |

| | |
|---|---|
| equipment for head cooling | water |
| equipment for oil cooling | water |

| | | | |
|---|---|---|---|
| motor: | Leroy/141kW/400V/50Hz/IP55/315MR | | |
| start-up: | VSD | | |
| motor eff. | 0.955 | motor line power cons. | 88.0 kW |
| | | coupling type. | CFA-30/90 |

operating conditions:

| | | | | | |
|---|---|---|---|---|---|
| suction pressure | 4.71 | bar_a | discharge pressure | 20.30 | bar_a |
| suction temperature | 2.50 | deg.C | discharge temperature | 122.26 | deg.C |
| suction specific volume | 0.2649 | m3/kg | disch. temp. at min. load | 133.37 | deg.C |
| enthalpy difference (ref.) | 1029.04 | kJ/kg | discharge specific volume | 0.0881 | m3/kg |
| suction side mass flow | 0.3310 | kg/s | condenser subcooled liquid density | 562.9 | kg/m3 |
| swept volume | 373.2 | m3/h | evaporator saturated liquid density | 634.3 | kg/m3 |
| cover cooling water flow | 0.5 | m3/h | pressure ratio (p2/p1) | 4.31 | |
| cover cooling pressure loss | 9.49 | kPa | | | |

errors and warnings:
NB: At certain VSD frequencies, resonance vibrations may occur.
NB: Skipping limited frequency ranges may be necessary.
NB: All data valid for factory built VSD unit only !
NB: External motor cooling or oversize motor may be necessary
NB: design limits check OK

Full load performance data for chillers and other refrigeration systems are according to ISO-R916.
Measurement tolerances according to ISO-917.
Data subject to change without notice.

SABROE BY JOHNSON CONTROLS

# Sabroe

## Refrigeration Plant Computation

**Version 21.06**

| | | | |
|---|---|---|---|
| File : 255662Q_108_HP | Ref : CMAD | Page : 2 | |
| Date : 2011/09/12 | Time : 14.21.02 | | |
| User : JCI - HOLME - YROE SALES | | | |
| Prog : COMP1/104509 | Print : MIE ver. 8.0.6001.18702 | | |

### EVAPORATOR

| | | | |
|---|---|---|---|
| evaporator type | ESRD 702001 | number of evaporators | 1.00 |
| primary side: | | | |
| primary refrigerant | R-717 | total capacity | 340.6 kW |
| evaporating temperature | 3.1 deg.C | mean temperature diff. | 3.00 K |
| | | fouling factor | 0.000035 m2.K/W |
| inlet velocity - prim. side | 3.28 m/s | outlet velocity - prim. side | 6.28 m/s |
| secondary side: | | | |
| secondary refrigerant (204) PROPYLENE_GLYCOL | | percentage by weight | 25.0 % |
| inlet temperature | 7.5 deg.C | freezing temperature | -10.4 deg.C |
| outlet temperature | 5.0 deg.C | total flow | 120.0 m3/h |
| pressure loss | 21.5 kPa | | |
| velocity | 1.75 m/s | | |
| density | 1025.0 kg/m3 | specific heat capacity | 3.981 kJ/kg.K |
| dynamic viscosity | 4.028 Cpoise | thermal conductivity | 0.478 W/m.K |
| inlet velocity - sec. side | 1.85 m/s | outlet velocity - sec. side | 1.85 m/s |
| min. wall temperature | 4.1 deg.C | | |
| | | secondary side pass number | 1 |
| built-in liquid separator performance: | | separator speed | 0.12 m/s |
| separator pressure loss | 0.0 K | velocity ratio (cmax/cgas) | 2.91 |
| special PHE output: | | | |
| no. of cassettes and type | 1*200 MG | service transfer coefficient | 1396.9 W/m2K |
| design/rating mode | rating | clean transfer coefficient | 1540.8 W/m2K |
| plate material | AISI-316 | refrigerant pressure loss | 0.13 mbg |
| plate thickness | 0.6 mm | margin | 5.00 % |
| max. pressure loss sec. side | 10.00 mbg | available liquid head | 0.40 mbg |
| primary side connection - in/out | 1/1 | quality of vapour | 0.85 |
| secondary side connection - in/out | 2/2 | excessive area | 0.00 % |
| hot side channel pressure loss | 19.7 kPa | | |
| cold side channel pressure loss | 0.25 mbg | | |

errors and warnings:
NB: suitable for closed systems only (dp-channel < 2.9 mbg.)
NB: nucleate boiling multiplier automatically disabled

Full load performance data for chillers and other refrigeration systems are according to ISO-R916.
Measurement tolerances according to ISO-917.
Data subject to change without notice.

# Sabroe

## Refrigeration Plant Computation

Version 21.06

| | | | | | |
|---|---|---|---|---|---|
| File | : 255662Q_108_HP | Ref | : CMAD | Page : | 3 |
| Date | : 2011/09/12 | Time | : 14.21.02 | | |
| User | : JCI - HOLME - YROE SALES | | | | |
| Prog | : COMP1/104509 | Print | : MIE ver. 8.0.6001.18702 | | |

CONDENSER

| | | | | | |
|---|---|---|---|---|---|
| condenser type | CRRD 802001 | | number of condensers | 1.00 | |
| primary side: | | | | | |
| primary refrigerant | R-717 | | total capacity | 422.4 | kW |
| condensing temperature | 49.9 | deg.C | mean temperature diff. | 1.60 | K |
| condenser liquid subcooling | 0.0 | K | | | |
| | | | fouling factor | 0.000020 | m2.K/W |
| secondary side: | | | | | |
| secondary refrigerant (200) WATER | | | | | |
| inlet temperature | 46.6 | deg.C | | | |
| outlet temperature | 49.2 | deg.C | total flow | 140.0 | m3/h |
| pressure loss | 22.5 | kPa | | | |
| velocity | 2.05 | m/s | | | |
| density | 989.0 | kg/m3 | specific heat capacity | 4.181 | kJ/kg.K |
| dynamic viscosity | 0.566 | Cpoise | thermal conductivity | 0.638 | W/m.K |
| inlet velocity - sec. side | 2.16 | m/s | outlet velocity - sec. side | 2.16 | m/s |
| special PHE output: | | | | | |
| no. of cassettes and type | 1*200 MG | | service transfer coefficient | 3367.8 | W/m2K |
| design/rating mode | rating | | clean transfer coefficient | 3850.7 | W/m2K |
| plate material | AISI-316 | | refrigerant pressure loss | 0.01 | mbg |
| plate thickness | 0.6 | mm | margin | 5.00 | % |
| max. pressure loss sec. side | 10.00 | mbg | | | |
| primary side connection - in/out | 1/1 | | superheated vapour temp. | 122.30 | deg.C |
| secondary side connection - in/out | 2/2 | | excessive area | 0.00 | % |
| hot side channel pressure loss | 0.00 | mbg | | | |
| cold side channel pressure loss | 19.4 | kPa | | | |

errors and warnings:
NB: suitable for closed systems only (dp-channel < 3.0 mbg.)

# Sabroe

## Refrigeration Plant Computation

**Version 21.06**

| | | | | | | | |
|---|---|---|---|---|---|---|---|
| File | : | 255662Q_108_HP | Ref | : | CMAD | Page : | 4 |
| Date | : | 2011/09/12 | Time | : | 14.21.02 | | |
| User | : | JCI - HOLME - YROE SALES | | | | | |
| Prog | : | COMP1/104509 | Print | : | MIE ver. 8.0.6001.18702 | | |

### ChillPAC UNIT DATA - ChillPAC108EV-C

| | | |
|---|---|---|
| plant load percentage | 55.0 | % |
| plant cooling capacity | 340.6 | kW |
| plant heating capacity | 422.4 | kW |
| totalt shaft power consumption | 84.0 | kW |
| total line power consumption | 88.0 | kW |
| capacity/shaft power ratio | 4.05 | |
| capacity/line power ratio | 3.87 | |

| | | |
|---|---|---|
| chiller unit approx. length | 4.84 | m |
| chiller unit exact width | 1.00 | m |
| chiller unit approx. height | 2.00 | m |
| unit approx. operating weight | 5525. | kg |
| unit approx. refrigerant charge | 51. | kg |
| unit approx. evaporator brine/water charge | 80. | kg |
| unit approx. condensor water charge | 80. | kg |
| number of vibration dampers | 6 | |
| chiller unit expansion valve | 1 x HFI-050FD | |
| unit expansion valve load | 37.7 | % |

errors and warnings: